

# Classification of symmetry enriched topological phases with exactly solvable models

Andrej Mesaros and Ying Ran

*Department of Physics, Boston College, Chestnut Hill, Massachusetts 02467, USA*

(Received 11 December 2012; published 4 April 2013)

Recently, a new class of quantum phases of matter—symmetry protected topological states, such as topological insulators—has attracted much attention. In presence of interactions, group cohomology provides a classification of these [Chen *et al.*, *Phys. Rev. B* **87**, 155114 (2013)]. These phases have short-ranged entanglement and no topological order in the bulk. However, when long-range entangled topological order is present, it is much less understood how to classify quantum phases of matter in the presence of global symmetries. Here we present a classification of bosonic gapped quantum phases with or without long-range entanglement in the presence or absence of on-site global symmetries. In  $2 + 1$  dimensions, the quantum phases in the presence of a global symmetry group  $SG$ , and with topological order described by a finite gauge group  $GG$ , are classified by the cohomology group  $H^3(SG \times GG, U(1))$ . Generally, in  $d + 1$  dimensions, such quantum phases are classified by  $H^{d+1}(SG \times GG, U(1))$ . Although we only partially understand to what extent our classification is complete, we present an exactly solvable local bosonic model, in which the topological order is emergent, for each given class in our classification. When the global symmetry is absent, the topological order in our models is described by the general Dijkgraaf-Witten discrete gauge theories. When the topological order is absent, our models become the exactly solvable models for symmetry protected topological phases [Chen *et al.*, *Phys. Rev. B* **87**, 155114 (2013)]. When both the global symmetry and the topological order are present, our models describe symmetry enriched topological phases. Our classification includes, but goes beyond, the previously discussed projective symmetry group classification. Measurable signatures of these symmetry enriched topological phases and generalizations of our classification are discussed.

DOI: [10.1103/PhysRevB.87.155115](https://doi.org/10.1103/PhysRevB.87.155115)

PACS number(s): 75.10.Kt, 73.43.-f

## I. INTRODUCTION

Recently there has been significant interest in topological phases of matter, which are quantum phases of matter beyond the Ginzburg-Landau symmetry-breaking description.<sup>1</sup> After the discovery of fractional quantum Hall states, the notion of topological order was proposed.<sup>2</sup> Topologically ordered phases of matter feature ground-state degeneracies on torus,<sup>3</sup> and anyonic quasiparticle excitations in the bulk in  $2 + 1$  dimensions.<sup>4</sup> These features are robust against arbitrary local perturbations. Therefore, the global symmetry is *not* a requirement for topologically ordered quantum phases.

More recently, symmetry protected topological (SPT) phases attracted a lot of attention. SPT phases are defined to have no topological order in the bulk (and thus no anyons in the bulk nor ground-state degeneracies on torus); nevertheless, their distinctions are protected by the global symmetry.<sup>5–13</sup> Examples of SPT phases include topological insulators and superconductors.<sup>14–18</sup> One experimental signature of the SPT phases are the symmetry protected gapless boundary states, which can be obtained from a Chern-Simons based classification of phases.<sup>19</sup> Another classification of interacting bosonic SPT phases for on-site global symmetries is provided in the original work by Chen *et al.*<sup>20</sup> using the group cohomology method. At the superficial level, there is no relation between the SPT phases and the topologically ordered phases. For example, in  $1 + 1d$ , it can be shown that in the presence of interactions, there is no topological order but there are nontrivial SPT phases,<sup>20–25</sup> such as the AKLT<sup>26,27</sup> integer spin chain. A recent beautiful work<sup>28</sup> shows that SPT phases and topologically ordered phases are related via certain duality in spatial dimensions higher than one.

How can one understand/classify gapped quantum phases when both the topological order and the global symmetry are present? This is an important question for both fundamental and practical purposes, and this paper is an attempt to answer it, at least partially. To illustrate the importance of this question, as an example, we can consider one famous topologically ordered phase: the Laughlin's  $\nu = 1/3$  fractional quantum Hall liquid<sup>29</sup> (FQHL), which has threefold ground-state degeneracy on torus<sup>2</sup> and anyonic quasiparticle excitations in the bulk. In the physical realization of the Laughlin FQHL in 2DEG, there is also a global symmetry: the  $U(1)$  charge conservation for electrons. One can imagine what would happen if the  $U(1)$  charge conservation was absent, for instance, if a small electronic pairing was introduced via proximity effect. Because the topological order is robust towards arbitrary perturbation, the threefold ground-state degeneracy and the anyonic statistics of quasiparticles would still be present.

Is the  $U(1)$  global symmetry unimportant for the FQHL physics then? Obviously, this is not the case. In fact, this  $U(1)$  symmetry allows one to find two striking experimental signatures of Laughlin's state: the quantized Hall conductance  $\sigma_{xy} = e^2/3h$  and the  $e^* = e/3$  fractional charge carried by quasiparticles. The second signature is very interesting: The quasiparticles of a topologically ordered phase can carry a fraction of the quantum number of the fundamental degrees of freedom (electrons here) in the quantum system. Such phenomena are often referred to as “symmetry fractionalization.” These phenomena only occur when the system has topological order. The  $e^* = e/3$  charge of quasiparticles is a remarkable demonstration of how the global symmetry can “act” on the topological order in a nontrivial fashion.<sup>30–32</sup>

Another collection of fascinating quantum phases is the quantum spin liquid (QSL). Quantum spin liquids are often

defined to be featureless Mott insulator phases, namely phases that respect full lattice symmetry as well as the  $SU(2)$  spin rotational symmetry, with a half-integer spin per unit cell. Based on the Hastings' generalization<sup>33</sup> of Lieb-Schultz-Mattis theorem<sup>34</sup> in higher dimensions, we know that gapped QSLs in two and higher spatial dimensions must host nontrivial ground-state degeneracies on torus. However, because there is no symmetry-breaking-induced ground-state degeneracy, this indicates that the gapped QSLs are topologically ordered.

How can one classify/understand QSL phases? For instance, recent numerical simulations<sup>35</sup> point out that the spin- $\frac{1}{2}$  Heisenberg model on a Kagome lattice hosts a gapped QSL phase. It is then an important issue to understand the nature of this QSL phase. As a matter of fact, numerical evidence for topological order described by a  $Z_2$  gauge theory has been found.<sup>36,37</sup> Is this topological order enough to determine the nature of this QSL phase? The answer is negative. It turns out that there are more than one QSL phase on the Kagome lattice even for a given  $Z_2$  topological order.<sup>38–42</sup> Their distinctions are protected by the global symmetries. Roughly speaking, the way that the global symmetries act on the topological order is different for different phases. These phenomena have been called “symmetry enriched topological phases” or “symmetry enriched topological order.”<sup>43–46</sup> When the global symmetries are absent, all these phases are no longer distinguishable and are adiabatically connected to one another. However, when the global symmetries are present, one necessarily encounters phase transitions while going from one phase to another. Therefore, for the Kagome lattice gapped spin liquid example, it remains an unresolved issue to understand which among all the symmetry enriched topological phases is the one found in the numerical simulations.

The above physical examples motivate us to consider the following questions. How are symmetry enriched topological (SET) phases generally classified? Or, how can one classify different ways in which the global symmetry “acts” on the topological order? What are the experimental/numerical signatures of different SET phases? The last question is quite urgent for the above Kagome QSL example: Although there are nice numerical methods (e.g., the topological entanglement entropy<sup>47,48</sup>) to detect the  $Z_2$  topological order,<sup>37,49–51</sup> due to the lack of theoretical understanding it is still unknown how to numerically distinguish different SET phases.

This paper attempts to address these questions to a certain level. We consider on-site global symmetries only; namely, the global symmetry transformation is a direct product of unitary transformations, and each transformation only acts in the local Hilbert space. In addition, we focus on bosonic systems with finite unitary symmetry groups  $SG$  and topological orders that can be described by finite gauge groups  $GG$ . Generalizations of these conditions are discussed at the end of the paper. Under these assumptions, we propose that gapped bosonic quantum phases with  $SG$  and  $GG$  are classified by group cohomology  $H^3(SG \times GG, U(1))$  in  $2 + 1$  dimensions, and generally  $H^{d+1}(SG \times GG, U(1))$  in  $d + 1$  dimensions ( $d \geq 2$ ). Here “ $\times$ ” is the direct product (or the cross product) of two groups, and we explain the notion of group cohomology shortly.

Let us consider some special limits of our classification. When the system does not have topological order,  $GG = Z_1$ , our classification becomes  $H^{d+1}(SG, U(1))$ . This, in fact,

goes back to the group cohomology classification of SPT phases.<sup>20</sup> When the system does not have global symmetry,  $SG = Z_1$ , our classification becomes  $H^{d+1}(GG, U(1))$ . In  $2 + 1$  dimensions, this coincides with the Dijkgraaf-Witten classification<sup>52</sup> of topological quantum field theories with discrete gauge groups.

When both the  $SG$  and the  $GG$  are nontrivial, we show that the indices of the classification  $H^{d+1}(SG \times GG, U(1))$  can be expanded as

$$\begin{aligned} H^{d+1}(SG \times GG, U(1)) \\ = H^{d+1}(SG, U(1)) \times H^{d+1}(GG, U(1)) \times SET(SG, GG), \end{aligned} \quad (1)$$

where  $SET(SG, GG)$  is introduced later.  $SET(SG, GG)$  describes the nontrivial interplay between the topological order and the global symmetry and classifies the SET phases.

Some detectable signatures of SET phases, for example, the symmetry protected degeneracy of excited states, are studied in this paper. We leave the general numerical/experimental signatures of SET phases as a subject for future investigation. Nevertheless, we provide exactly solvable local bosonic models for every phase in our classification, in which the topological order is emergent. These models would be useful tools to further study the properties of these phases, including detectable signatures.

The plan of this paper is as follows. In Sec. II, we provide the mathematical background of our classification. We review a previously known partial classification of SET phases, the projective symmetry group (PSG), and comment on the general notion of “symmetry fractionalization.” In particular, we show that our classification includes the mathematical structure underlying the PSG classification in  $2 + 1$  dimensions and goes beyond it. Namely, our classification contains phases that are *not* described by the PSG. In  $3 + 1$  dimensions, our classification becomes very different from the PSG classification and we explain the reason in Sec. VI. In Sec. III, we focus on  $2 + 1$  dimensions and present the geometric interpretation of group cohomology, leading to a class of exactly solvable models. Each model corresponds to a phase in our classification. Generalizations to higher dimensions are briefly discussed. Staying in  $2 + 1$  dimensions, in Sec. IV we study the elementary excitations of these models, namely gauge fluxes and charges, by introducing stringlike operators. In Sec. V, we will solve these models in  $2 + 1$  dimensions for some illuminating examples. One particularly important case is the simplest example that is *not* described by the PSG classification nor “symmetry fractionalization.” In that example the global symmetry transformation interchanges the quasiparticle species. Detectable signatures of these examples will be studied. In Sec. VI we consider generalizations of our study, comment on relations with previous work, and conclude.

## II. THE CLASSIFICATION

### A. Mathematical preparation

#### 1. Definition of the cohomology group

We begin with a brief introduction to group cohomology. A detailed introduction can be found in Ref. 20; in this

paper, we do not present the most general definition of group cohomology.

For a finite group  $G$  and an Abelian group  $M$  ( $M$  does not need to be finite or discrete) one can consider an arbitrary function that maps  $n$  elements of  $G$  to an element in  $M$ ;  $\omega : G^n \rightarrow M$  or equivalently  $\omega(g_1, g_2, \dots, g_n) \in M$ ,  $\forall g_1, g_2, \dots, g_n \in G$ . Such a group function is called an  $n$ -cochain. The set of all  $n$ -cochains, which is denoted as  $C^n(G, M)$ , forms an Abelian group in the usual sense:  $(\omega_1 \cdot \omega_2)(g_1, g_2, \dots, g_n) = \omega_1(g_1, g_2, \dots, g_n) \cdot \omega_2(g_1, g_2, \dots, g_n)$ , in which the identity  $n$ -cochain is a group function whose value is always the identity in  $M$ .

One can define a mapping  $\delta$  from  $C^n(G, M)$  to  $C^{n+1}(G, M)$ :  $\forall \omega \in C^n(G, M)$  define  $\delta\omega \in C^{n+1}(G, M)$  as

$$\begin{aligned} \delta\omega(g_1, \dots, g_{n+1}) &= \omega(g_2, \dots, g_{n+1}) \cdot \omega^{(-1)^{n+1}}(g_1, \dots, g_n) \\ &\times \prod_{i=1}^n \omega^{(-1)^i}(g_1, \dots, g_{i-1}, g_i \cdot g_{i+1}, g_{i+2}, \dots, g_{n+1}). \end{aligned} \tag{2}$$

It is easy to show that the mapping  $\delta$  is nilpotent:  $\delta^2\omega = 1$  [here 1 denotes the identity  $(n + 2)$ -cochain]. In addition, for two  $n$ -cochains  $\omega_1, \omega_2$ , obviously  $\delta$  satisfies  $\delta(\omega_1 \cdot \omega_2) = (\delta\omega_1) \cdot (\delta\omega_2)$ .

An  $n$ -cochain  $\omega(g_1, \dots, g_n)$  is called an  $n$ -cocycle if and only if it satisfies the condition  $\delta\omega = 1$ , where 1 is the identity element in  $C^{n+1}(G, M)$ . When this condition is satisfied, we also say that  $\omega(g_1, \dots, g_n)$  is an  $n$ -cocycle of group  $G$  with coefficients in  $M$ . The set of all  $n$ -cocycles, denoted by  $Z^n(G, M)$ , forms a subgroup of  $C^n(G, M)$ .

Not all different cocycles are inequivalent. Below we define an equivalence relation in  $Z^n(G, M)$ . Because  $\delta$  is nilpotent, for any  $(n-1)$ -cochain  $c(g_1, \dots, g_{n-1})$ , we can find the  $n$ -cocycle  $\delta c$ . If an  $n$ -cocycle  $b$  can be represented as  $b = \delta c$ , for some  $c \in C^{n-1}(G, M)$ ,  $b$  is called an  $n$ -coboundary. The set of all  $n$ -coboundaries, denoted by  $B^n(G, M)$ , forms a subgroup of  $Z^n(G, M)$ . Two  $n$ -cocycles  $\omega_1, \omega_2$  are equivalent (denoted by  $\omega_1 \sim \omega_2$ ) if and only if they differ by an  $n$ -coboundary:  $\omega_1 = \omega_2 \cdot b$ , where  $b \in B^n(G, M)$ .

The  $n$ th cohomology group of group  $G$  with coefficients in  $M$ ,  $H^n(G, M)$ , is formed by the equivalence classes in  $Z^n(G, M)$ . More precisely,  $H^n(G, M) = Z^n(G, M)/B^n(G, M)$ .

In this paper we make a lot of use of 3-cocycles  $\omega$ . We always choose them to be in ‘‘canonical’’ form, which means that  $\omega(g_1, g_2, g_3) = 1$  if any of  $g_1, g_2, g_3$  is equal to  $\mathbb{1}$  (the identity element of group  $G$ ). For any of the inequivalent cocycles mentioned above, it is always possible to choose a gauge such that  $\omega$  becomes canonical.<sup>20</sup> Specifically, the explicit elementary cocycles that we use in studying examples of our models in Sec. V are canonical.

So far the notions of cocycle and cohomology group are quite formal. However, it turns out that they have clear geometric/topological meanings, which we describe in Sec. III.

### 2. Examples

*$H^1(G, U(1))$  and one-dimensional representations of groups.* Let us consider the first cohomology group of a finite group  $G$  with coefficients in  $U(1)$ :  $H^1(G, U(1))$ . In this case,

the cocycle condition becomes

$$\omega(g_1) \cdot \omega(g_2)/\omega(g_1 \cdot g_2) = 1. \tag{3}$$

This means the 1-cocycle  $\omega(g)$  is a one-dimensional unitary representation of the group  $G$ . Clearly, different 1-cocycles are different representations. A 0-cochain is defined to be a constant  $c_0 \in U(1)$ . Consequently, a 1-cocycle is a 1-coboundary if and only if it is identity:  $\omega(g) = c_0/c_0 = 1$ . We conclude that the  $H^1(G, U(1))$  is formed by inequivalent one-dimensional unitary representations of  $G$ .

For instance,

$$H^1(Z_n, U(1)) = Z_n, \quad H^1(Z_n^k, U(1)) = Z_n^k. \tag{4}$$

More generally, for any finite Abelian group  $G$ , due to a fundamental theorem, we know that  $G$  can be decomposed as  $G = Z_{n_1}^{k_1} \times Z_{n_2}^{k_2} \times \dots \times Z_{n_q}^{k_q}$ . Because we know the one-dimensional representations of all the components, clearly,

$$H^1(G, U(1)) = G, \quad \forall \text{ finite Abelian } G. \tag{5}$$

*$H^1(G, Z)$  and finite groups.* Following the above discussion,  $H^1(G, Z)$  is formed by the group of all group homomorphisms from  $G$  to  $Z$ . It is straightforward to show that the only group homomorphism between a finite  $G$  and  $Z$  is the trivial one.

*$H^2(G, U(1))$  and projective representations of groups.* The condition for 2-cocycles is

$$\omega(g_1, g_2) \cdot \omega(g_1 \cdot g_2, g_3) = \omega(g_2, g_3) \cdot \omega(g_1, g_2 \cdot g_3). \tag{6}$$

In fact, the 2-cocycle is related to the so-called projective representations of groups. In usual unitary group representations, each group element  $g$  in  $G$  is represented by a unitary matrix  $D(g)$ , which satisfies  $D(g_1) \cdot D(g_2) = D(g_1 \cdot g_2)$ . However, for projective representations, this relation can be modified by a phase factor  $\omega(g_1, g_2) \in U(1)$ :  $D(g_1) \cdot D(g_2) = \omega(g_1, g_2)D(g_1 \cdot g_2)$ . The phase factor  $\omega(g_1, g_2)$ , which is a function of  $g_1, g_2$ , is called a factor system. A factor system cannot be arbitrary. In order to satisfy the associativity condition,  $[D(g_1) \cdot D(g_2)] \cdot D(g_3) = D(g_1) \cdot [D(g_2) \cdot D(g_3)]$ , the factor system must satisfy Eq. (6), the same condition as for 2-cocycles.

What is a 2-coboundary? A 2-coboundary  $\omega(g_1, g_2)$  can be written as  $\omega(g_1, g_2) = c(g_1) \cdot c(g_2)/c(g_1 \cdot g_2)$  for a certain 1-cochain  $c(g)$ . If two 2-cocycles,  $\omega_1, \omega_2$ , differ by a 2-coboundary,

$$\omega_1(g_1, g_2) = \omega_2(g_1, g_2) \cdot \frac{c(g_1) \cdot c(g_2)}{c(g_1 \cdot g_2)}, \tag{7}$$

it is obvious that they correspond to equivalent projective representations, because one can absorb the 1-cochain into  $D(g)$  by redefining  $\tilde{D}(g) = c(g) \cdot D(g)$ , after which the two factor systems becomes the same (this is actually the definition of equivalent projective representations). We conclude that  $H^2(G, U(1))$  classifies all inequivalent factor systems of projective representations.

The calculation of  $H^2(G, U(1))$  is nontrivial. We list some useful results:

$$H^2(Z_n, U(1)) = Z_1, \quad H^2(Z_n^k, U(1)) = Z_n^{k(k-1)/2}, \tag{8}$$

$$H^2(Z_n \times Z_m, U(1)) = Z_{\text{gcd}(n,m)},$$

where  $Z_1$  is the trivial group.

$H^3(G, U(1))$ . The 3-cocycle condition is

$$\begin{aligned} &\omega(g_1, g_2, g_3) \cdot \omega(g_2, g_3, g_4) \cdot \omega(g_1, g_2 \cdot g_3, g_4) \\ &= \omega(g_1 \cdot g_2, g_3, g_4) \cdot \omega(g_1, g_2, g_3 \cdot g_4), \end{aligned} \quad (9)$$

and a 3-cocycle  $\omega$  is a 3-coboundary if and only if it can be represented as

$$\omega(g_1, g_2, g_3) = \frac{c(g_2, g_3) \cdot c(g_1, g_2 \cdot g_3)}{c(g_1, g_2) \cdot c(g_1 \cdot g_2, g_3)}. \quad (10)$$

These equations may look strange. However, after we introduce a geometric interpretation in Sec. III, their meanings become clear.

We list some useful results for  $H^3(G, U(1))$ :

$$\begin{aligned} H^3(Z_n, U(1)) &= Z_n, \\ H^3(Z_n^k, U(1)) &= Z_n^{k+k(k-1)/2+k(k-1)(k-2)/3!}. \end{aligned} \quad (11)$$

For instance,  $H^3(Z_2^2, U(1)) = Z_2^3$  and  $H^3(Z_2^3, U(1)) = Z_2^7$ .

### 3. Some useful theorems

First, it is known that for any finite group  $G$ , its every  $n$ th cohomology group with  $n > 0$  is a finite Abelian group. Below we list a couple of theorems on group cohomology that are used in the following.

*Universal coefficients theorem.* This theorem relates cohomology groups with different coefficients:

$$H^n(G, \mathbf{B}) = [H^n(G, Z) \otimes \mathbf{B}] \times \text{Tor}(H^{n+1}(G, Z), \mathbf{B}). \quad (12)$$

This formula allows one to compute cohomology groups with coefficients in some Abelian group  $\mathbf{B}$  by using the cohomology groups with coefficients in the group of integers  $Z$ .

Here “ $\times$ ” is the usual direct product of groups, and we need to define the two new operations: “ $\otimes$ ” and “Tor”. “ $\otimes$ ” stands for the “symmetric tensor product” (over  $Z$ ) between two Abelian groups, while “Tor” stands for the “torsion product.”

Instead of explaining the rigorous mathematical definitions of these products, we simply list some useful results.  $A \otimes B$  always equals  $B \otimes A$  (up to isomorphism), and

$$\begin{aligned} Z_n \otimes Z_m &= Z_{\text{gcd}(n,m)}, \quad Z_n \otimes Z = Z_n, \\ Z_n \otimes U(1) &= Z_1, \quad Z \otimes U(1) = U(1), \\ Z \otimes Z &= Z, \quad (A \times B) \otimes C = (A \otimes C) \times (B \otimes C). \end{aligned} \quad (13)$$

The last relation means that  $\otimes$  is distributive.

Concerning the torsion product, one also has  $\text{Tor}(A, B) = \text{Tor}(B, A)$ . In addition,

$$\begin{aligned} \text{Tor}(Z_n, Z_m) &= Z_{\text{gcd}(n,m)}, \\ \text{Tor}(Z_n, U(1)) &= Z_n, \\ \text{Tor}(A, Z) &= Z_1, \quad \forall A, \\ \text{Tor}(A \times B, C) &= \text{Tor}(A, C) \times \text{Tor}(B, C). \end{aligned} \quad (14)$$

The torsion product is also distributive (the last relation above).

Using the universal coefficients theorem, one can compute the cohomology groups with coefficients in  $Z$  from those with coefficients in  $U(1)$ , and vice versa:

$$\begin{aligned} H^n(G, U(1)) &= [H^n(G, Z) \otimes U(1)] \times \text{Tor}(H^{n+1}(G, Z), U(1)) \\ &= H^{n+1}(G, Z), \quad \text{for } n > 0, \end{aligned} \quad (15)$$

where we used the fact that  $H^n(G, Z)$  is a finite Abelian group for  $n > 0$  so that  $[H^n(G, Z) \otimes U(1)] = Z_1$ . Note that the above equation is invalid if  $n = 0$ . At this moment, let us define the 0th cohomology group. In this paper,  $H^0(G, M) = M$ . Therefore,  $[H^0(G, Z) \otimes U(1)] = U(1) \neq Z_1$ .

Using Eqs. (15) and (5), we have

$$H^2(G, Z) = G, \quad \forall \text{ finite Abelian } G. \quad (16)$$

*The Künneth formula.* This theorem allows one to compute the cohomology group of a direct product of groups, using the cohomology groups of its components:

$$\begin{aligned} H^n(A \times B, Z) &= \prod_{i=0}^n [H^i(A, Z) \otimes H^{n-i}(B, Z)] \\ &\quad \times \prod_{i=0}^{n+1} \text{Tor}(H^i(A, Z), H^{n+1-i}(B, Z)), \end{aligned} \quad (17)$$

where “ $\prod$ ” is the usual direct product. For example, this formula and the basic results

$$H^p(Z_n, Z) = \begin{cases} Z_n & \text{if } p \text{ is even,} \\ 0 & \text{if } p \text{ is odd,} \\ Z & \text{if } p = 0, \end{cases} \quad (18)$$

together with Eq. (15), allow one to obtain the results for  $H^p(Z_n^k, U(1))$  listed previously.

### B. The notion of symmetry fractionalization and the projective symmetry group

The main goal of this paper is to address the nontrivial interplay between global symmetry and topological order. What is already known about that interplay? One phenomenon famously connected to such an interplay is the so-called “symmetry fractionalization.”

Topologically ordered phases feature anyonic quasiparticle excitations in the bulk. In fact, in some sense these quasiparticles are nonlocal, because one cannot create a single quasiparticle excitation in a system with periodic boundary conditions (PBCs). One must at least create a pair: a quasiparticle and its anti-quasiparticle. Therefore, a single anyonic quasiparticle state is not in the excitation spectrum of a system with PBC.

The fact that a single anyonic quasiparticle excitation is not a physical excitation in a system with PBC has an important physical consequence.<sup>53</sup> When the system has a certain global symmetry group  $SG$ , based on quantum mechanics, we know that all excited states of the quantum system can be labeled by irreducible representations (irreps) of  $SG$ . The irreps characterize how the ground state and excited states transform under the global symmetry. Then it is natural to imagine that each anyonic quasiparticle also has to transform as a certain irrep of  $SG$ . However, this does not need to be true, exactly because a single quasiparticle is not a physical excited state.

Let us consider a famous example, the  $\nu = 1/3$  Laughlin state. There the physical system has a  $U(1)$  charge conservation symmetry, and therefore any physical state should be an irrep of this  $U(1)$ :  $|\psi\rangle \rightarrow e^{im\theta}|\psi\rangle$ , for  $\forall e^{i\theta} \in U(1)$ . Here the integer  $m \in Z$  is nothing but the total electric charge of the state. However, we were also told that the anyonic quasiparticle

carries  $1/3$ , a noninteger, electric charge. A fractional charge is *not* an irrep of the global symmetry.

Clearly, the fractional charge of an anyonic quasiparticle can be realized exactly because the single anyonic quasiparticle is not a physical state. Only when there are three (generally multiple of three) quasiparticles in the bulk can it be a physical state, which carries one more electric charge compared to the ground state. This phenomenon is called symmetry fractionalization.

In this example, we can ask a further question: Why do the quasiparticles have to carry  $1/3$ , not  $1/5$ , or some other fraction of electric charge? Or, what is the guiding principle that dictates this fractional charge?

One obvious guiding principle is the fusion rule. We know that three quasiparticles become an electron after fusion, which must carry electric charge one. Consequently, each quasiparticle must carry  $1/3$  charge. In fact, this point of view is conceptually very general. For example, one may even be able to consider topologically ordered phases with non-Abelian quasiparticles. However, the mathematical framework behind this point of view, for the most general topologically ordered phases, is technically highly nontrivial<sup>54</sup> and is beyond the scope of this paper.

In this paper, we choose a different point of view, which involves a simpler mathematical framework: projective representations of symmetry group. The trade-off is that we can only use this point of view to understand symmetry fractionalization in certain subclasses of topologically ordered phases.<sup>55</sup> However, this is enough for the purpose of this paper.

The point of view that we choose is the following. Because only multiples of three quasiparticles correspond to physical states, we can define a so-called invariant gauge group (IGG):  $IGG = Z_3 = \{1, e^{i2\pi/3}, e^{i4\pi/3}\}$ . We can multiply each quasiparticle in the system by a fixed element in IGG. Clearly, the total phase becomes unity and the physical wave function is not modified.

This IGG tells us that when we implement the global  $U(1)$  transformation on each quasiparticle, it is perfectly fine to have a phase ambiguity, if and only if (iff) this phase ambiguity is an element in  $IGG$ , because this ambiguity does not modify the physical state at all. Therefore, a single quasiparticle does not have to form an irrep of  $SG$ , but it can form a so-called projective representation of  $SG$  with coefficients in  $IGG$ . Formally, this means that a single quasiparticle can transform under the global  $U(1)$  as  $\psi_{qp} \rightarrow D(e^{i\theta})\psi_{qp}$ ,  $\forall e^{i\theta} \in U(1)$ , where  $D(e^{i\theta})$  only needs to be a projective representation:

$$D(e^{i\theta_1}) \cdot D(e^{i\theta_2}) = \omega(e^{i\theta_1}, e^{i\theta_2})D(e^{i(\theta_1+\theta_2)}), \quad (19)$$

where  $\omega(e^{i\theta_1}, e^{i\theta_2}) \in IGG$  (this is why we say that the projective representation has coefficients in  $IGG$ ). In addition, as we learned in Sec. II A2, the associativity condition is satisfied iff  $\omega(e^{i\theta_1}, e^{i\theta_2}) \in H^2(U(1), IGG)$ , a 2-cocycle of  $U(1)$  group with coefficients in  $IGG$ .

In fact, the  $1/3$  electric charge (in general,  $n/3$  fractional charge with  $n$  being an integer) is exactly a projective representation of  $U(1)$  with coefficients in  $IGG$ . One can check it explicitly: Let us define the transformation law of a single quasiparticle under  $U(1)$  as  $D(e^{i\theta}) = e^{i\theta/3}$ ,  $\forall \theta \in [0, 2\pi)$ . Clearly,  $\omega(e^{i\theta_1}, e^{i\theta_2}) = e^{i2\pi/3}$ , iff  $\theta_1 + \theta_2 \geq 2\pi$ ,  $\forall \theta_{1,2} \in [0, 2\pi)$ , and

$\omega(e^{i\theta_1}, e^{i\theta_2}) = 1$  otherwise. This  $\omega(e^{i\theta_1}, e^{i\theta_2})$  is a 2-cocycle  $\in H^2(U(1), IGG)$ , because the associativity condition is obviously satisfied by  $D(e^{i\theta})$ .

In this example, we learned that a quasiparticle of a topologically ordered phase can transform under the global symmetry group  $SG$  as a projective representation of  $SG$  with coefficients in a certain Abelian group  $IGG$ . This point of view is also quite general and is enough to characterize symmetry fractionalization in this paper. Actually, we use this point of view to classify symmetry fractionalization. First, we comment on our choice of notation.

In this paper, ‘‘symmetry fractionalization’’ is a phrase reserved to characterize how the global symmetry is implemented *locally* on a single quasiparticle. Here ‘‘locally’’ is the key word. It basically means that when we claim symmetry fractionalization, we already made a basic assumption: that the global symmetry transformations can indeed be implemented by local transformations of each quasiparticle.

*The basic assumption of symmetry fractionalization.* Consider an excited state of a topologically ordered phase with a global symmetry group  $SG$ , having  $n$ -quasiparticles (which do not have to be of the same type) spatially located at positions  $\mathbf{r}_1, \mathbf{r}_2, \dots, \mathbf{r}_n$ , far apart from one another. Let us denote this state by  $|\psi(\mathbf{r}_1, \mathbf{r}_2, \dots, \mathbf{r}_n)\rangle$ . For any symmetry transformation  $U(g)$  by a group element  $g \in SG$ , clearly  $U(g)$  will generally transform this state into another state:  $U(g) : |\psi(\mathbf{r}_1, \mathbf{r}_2, \dots, \mathbf{r}_n)\rangle \rightarrow |\tilde{\psi}(\mathbf{r}_1, \mathbf{r}_2, \dots, \mathbf{r}_n)\rangle$ . The basic assumption of symmetry fractionalization is that there exist local operators  $U_1(g), U_2(g), \dots, U_n(g)$ , such that  $U_i(g)$  is a local operator acting only in a finite region around the spatial position  $\mathbf{r}_i$ , and does not touch the other quasiparticles; in addition,  $U_1(g), U_2(g), \dots, U_n(g)$  satisfy

$$U_1(g) \cdot U_2(g) \cdots U_n(g) |\psi(\mathbf{r}_1, \mathbf{r}_2, \dots, \mathbf{r}_n)\rangle = U(g) |\psi(\mathbf{r}_1, \mathbf{r}_2, \dots, \mathbf{r}_n)\rangle = |\tilde{\psi}(\mathbf{r}_1, \mathbf{r}_2, \dots, \mathbf{r}_n)\rangle \quad (20)$$

Pictorially, this assumption is shown in Fig. 1.

Wen<sup>56</sup> first attempted to classify symmetry fractionalization while investigating the parton mean-field states of QSLs in the presence of global symmetries such as lattice space group symmetries, time-reversal symmetry, and spin-rotation

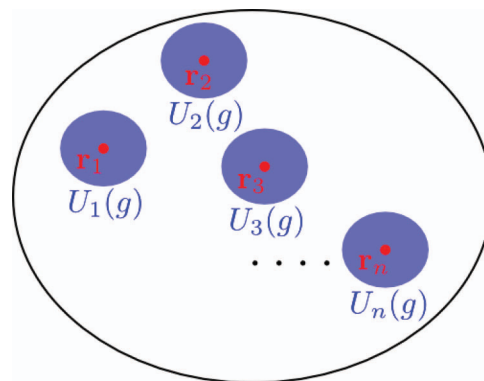


FIG. 1. (Color online) Illustration of the basic assumption of symmetry fractionalization Eq. (20): Under a symmetry transformation  $U(g)$  with  $\forall g \in SG$ , an excited state is transformed by the product of local transformation operators  $U_i(g)$ , with each operator only acting on one quasiparticle locally.

symmetry. In Ref. 56, Wen introduced the notion of PSG, a very useful tool to classify parton states, as well as the low-energy gauge fluctuations, in the presence of these global symmetries. We do not provide a detailed review of the PSG classification here; however, we introduce the core mathematical structure underlying the PSG and comment on the connection between PSG and the current work, in Sec. II C. Also, a brief introduction to the parton construction and PSG can be found in Appendix A.

One way to understand PSG is via the low-energy effective theory of a state with topological order. Let us consider the following situation: There is a quantum state whose topological order is described by a gauge group  $GG$ . Therefore, there are gauge charge excitations of the gauge group  $GG$  in the system, which are anyonic quasiparticles. In order to write an effective theory in terms of these gauge charge quasiparticles, it is crucial to understand how they transform under the global symmetry  $SG$ . Similarly to the usual Ginzburg-Landau theory, any local term that is allowed by global symmetry will appear in the effective theory. Naively, one may expect that the gauge charges must form representations of the symmetry group  $SG$ .

However, Wen pointed out<sup>56</sup> that these gauge charges do not have to form representations of the  $SG$ . Instead, gauge charges transform under a larger group: the  $PSG$ . The relation between  $PSG$ ,  $SG$ , and  $GG$  is given by

$$PSG/GG = SG. \quad (21)$$

Mathematically,  $PSG$  is a group extension of  $SG$  by the group  $GG$ . From here to the end of this section, we assume for simplicity that  $GG$  is a finite Abelian group. In this case,  $PSG$  can be shown to be the central extension (i.e.,  $GG$  is in the center of  $PSG$ ) of  $SG$  by  $GG$  (see Appendix A). The classification of how gauge charge quasiparticles transform under the  $SG$  becomes the classification of all inequivalent central extensions of the group. There is a nice mathematical theorem (see, for example, Ref. 57) stating that all inequivalent central extensions of the group  $SG$  by  $GG$  are classified by  $H^2(SG, GG)$ .

The mathematical structure  $H^2(SG, GG)$  underlying the PSG classification, which has been independently observed by several people,<sup>58</sup> is somewhat mysterious at this moment. However, in fact, its physical meaning can be easily understood. To proceed, again for simplicity, let us assume  $GG$  has the form  $GG = Z_n \times Z_m$ , and one can easily generalize the following discussion to any finite Abelian gauge group. In this case, in order to understand the symmetry transformations of the gauge charges, we only need to consider two fundamental gauge charge excitations:  $\psi_1$  and  $\psi_2$ , which carry gauge charge  $(1, 0)$  and  $(0, 1)$ , respectively. [Note that we adopt the notation  $(a, b)$  to label gauge charge here,  $0 \leq a < n, 0 \leq b < m$ .] This is sufficient because one can build any gauge charge quasiparticle by fusing  $\psi_1$  and  $\psi_2$ .

What are the most general possible ways in which  $\psi_1$  and  $\psi_2$  can transform under  $SG$ ? This is a big question and we attempt to provide an answer later in this paper. In this section, however, let us consider a smaller question: Under the assumption of symmetry fractionalization, what are the most general possible ways in which  $\psi_1$  and  $\psi_2$  transform under  $SG$ ?

Under this assumption, symmetry transformations of quasiparticles are realized by local operators, which cannot change the quasiparticle's species (or more precisely, the superselection sector of a quasiparticle). Therefore, the gauge charge will be invariant under  $SG$  transformation:  $\psi_1$  only transforms into  $\psi_1$  while  $\psi_2$  only transforms into  $\psi_2$ . However, similarly to the situation with fractional charge in fractional quantum Hall states discussed above,  $\psi_1$  (or  $\psi_2$ ) does not need to form a representation of  $SG$ . This is because any excited states with PBC must contain a multiple of  $n$  number of  $Z_n$  gauge charges  $\psi_1$ , and a multiple of  $m$  number of  $Z_m$  gauge charges  $\psi_2$ . Consequently, when we define symmetry transformations of  $\psi_1$  ( $\psi_2$ ), it is perfectly fine to have a phase  $e^{i2\pi \frac{k_1}{n}}$  ( $e^{i2\pi \frac{k_2}{m}}$ ) ambiguity. The state  $\psi_1$  ( $\psi_2$ ) only needs to form a projective representation of  $SG$  with coefficients in the  $Z_n$  ( $Z_m$ ) subgroup of  $U(1)$ , which is exactly classified by  $H^2(SG, Z_n)$  ( $H^2(SG, Z_m)$ ). Finally, because we can pair up any two transformation laws of  $\psi_1$  and  $\psi_2$ , the symmetry transformations of gauge charge quasiparticles with  $GG = Z_n \times Z_m$  are classified by  $H^2(SG, Z_n) \times H^2(SG, Z_m)$ .

Based on the universal coefficients theorem, it is straightforward to show that

$$H^2(SG, Z_n \times Z_m) = H^2(SG, Z_n) \times H^2(SG, Z_m), \quad (22)$$

which is exactly the mathematical structure  $H^2(SG, GG)$  underlying the PSG classification.

Through this example, we learned that  $H^2(SG, GG)$  is a classification of different ways in which anyonic quasiparticles transform under the global symmetry  $SG$ , under the assumption of symmetry fractionalization. Therefore, in this paper we refer to  $H^2(SG, GG)$  as the symmetry fractionalization classification and the classes contained in  $H^2(SG, GG)$  as the symmetry fractionalization classes.

There is one important point that we have not mentioned. We have shown that  $H^2(SG, GG)$  classifies how gauge charges transform under  $SG$ . However, we also know that there are other quasiparticle excitations in the system, such as gauge flux excitations. For instance, in a  $GG = Z_2$  topologically ordered phase, there are three species of nontrivial quasiparticles:  $Z_2$  gauge charge  $e$ ,  $Z_2$  gauge flux  $m$ , and their bound state  $em$ . In a usual topologically ordered state described by an Abelian gauge group  $GG$ , the gauge charges and gauge fluxes are dual to each other in  $2 + 1$  dimensions. For instance, it does not matter if one labels  $e$  or  $m$  as the gauge charge in the usual  $Z_2$  gauge theory.

In fact, the above discussion indicates that  $H^2(SG, GG)$  is only a classification of symmetry fractionalization for  $GG$  gauge charges (or gauge fluxes) only, but not for both gauge charges and gauge fluxes. That means that the full classification of symmetry fractionalization should go beyond  $H^2(SG, GG)$ . However, we see shortly in Sec. II C that our classification of SET phases only contains  $H^2(SG, GG)$ . In addition, in our exactly solvable models, we show that this  $H^2(SG, GG)$  only corresponds to the symmetry fractionalization of the gauge fluxes. It turns out that in these exactly solvable models, the gauge charges always have trivial symmetry fractionalization.<sup>59</sup> We comment on this issue in Sec. II C and Sec. VI.

Now let us consider some simple examples to see the power of  $H^2(SG, GG)$ . For the reason mentioned in the previous paragraph, in the following examples we describe  $H^2(SG, GG)$  as the symmetry fractionalization classification of the *gauge fluxes*.

(1)  $GG = Z_2$  and  $SG = Z_2$ . Let us denote the generator of  $SG$  as  $\sigma$ , and denote by  $D_m(\sigma)$  the transformation of the  $Z_2$  gauge flux  $m$  by  $\sigma$ . Because  $SG = Z_2$ , we have

$$\sigma^2 = 1. \tag{23}$$

The universal coefficients theorem allows us to compute

$$H^2(SG, GG) = H^2(Z_2, Z_2) = Z_2. \tag{24}$$

It means that there are two symmetry fractionalization classes of the  $Z_2$  gauge flux. They correspond to

$$D_m(\sigma)^2 = \pm 1. \tag{25}$$

These two possible signs are exactly the two inequivalent cocycles in  $H^2(Z_2, Z_2)$ . The positive sign is the trivial symmetry fractionalization class, while the negative sign is the nontrivial class.

(2)  $GG = Z_2^2$  and  $SG = Z_2$ . Let us denote the generator of  $SG$  by  $\sigma$ . Now there are two fundamental  $Z_2$  gauge fluxes:  $m_1$ , the  $\pi$  flux in the first  $Z_2$  gauge group, and  $m_2$ , the  $\pi$  flux in the second  $Z_2$  gauge group. Straightforward computation gives

$$H^2(SG, GG) = H^2(Z_2, Z_2^2) = Z_2^2. \tag{26}$$

There are four classes. The corresponding transformations of the  $Z_2$  gauge fluxes  $m_1, m_2$ , denoted by  $D_{m_1}(\sigma), D_{m_2}(\sigma)$ , satisfy

$$D_{m_1}(\sigma)^2 = \pm 1, \quad D_{m_2}(\sigma)^2 = \pm 1. \tag{27}$$

(3)  $GG = Z_2$  and  $SG = Z_2^2$ . Let us denote the two generators of  $SG$  by  $\sigma, \tau$ . Because  $SG = Z_2^2$ , we have

$$\sigma^2 = 1, \quad \tau^2 = 1, \quad \sigma\tau = \tau\sigma. \tag{28}$$

Straightforward computation gives

$$H^2(SG, GG) = H^2(Z_2^2, Z_2) = Z_2^3. \tag{29}$$

There are eight classes. The corresponding transformations of the  $Z_2$  gauge flux  $m$ , denoted by  $D_m(\sigma)$  and  $D_m(\tau)$ , satisfy

$$D_m(\sigma)^2 = \pm 1, \quad D_m(\tau)^2 = \pm 1, \tag{30}$$

$$D_m(\sigma)D_m(\tau) = \pm D_m(\tau)D_m(\sigma).$$

### C. The classification and connection to previous work

Quite some time ago, Dijkgraaf and Witten pointed out that the topological orders in  $2 + 1$  dimensions, described by discrete gauge theories with a gauge group  $GG$  are classified by its third cohomology group:  $H^3(GG, U(1))$ .<sup>52</sup> Different topological orders labeled by  $H^3(GG, U(1))$  can be viewed as different discrete versions of the Chern-Simons terms.<sup>60–62</sup> For example, because  $H^3(Z_2, U(1)) = Z_2$ , there are two distinct topological orders described by a  $Z_2$  gauge group. In the language of the  $K$  matrix, the two topological orders are described by  $K = \begin{pmatrix} 0 & 2 \\ 2 & 0 \end{pmatrix}$  and  $K = \begin{pmatrix} 2 & 0 \\ 0 & -2 \end{pmatrix}$ , respectively. The first one is the usual  $Z_2$  gauge theory while the second one is

the so-called double-semion theory. The quasiparticle anyonic statistics in the two theories are different.

Recently, an original work by Chen *et al.*<sup>20</sup> showed that bosonic SPT phases protected by a global (unitary) on-site symmetry group  $SG$  in  $2 + 1$  dimensions are also classified by  $H^3(SG, U(1))$ . Here different phases labeled by  $H^3(SG, U(1))$  can be viewed as different topological  $\theta$  terms on a discrete space-time. For instance, because  $H^3(Z_2, U(1)) = Z_2$ , there are two distinct Ising paramagnetic (namely disordered) phases (without topological order) in  $2 + 1$  dimensions. One is the usual Ising paramagnet, while the other one is the nontrivial Ising SPT phase which features symmetry protected gapless edge states.

It appears that the mathematical object  $H^3(G, U(1))$  shows up in these two completely different physical contexts, and one may wonder if there is a certain underlying relation between them. A recent beautiful work by Levin and Gu<sup>28</sup> demonstrated such an underlying relation explicitly. It was known that the deconfined phase of a usual  $Z_2$  gauge theory is dual to the usual Ising paramagnetic phase. What was shown in Ref. 28 is that following the same duality, using exactly solvable models, the double-semion gauge theory is dual to the nontrivial SPT phase. It was proposed that such dualities between the Dijkgraaf-Witten theories and the SPT phases are general.<sup>63</sup>

The observation made by Levin and Gu is illuminating and motivated us to consider the cases where both a global on-site symmetry group  $SG$  and a topological order described by a gauge group  $GG$  are present. Let us consider such a gapped quantum phase. On one hand, one can imagine following the route of duality transformation to transform  $SG$  into a gauge group and eventually having a quantum phase with topological order described by the gauge group  $SG \times GG$ . On the other hand, one can follow the backward duality transformation to transform  $GG$  into a global on-site symmetry, which eventually gives a quantum phase with a global on-site symmetry  $SG \times GG$ . If the initial phases are distinct, it is natural to expect that the phases after duality are also distinct, and vice versa.

Therefore, it is reasonable to expect that, in  $2 + 1$  dimensions, bosonic phases with both a global on-site symmetry group  $SG$  and a topological order described by a gauge group  $GG$  are classified by  $H^3(SG \times GG, U(1))$ . We construct exactly solvable models for these phases shortly, and we solve these models in some examples and discuss the measurable differences between different phases.

Intuitively, a classification of phases having both  $SG$  and  $GG$  should at least include  $H^3(SG, U(1))$  and  $H^3(GG, U(1))$ . This is because one can always consider a system where the degrees of freedom which give rise to the topological order and the degrees of freedom on which the symmetry group acts completely decouple from each other. For instance, we can consider a bilayer system in which the global symmetry  $SG$  only acts nontrivially on the first layer, while the topological order described by  $GG$  only lives on the second layer (see Fig. 2). In this case, the possible phases living on the first (second) layer would be classified by  $H^3(SG, U(1))$  ( $H^3(GG, U(1))$ ). Because one can tune these phases separately, a classification of phases with both  $SG$  and  $GG$  should actually at least include the cross product:  $H^3(SG, U(1)) \times H^3(GG, U(1))$ .

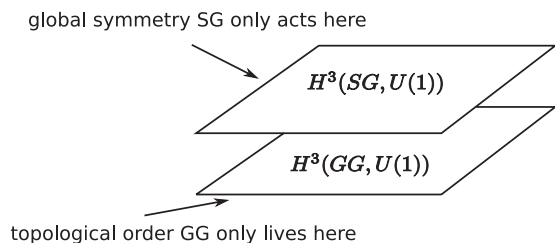


FIG. 2. A bilayer system in which the topological order and the global symmetry decouple.

These indices are labeling the phases with no interplay between the global symmetry and the topological order.

This intuitive argument also indicates that, if a classification contains more phases than  $H^3(SG, U(1)) \times H^3(GG, U(1))$ , the extra phases must have nontrivial interplay between the global symmetry and the topological order.

Using the Künneth formula and the universal coefficients theorem, we can immediately examine whether our classification is consistent with the above physical intuition:

$$\begin{aligned}
 H^3(SG \times GG, U(1)) &= H^4(SG \times GG, Z) \\
 &= H^4(SG, Z) \times H^4(GG, Z) \times SET(SG, GG) \\
 &= H^3(SG, U(1)) \times H^3(GG, U(1)) \times SET(SG, GG). \quad (31)
 \end{aligned}$$

Note that to obtain the first two terms, we have used  $H^0(G, Z) = Z$  and  $K \otimes Z = K$ ,  $\forall$  Abelian finite group  $K$ . Here we define the Abelian group  $SET(SG, GG)$  as all the other terms in the Künneth expansion formula. For reasons that become clear shortly, we further decompose  $SET(SG, GG)$  into two parts:

$$SET(SG, GG) \equiv SFC(SG, GG) \times EXTRA(SG, GG), \quad (32)$$

where

$$\begin{aligned}
 SFC(SG, GG) \equiv [H^2(SG, Z) \otimes H^2(GG, Z)] \\
 \times \text{Tor}(H^3(SG, Z), H^2(GG, Z)), \quad (33)
 \end{aligned}$$

and

$$EXTRA(SG, GG) \equiv \text{Tor}(H^2(SG, Z), H^3(GG, Z)), \quad (34)$$

where we used the fact that  $H^1(G, Z) = Z_1$ ,  $\forall$  finite  $G$ . In Eq. (31), we see that indeed our classification contains  $H^3(SG, U(1)) \times H^3(GG, U(1))$ , which is what one expects. When we choose the indices in  $SET(SG, GG)$  to be trivial, i.e., the identity group element in  $SET(SG, GG)$ , these terms label the phases in which the topological order and the global symmetry are decoupled. Clearly, the indices in  $SET(SG, GG)$  are characterizing the nontrivial interplay between the topological order and global symmetry; namely, global symmetry and topological order together enrich the classification. The notation  $SET(SG, GG)$  follows from “symmetry enriched topological order.”

The potential physical meaning of  $SFC(SG, GG)$  becomes clear if  $GG$  is an Abelian group. In this case we can consider the symmetry fractionalization classes, which are given by  $H^2(SG, GG)$  as discussed in Sec. II B. Using the universal

coefficients theorem,

$$\begin{aligned}
 H^2(SG, GG) &= [H^2(SG, Z) \otimes GG] \times \text{Tor}(H^3(SG, Z), GG) \\
 &= SFC(SG, GG) \text{ if } GG \text{ is Abelian,} \quad (35)
 \end{aligned}$$

where we used the fact that  $H^2(GG, Z) = H^1(GG, U(1)) = GG$ , if  $GG$  is a finite Abelian group. Indeed, in this case,  $SFC(SG, GG)$  has exactly the same mathematical structure as the symmetry fractionalization classification, leading to the notation “SFC.”

When  $GG$  is non-Abelian, the PSG is no longer related to the central extensions of the  $SG$  by  $GG$ , and  $H^2(SG, GG)$  is not even well-defined. In this case, the mathematical structure underlying PSG, for symmetry fractionalization classes, was unknown. However,  $SFC(SG, GG)$  in Eq. (33) is still well-defined. We propose that  $SFC(SG, GG)$  is the correct counterpart of  $H^2(SG, GG)$  when  $GG$  is non-Abelian.

At this moment, the expansion formula Eq. (31) is completely mathematical. It appears that the above discussion is attaching physical meaning to the terms in this formula, such as symmetry fractionalization for  $SFC(SG, GG)$ , without justification. In fact, we do not mathematically prove our physical interpretation of the formula Eq. (31) generally, although we believe it. However, because we have exactly solvable models for every phase in the classification  $H^3(SG \times GG, U(1))$ , we can at least justify our physical interpretation in some examples by solving these models. We show in Sec. V that, in all the examples that we study, our physical interpretation is correct.

As mentioned earlier, a full classification of symmetry fractionalization classes should go beyond  $H^2(SG, GG)$  even when  $GG$  is Abelian, because one should at least consider the symmetry fractionalization classes for both gauge charges and gauge fluxes. However, in the expansion Eq. (31), only  $SFC(SG, GG)$  appears. We show that in the exactly solvable models, this  $SFC(SG, GG)$  is characterizing all the symmetry fractionalization classes for gauge fluxes only. It turns out that gauge charges in these models always have trivial symmetry fractionalization. Intuitively, this means that our classification for the symmetry fractionalization is incomplete. This may be due to the fact that we only consider quantum phases with exactly solvable model realizations, which puts constraints on our classification.

The extra indices  $EXTRA(SG, GG)$  in the expansion Eq. (31) have a completely different mathematical structure than symmetry fractionalization classes, and intuitively this term must be related to the nontrivial interplay between the global symmetry and the topological order, but should not be associated with symmetry fractionalization. Indeed, we show that  $EXTRA(SG, GG)$  is related to the phenomena in which global symmetry transformations interchange the quasiparticle species (or more precisely, the superselection sectors). For instance, in the example mentioned in Sec. II B, in which  $GG = Z_n \times Z_m$ ,  $EXTRA(SG, GG)$  characterizes the phenomena where the global symmetry could transform a  $\psi_1$  gauge flux into a  $\psi_2$  gauge flux under certain conditions. Such a nontrivial interplay between the global symmetry and the topological order is beyond symmetry fractionalization, because it violates the basic assumption of symmetry fractionalization:



It is impossible to change quasiparticle species by operators acting on the quasiparticles only locally.

Before we move to the exactly solvable models, let us present the examples that we solve in Sec. V. We consider three simple cases.

$$(1) \quad SG = Z_2, GG = Z_2:$$

$$H^3(SG \times GG, U(1)) = Z_2^3, \quad (36)$$

and among these,

$$\begin{aligned} H^3(SG, U(1)) = Z_2, \quad H^3(GG, U(1)) = Z_2 \\ SFC(SG, GG) = Z_2, \quad EXTRA(SG, GG) = Z_1. \end{aligned} \quad (37)$$

This means that among  $Z_2^3$  indices, one  $Z_2$  is labeling the two SPT phases, one  $Z_2$  is labeling the two Dijkgraaf-Witten topological orders. The remaining  $Z_2$  is labeling the symmetry fractionalization classes, whose physical meaning is presented in Eq. (25). In this case there is no SET indices beyond the symmetry fractionalization classification.

$$(2) \quad SG = Z_2^2, GG = Z_2:$$

$$H^3(SG \times GG, U(1)) = Z_2^7, \quad (38)$$

and among them,

$$\begin{aligned} H^3(SG, U(1)) = Z_2^3, \quad H^3(GG, U(1)) = Z_2 \\ SFC(SG, GG) = Z_2^3, \quad EXTRA(SG, GG) = Z_1. \end{aligned} \quad (39)$$

This means that among  $Z_2^7$  indices, one  $Z_2^3$  is labeling the eight SPT phases, one  $Z_2$  is labeling the two Dijkgraaf-Witten topological orders. The remaining  $Z_2^3$  is labeling the symmetry fractionalization classes, whose physical meaning is presented in Eq. (30). In this case there is also no SET indices beyond the symmetry fractionalization classification.

$$(3) \quad SG = Z_2, GG = Z_2^2:$$

$$H^3(SG \times GG, U(1)) = Z_2^7, \quad (40)$$

and among them,

$$\begin{aligned} H^3(SG, U(1)) = Z_2, \quad H^3(GG, U(1)) = Z_2^3 \\ SFC(SG, GG) = Z_2^2, \quad EXTRA(SG, GG) = Z_2. \end{aligned} \quad (41)$$

This means that among  $Z_2^7$  indices, one  $Z_2$  is labeling the two SPT phases, one  $Z_2^3$  is labeling the eight Dijkgraaf-Witten topological orders. One  $Z_2^2$  is labeling the symmetry fractionalization classes, whose physical meaning is presented in Eq. (27). Finally, the remaining  $Z_2$  in  $EXTRA(SG, GG)$  labels the phases beyond the symmetry fractionalization. This is the simplest example in which SET phases beyond symmetry fractionalization are realized.

### III. EXACTLY SOLVABLE MODELS

In this section we introduce the exactly solvable models which exhibit all the phases from the general classification introduced above. First we recall the Dijkgraaf-Witten topological invariant and then introduce the general form of our exactly solvable models.

#### A. The geometric interpretation of group cohomology and the Dijkgraaf-Witten topological invariants

##### 1. The geometric interpretation of group cohomology

In Sec. II A we introduced group cohomology, which appears to be a group theoretical concept. However, group cohomology is actually about topology. In this section, we introduce the geometric interpretation of group cohomology, which is the mathematical foundation of our exactly solvable models.

An  $n$ -cocycle  $\omega \in H^n(G, U(1))$  of a group  $G$  allows one to construct a topological invariant for  $n$ -dimensional manifolds. Generally, different elements of  $H^n(G, U(1))$  correspond to different topological invariants of  $n$ -manifolds. Below we illustrate the construction of such topological invariants.

Let us consider a three-dimensional manifold as an example. We know that tetrahedra can be viewed as building blocks for arbitrary 3-manifolds. To begin with, we show that a 3-cocycle  $\omega \in H^3(G, U(1))$  allows one to assign a complex number to a tetrahedron following a simple procedure.

The procedure contains two steps (see Fig. 3). The first step is called *ordering*, in which one chooses an ordering of the four vertices of the tetrahedron. We can represent this ordering by assigning arrows going from lower to higher ordered vertices on the edges of the tetrahedron. For any given face (i.e., a triangle) of the tetrahedron, obviously the three arrows never form an oriented loop.

The second step is called *coloring*, in which one assigns a group element to every edge of the tetrahedron. The coloring must be consistent with certain rules below. Note that an

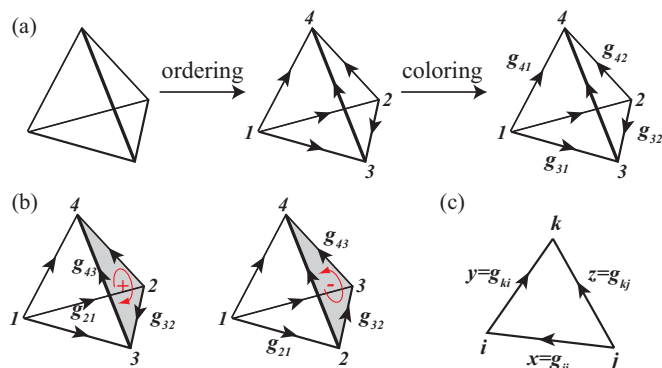


FIG. 3. (Color online) The 3-cocycle  $\omega(h_1, h_2, h_3)$  assigns a  $U(1)$  complex number (i.e., a phase) to a 3-simplex (tetrahedron). (a) Left to center: the “ordering” of tetrahedron’s four vertices; we choose here  $1 \rightarrow 2 \rightarrow 3 \rightarrow 4$ . An edge is oriented from lower to higher vertex, so no triangle forms an oriented loop. (Alternatively, one orients all edges without forming oriented triangle loops, and a consistent underlying vertex ordering is guaranteed.) Center to right: “Coloring” assigns group element  $g_{ij}$  to  $j \rightarrow i$  edge, with  $g_{ji} = g_{ij}^{-1}$ . (Four of six elements are shown explicitly.) The shown tetrahedron  $1 \rightarrow 2 \rightarrow 3 \rightarrow 4$  is assigned the phase  $\omega(g_{43}, g_{32}, g_{21})^\epsilon = \omega(g_{43}, g_{32}, g_{21})$ . The exponent  $\epsilon = \pm 1$  is determined by (b) chirality. For tetrahedron  $1 \rightarrow 2 \rightarrow 3 \rightarrow 4$ , looking from vertex 1, (counter-)clockwise loop 234 means  $\epsilon = -1$  (+1), which is realized in the right (left) tetrahedron. (c) The zero-flux rule applies to all tetrahedron faces, i.e., triangles. Generally,  $g_{ki} \cdot g_{ij} \cdot g_{jk} = \mathbb{1}$ , the group identity element. Recall that  $g_{jk} = g_{kj}^{-1}$ . Choosing an ordering and assigning elements to ordered bonds, like shown, leads to the constraint  $z = y \cdot x$ .

edge already has an arrow, or orientation, associated with it. The assigned group element for a given edge should then be understood in the following way: If we assign the group element  $g \in G$  to follow the direction of the arrow, then we automatically assign group element  $g^{-1} \in G$  to the direction opposite to the arrow. Let us denote the group element assigned to the bond connecting vertices  $j$  and  $i$  as  $g_{ij}$ , following the orientation from  $j$  to  $i$ :  $j \rightarrow i$ . We then automatically assign  $g_{ji} = g_{ij}^{-1}$ .

In addition, the three assigned group elements for any given face must satisfy the constraint  $g_{ij} \cdot g_{jk} \cdot g_{ki} = \mathbb{1}$ , where  $\mathbb{1}$  is the identity element in group  $G$  and  $i, j, k$  are the three vertices of the face. We call this constraint the “zero-flux rule” throughout this paper. With this constraint, it is easy to show that among the six group elements for the six edges of the tetrahedron, only three are independent. In particular, let us denote the ordered vertices by  $1, 2, 3, 4$ ; then,  $g_{43}, g_{32}, g_{21}$  completely determine all the other group elements.

Given a 3-cocycle  $\omega(x, y, z) \in H^3(G, U(1))$ , one assigns the complex number  $\omega(g_{43}, g_{32}, g_{21})^\epsilon$  to an ordered and colored tetrahedron. [Sometimes we use the  $\omega^\epsilon(g_{43}, g_{32}, g_{21})$  notation.] Here  $\epsilon = \pm 1$  depending on the chirality of the ordered vertices. One can determine this chirality by the right-hand rule: Imagine looking at the face formed by vertices 2-3-4 from the vertex 1; if the vertices 2-3-4 form a counterclockwise (clockwise) loop, the chirality of the ordering is positive (negative) and  $\epsilon = 1$  ( $\epsilon = -1$ ).

This assignment of  $\omega(g_{43}, g_{32}, g_{21})^\epsilon$  to an ordered and colored tetrahedron allows a simple geometric interpretation of the cocycle condition Eq. (9); see Fig. 4. To see this, consider an ordered and colored tetrahedron and the associated complex number  $\omega(g_{43}, g_{32}, g_{21})^\epsilon$ . One can now add one more vertex  $a$  inside the tetrahedron. With vertex  $a$ , the original tetrahedron can be triangulated into four smaller tetrahedra.

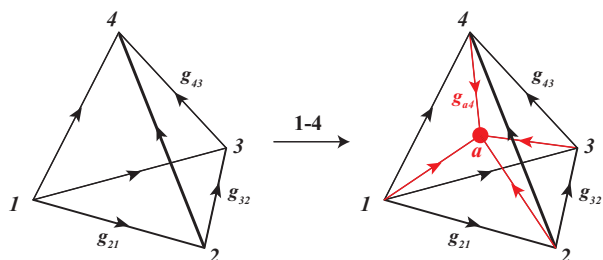


FIG. 4. (Color online) The 1-4 move (three dimensions) changes triangulation but not total product of phases  $\prod_I W(\sigma_I)^{\epsilon_I}$  of 3-simplices  $\sigma_I$ . (Left) The initial tetrahedron is assigned the phase  $W_0 \equiv \omega(g_{43}, g_{32}, g_{21})^{-1}$  (see Fig. 3). (Right) The vertex  $a$  is added, and we choose the ordering such that  $1 \rightarrow 2 \rightarrow 3 \rightarrow 4 \rightarrow a$  [obvious from chosen orientations of new (red) edges]. There are now four smaller tetrahedra, with phases 1, tetrahedron  $1 \rightarrow 2 \rightarrow 4 \rightarrow a$ ,  $W_1 \equiv \omega(g_{a4}, g_{42}, g_{21})$ ; 2, tetrahedron  $2 \rightarrow 3 \rightarrow 4 \rightarrow a$ ,  $W_2 \equiv \omega(g_{a4}, g_{43}, g_{32})$ ; 3, tetrahedron  $1 \rightarrow 3 \rightarrow 4 \rightarrow a$ ,  $W_3 \equiv \omega(g_{a4}, g_{43}, g_{31})^{-1}$ ; 4, tetrahedron  $1 \rightarrow 2 \rightarrow 3 \rightarrow a$ ,  $W_4 \equiv \omega(g_{a3}, g_{32}, g_{21})^{-1}$ . The 3-cocycle condition, Eq. (9), says the total phase does not change by the move:  $W_0 = W_1 W_2 W_3 W_4$ . Note that only one independent new group element is introduced (we marked the  $g_{a4}$ ), and from zero-flux rule  $g_{a3} = g_{a4} \cdot g_{43}$ . Changing our choice of ordering for  $a$  relative to  $1, 2, 3, 4$  would lead to an equivalent 3-cocycle condition.

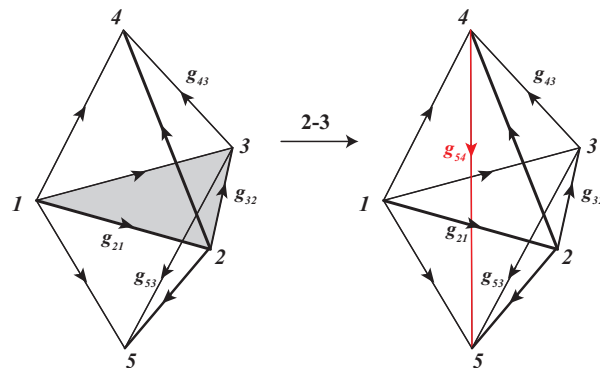


FIG. 5. (Color online) The 2-3 move (three dimensions) changes triangulation but not total product of phases  $\prod_I W(\sigma_I)^{\epsilon_I}$ . (Left) Two initial tetrahedra, 1234 and 1235, are assigned the total phase  $W_0 \equiv \omega(g_{53}, g_{32}, g_{21})\omega(g_{43}, g_{32}, g_{21})^{-1}$  (see Fig. 3). (Right) One edge (red) is added, and we choose the ordering  $4 \rightarrow 5$ . The volume is now divided into three smaller tetrahedra, with phases 1, tetrahedron  $1 \rightarrow 2 \rightarrow 4 \rightarrow 5$ ,  $W_1 \equiv \omega(g_{54}, g_{42}, g_{21})$ ; 2, tetrahedron  $2 \rightarrow 3 \rightarrow 4 \rightarrow 5$ ,  $W_2 \equiv \omega(g_{54}, g_{43}, g_{32})$ ; 3, tetrahedron  $1 \rightarrow 3 \rightarrow 4 \rightarrow 5$ ,  $W_3 \equiv \omega(g_{54}, g_{43}, g_{31})^{-1}$ . The 3-cocycle condition, Eq. (9), says the total phase does not change by the move:  $W_0 = W_1 W_2 W_3$ . Note that the new group element  $g_{54}$  is not independent, e.g.,  $g_{54} = g_{52} \cdot g_{42}^{-1}$ .

One can further continue the ordering and coloring procedure for the four smaller tetrahedra. Since we already have the ordering and coloring for the large tetrahedron, we only need to assign an order to vertex  $a$ , as well as to color the four newly created edges  $1a, 2a, 3a$ , and  $4a$ . Actually, according to the zero-flux rule, it is easy to show that only one of the four new edges is independent. After we complete ordering and coloring the four small tetrahedra, we have four new complex numbers, each of which is associated with a small tetrahedron. It is straightforward to show that, no matter how one performs the complete ordering and coloring procedure, the cocycle condition Eq. (9) dictates that the product of the four new complex numbers exactly equals the original complex number  $\omega(g_{43}, g_{32}, g_{21})^\epsilon$ .

Such a procedure of completing the triangulation and ordering and coloring of tetrahedra after adding a vertex is called a 1-4 move. A specific example of a 1-4 move is shown in Fig. 4.

Similarly, there is a 2-3 move; see Fig. 5. Namely, one can consider two face-sharing tetrahedra, both of which have been ordered and colored. There are then two complex numbers, each of which is associated with a tetrahedron. One can now connect the two vertices that are on opposite sides of the shared face, and the volume enclosed by the original two tetrahedra can be triangulated into three tetrahedra. One can continue the ordering and coloring procedure for the three tetrahedra and obtain three new complex numbers. It is also easy to show that, no matter how one performs the further ordering and coloring procedure, the cocycle condition Eq. (9) dictates that the product of the three new complex numbers equals the product of the two original complex numbers. A specific example of such a 2-3 move is illustrated in Fig. 5.

In this paper we use “canonical” 3-cocycles  $\omega$ , meaning that  $\omega(g_1, g_2, g_3) = 1$  if any of  $g_1, g_2, g_3$  is equal to  $\mathbb{1}$  (the identity element of group  $G$ ). It is always possible to choose a gauge for

$\omega$  such that it becomes canonical.<sup>20</sup> Specifically, the explicit elementary cocycles that we use in studying examples of our models in Sec. V are going to be canonical.

**2. The Dijkgraaf-Witten topological invariants**

The above examples of 1-4 move and 2-3 move suggest that the products of the assigned complex numbers  $\omega(g_{lk}, g_{kj}, g_{ji})^\epsilon$  for a given volume may be related to a certain invariant that is independent of the triangulation, ordering, and coloring procedure. This is indeed true, as stated by two mathematical theorems presented in the following.

Let us first consider a closed 3-manifold  $M$  without a boundary. One can triangulate  $M$  by a finite number of 3-simplices (i.e., tetrahedra) and then order the vertices of this triangulation. Next, one can have a coloring  $\varphi$  of all the edges in the triangulation obeying the zero-flux rule. Note that under a fixed triangulation and ordering of vertices, there can be many different colorings. Let us denote a 3-simplex of the triangulation, together with the ordering of its vertices, by  $\sigma_I$ , where  $I = 1, 2, \dots, S$  labels 3-simplices and  $S$  is the total number of 3-simplices. For a given coloring  $\varphi$ , let us also denote the assigned complex number  $\omega(g_{lk}, g_{kj}, g_{ji})^\epsilon$  for the simplex- $\sigma_I$  as  $W(\sigma_I, \varphi)^{\epsilon(\sigma_I)}$ , and we can further compute the product of all these complex numbers for 3-simplices:  $\prod_{I=1}^S W(\sigma_I, \varphi)^{\epsilon(\sigma_I)}$ . For each given coloring  $\varphi$ , we have one such product.

*Theorem 1.* The sum of such products for all possible colorings, with an appropriate normalization factor, is a topological invariant of the closed manifold  $M$ :<sup>52</sup>

$$Z_M = \frac{1}{|G|^V} \sum_{\substack{\varphi \in \text{all} \\ \text{possible} \\ \text{colorings}}} \prod_{I=1}^S W(\sigma_I, \varphi)^{\epsilon(\sigma_I)}. \quad (42)$$

Here  $|G|$  is the number of elements in group  $G$ , and  $V$  is the number of vertices in the triangulation. Note that without Theorem 1, one would naively expect that  $Z_M$  depends on both the triangulation and the ordering of vertices (while different colorings are already summed over). However, with Theorem 1, we know that  $Z_M$  does not depend on either of them; it only depends on the topology of the manifold  $M$  and the 3-cocycle  $\omega \in H^3(G, U(1))$ . One can further show that equivalent 3-cocycles (i.e., 3-cocycles differing by a 3-coboundary) give exactly the same topological invariant  $Z_M$ ;<sup>52</sup> namely,  $Z_M$  only depends on inequivalent elements in  $H^3(G, U(1))$ .

The topological invariant  $Z_M$  is exactly the partition function of the Dijkgraaf-Witten (DW) topological quantum field theory (TQFT) for discrete gauge group  $G$  in  $2 + 1$  dimensions.<sup>52,64</sup> In order to have a well-defined TQFT, it turns out that one not only needs to define partition functions for closed space-time manifolds, but one also needs to define quantum transition amplitudes for space-time manifolds with boundaries. This is given by the second theorem.

Consider a 3-manifold  $M$  with boundary  $\partial M$ .  $\partial M$  is formed by a collection of closed 2-manifolds. One can triangulate  $\partial M$  by a finite number of 2-simplices (i.e., triangles), order the vertices of the 2-simplices, and then color their edges again following the zero-flux rule (i.e.,  $g_{ij}g_{jk}g_{ki} = \mathbb{1}$  for all

2-simplices). Let us denote the triangulation, ordering, and coloring of the boundary  $\partial M$  by  $\tau$ .

Next, we fix the coloring  $\tau$  and extend it into the bulk of  $M$ . This means that we consider a triangulation of  $M$ , an ordering of its vertices, and a coloring  $\varphi$  such that they become exactly the same as  $\tau$  when limited to the boundary  $\partial M$ . In this case, we also say that the bulk triangulation, ordering, and coloring in  $M$  are compatible with  $\tau$  on  $\partial M$ . For instance, the triangular faces of a tetrahedron can be viewed as the boundary of a three-dimensional ball. Then a 1-4 move can be viewed as a specific extension of the boundary  $\tau$  into the bulk of the ball.

Now let us fix the bulk triangulation and ordering of vertices in  $M$  that is compatible with  $\tau$ . There are still many possible colorings  $\varphi$  in  $M$  that are compatible with  $\tau$ , and they form a set which we denote as  $\text{Col}(M, \tau)$ . As in Theorem 1, with a fixed  $\varphi \in \text{Col}(M, \tau)$  one can compute the product of complex numbers  $\prod_{I=1}^S W(\sigma_I, \varphi)^{\epsilon(\sigma_I)}$  assigned to all the 3-simplices in the bulk of  $M$ . It turns out the sum of all such products satisfies the following theorem.

*Theorem 2.* The complex number  $Z_M(\tau)$  does not depend on the triangulation of  $M$  or the ordering of its vertices, whenever the topology of  $M$  and  $\tau$  on  $\partial M$  are fixed:<sup>52,64</sup>

$$Z_M(\tau) = \frac{1}{|G|^{V + \frac{V_{\partial M}}{2}}} \sum_{\varphi \in \text{Col}(M, \tau)} \prod_{I=1}^S W(\sigma_I, \varphi)^{\epsilon(\sigma_I)}. \quad (43)$$

Here  $V$  is the total number of vertices inside  $M$  (i.e., not including  $\partial M$ ), while  $V_{\partial M}$  is the number of vertices in  $\partial M$ . Obviously,  $Z_M(\tau)$  becomes  $Z_M$  in Eq. (42) when  $M$  does not have a boundary.

To see the physical meaning of  $Z_M(\tau)$ , let us consider a special case:  $M = \mathbf{B} \times [0, 1]$ , where  $\mathbf{B}$  is a certain closed orientable 2-manifold.  $\partial M$  is formed by two disconnected but identical closed 2-manifolds:  $\mathbf{B}_1 \cong \mathbf{B}$  and  $\mathbf{B}_2 \cong \mathbf{B}$ , corresponding to  $0 \in [0, 1]$  and  $1 \in [0, 1]$ , respectively (see Fig. 6).

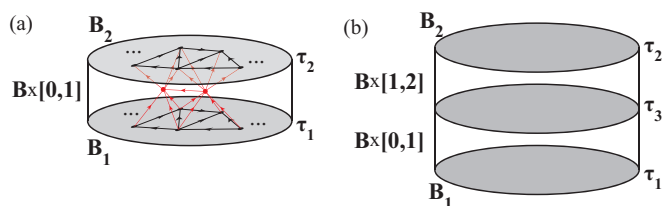


FIG. 6. (Color online) The DW topological invariant  $Z_M$  and TQFT for manifold  $M$  with boundary. (a) Two copies of 2-manifold  $B$ :  $B_1, B_2$ , with colorings  $\tau_1, \tau_2$ , form the boundary of 3-manifold  $M = B \times [0, 1]$ . The triangulation and ordering in  $B_1$  and  $B_2$  are chosen identical, as sketched. The triangulation and ordering in the bulk of  $M$  (example red vertices and edges) does not influence the value of DW invariant  $Z_M(\tau = \tau_1 \cup \tau_2)$ . A coloring  $\tau_i$  of  $B$  represents a quantum state  $|\tau_i\rangle$ , and then  $Z_M(\tau) = \langle \tau_2 | P | \tau_1 \rangle$  is a quantum amplitude of operator  $P$  in the DW TQFT associated with  $B$ . The image of  $P$  is the ground-state manifold of the TQFT. (b) The operator  $P$  is a projector: The quantum amplitude  $\langle \tau_2 | P^2 | \tau_1 \rangle$  is sketched, representing a product of amplitudes of  $P$  from  $\tau_1$  to  $\tau_3$ , and  $\tau_3$  to  $\tau_2$ , with a sum over colorings  $\tau_3$ . This becomes a sum over internal colorings in space  $M = B \times [0, 2]$  with boundary  $B_1 \cup B_2$ . The latter is equal to the amplitude  $\langle \tau_2 | P | \tau_1 \rangle$  from panel (a).

We can then triangulate and order the vertices on  $\mathbf{B}_1$  and  $\mathbf{B}_2$  in the same fashion.

For each edge  $ij$  of the triangulation of  $\mathbf{B}_1$ , we construct a  $|G|$ -dimensional local Hilbert space  $\mathcal{H}_{ij}^{\text{DW}} \equiv \{g_{ij} \in G\}$ ; namely, each group element labels a quantum state in  $\mathcal{H}_{ij}$ . Then we consider the tensor product of all such local Hilbert spaces  $\mathcal{H}^{\text{DW}} \equiv \otimes_{\text{all edges}} \mathcal{H}_{ij}^{\text{DW}}$ . Now we can associate each possible coloring on  $\mathbf{B}_1$  with a quantum state in  $\mathcal{H}^{\text{DW}}$ . Because a coloring must satisfy the zero-flux rule, clearly all possible colorings of  $\mathbf{B}_1$  span a subspace  $\tilde{\mathcal{H}}^{\text{DW}} \subset \mathcal{H}^{\text{DW}}$ . All possible colorings of  $\mathbf{B}_2$  then also form the exact same Hilbert subspace  $\tilde{\mathcal{H}}^{\text{DW}}$ .

Let us choose a coloring  $|\tau_1\rangle \in \tilde{\mathcal{H}}^{\text{DW}}$  on  $\mathbf{B}_1$ , and another coloring  $|\tau_2\rangle \in \tilde{\mathcal{H}}^{\text{DW}}$  on  $\mathbf{B}_2$ .  $\tau_1$  and  $\tau_2$  completely specify the triangulation, ordering, and coloring  $\tau$  on  $\partial M$ . Theorem 2 means that there is a well-defined quantum transition amplitude from the state  $|\tau_1\rangle$  to the state  $|\tau_2\rangle$ :

$$\langle \tau_2 | P | \tau_1 \rangle \equiv Z_M(\tau). \quad (44)$$

Because all possible  $|\tau_1\rangle$  ( $|\tau_2\rangle$ ) form a basis of  $\tilde{\mathcal{H}}^{\text{DW}}$ , this equation defines a quantum operator  $P$  on  $\tilde{\mathcal{H}}^{\text{DW}}$ .

Theorem 2 immediately dictates that  $P$  is a projector:  $P^2 = P$ . This is because after we insert an identity operator  $\sum_{\tau_3} |\tau_3\rangle \langle \tau_3| = \mathbb{1}$  in  $\tilde{\mathcal{H}}^{\text{DW}}$ ,  $\langle \tau_2 | P | \tau_1 \rangle = \sum_{\tau_3} \langle \tau_2 | P | \tau_3 \rangle \langle \tau_3 | P | \tau_1 \rangle$  has a simple geometric interpretation (see Fig. 6): We can consider two copies of the manifold  $M$ ,  $M_1 = \mathbf{B} \times [0, 1]$  and  $M_2 = \mathbf{B} \times [1, 2]$ , so that  $\langle \tau_3 | P | \tau_1 \rangle$  ( $\langle \tau_2 | P | \tau_3 \rangle$ ) is the quantum amplitude due to an internal triangulation and ordering of  $M_1$  ( $M_2$ ). We can then glue the top boundary of  $M_1$  with the bottom boundary of  $M_2$ . After the gluing, the vertices on the glued boundary  $\mathbf{B} \times \{1\}$  become internal vertices. Then  $\sum_{\tau_3} \langle \tau_2 | P | \tau_3 \rangle \langle \tau_3 | P | \tau_1 \rangle$  can be simply interpreted as the quantum amplitude due to an internal triangulation and ordering of  $M_1 \cup M_2 \cong M$ , which must be the same as  $\langle \tau_2 | P | \tau_1 \rangle$  according to Theorem 2.

Because  $P$  is a projector, the image of  $P$  forms a subspace in the Hilbert space  $\text{Img}(P) \subset \tilde{\mathcal{H}}^{\text{DW}}$  in which  $P$  acts as identity.  $\text{Img}(P)$  turns out to be the ground-state sector associated with the DW TQFT for the closed 2-manifold  $\mathbf{B}$ . One can also prove<sup>52</sup> that the dimension of  $\text{Img}(P)$  (i.e., the ground-state degeneracy of the TQFT) and the partition function of the closed space-time 3-manifold  $\tilde{M} \equiv \mathbf{B} \times S^1$  are identical:  $\dim[\text{Img}(P)] = Z_{\tilde{M}=\mathbf{B} \times S^1}$ .

At this point, it is useful to introduce an example. Consider the simplest group  $G = Z_2$ . According to Eqs. (15) and (18),  $H^3(Z_2, U(1)) = Z_2$ . This means that there are two inequivalent 3-cocycles and let us choose the trivial one:  $\omega(x, y, z) = 1$ ,  $\forall x, y, z \in Z_2$ , which gives rise to a DW TQFT. This particular TQFT turns out to be a familiar one: the  $Z_2$  gauge theory of the toric code model.<sup>65</sup> We can then use Theorem 1 to compute the partition function  $Z_M$  for a closed 3-manifold  $M$  and use Theorem 2 to compute the ground-state degeneracy via the projector  $P$ . For instance, for a 3-sphere and a 3-torus,  $Z_{S^3} = 1/2$  and  $Z_{T^3} = 4$ , respectively. The latter result implies that the ground-state degeneracy on a torus is 4, since  $T^3 = T^2 \times S^1$ . More generally, the ground-state degeneracy on a closed orientable 2-manifold  $\mathbf{B}$  is  $\dim[\text{Img}(P)] = 4^g$ , where  $g$  is the genus of  $\mathbf{B}$ .

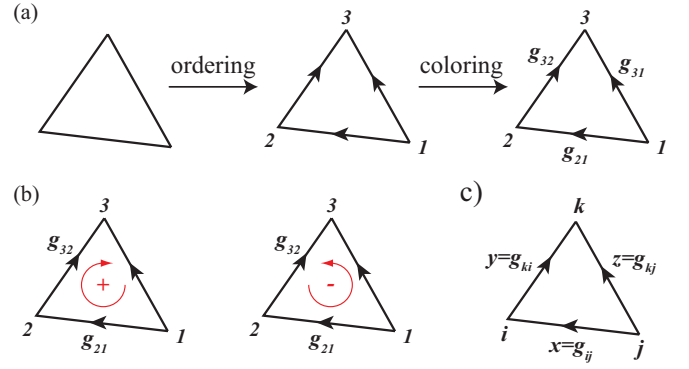


FIG. 7. (Color online) The 2-cocycle  $\omega(h_1, h_2)$  assigns a  $U(1)$  complex number (i.e., a phase) to a 2-simplex (triangle). (a) Left to center: the “ordering” of triangle’s three vertices; we choose here  $1 \rightarrow 2 \rightarrow 3$ . An edge is oriented from lower to higher vertex, so no triangle forms an oriented loop. (Alternatively, one orients all edges without forming oriented triangle loops, and a consistent underlying vertex ordering is guaranteed.) Center to right: “Coloring” assigns group element  $g_{ij}$  to  $j \rightarrow i$  edge, with  $g_{ji} = g_{ij}^{-1}$ . The shown triangle  $1 \rightarrow 2 \rightarrow 3$  is assigned the phase  $W = \omega(g_{32}, g_{21})^\epsilon = \omega(g_{32}, g_{21})$ . The exponent  $\epsilon = \pm 1$  is determined by (b) chirality. For triangle  $1 \rightarrow 2 \rightarrow 3$ , (counter-)clockwise loop 123 means  $\epsilon = +1$  ( $-1$ ), which is realized in the left (right) triangle. (c) The zero-flux rule applied to a triangle. Generally,  $g_{ki} \cdot g_{ij} \cdot g_{jk} = \mathbb{1}$ , the group identity element. Recall that  $g_{jk} = g_{kj}^{-1}$ . Choosing an ordering and assigning elements to ordered bonds as shown leads to the constraint  $z = y \cdot x$ .

### 3. The generalization to other dimensions

The above discussion has been limited to  $2 + 1$  dimensions. In fact, the geometric interpretation of an  $n$ -cocycle can be easily generalized to any  $n \geq 2$  space-time dimensions. Some aspects of this generalization have been discussed in Ref. 20. Here for the purpose of the current paper, we briefly discuss the  $n = 2$  and the  $n = 4$  cases.

*Geometric interpretation of a 2-cocycle*  $\omega(x, y) \in H^2(G, U(1))$  (see Fig. 7). Let us choose a 2-cocycle  $\omega(x, y) \in H^2(G, U(1))$ . Consider a 2-simplex (i.e., triangle). Again, one needs to perform the ordering and coloring procedure. Let us choose an ordering of the vertices  $1 \rightarrow 2 \rightarrow 3$ . We then color the edges by group elements  $g_{31}, g_{32}, g_{21}$  under the zero-flux rule:  $g_{31} = g_{32}g_{21}$ . Therefore, we can choose  $g_{32}, g_{21}$  to be the only independent elements. Next, we assign the complex number  $\omega(g_{32}, g_{21})^\epsilon$  to this 2-simplex. Here  $\epsilon = \pm 1$  depending on the chirality of the ordering of vertices: If  $1 \rightarrow 2 \rightarrow 3$  is clockwise (counterclockwise),  $\epsilon = 1$  ( $\epsilon = -1$ ).

The geometric interpretation of the 2-cocycle condition Eq. (6) can now be understood as the invariance of the product of these assigned complex numbers in a 1-3 move or a 2-2 move (see Fig. 8). For instance, in a 1-3 move, we consider an ordered and colored triangle, together with the assigned complex number  $\omega(g_{32}, g_{21})^\epsilon$ . Then we add one new vertex inside the triangle. After connecting the new vertex with the original three vertices, three new edges are created and the original triangle is thus further triangulated into three smaller triangles. We now can choose any ordering and coloring of the new vertex and new edges under the zero-flux rule, which then assigns three new complex numbers for the three smaller triangles. The 2-cocycle condition Eq. (6) dictates that

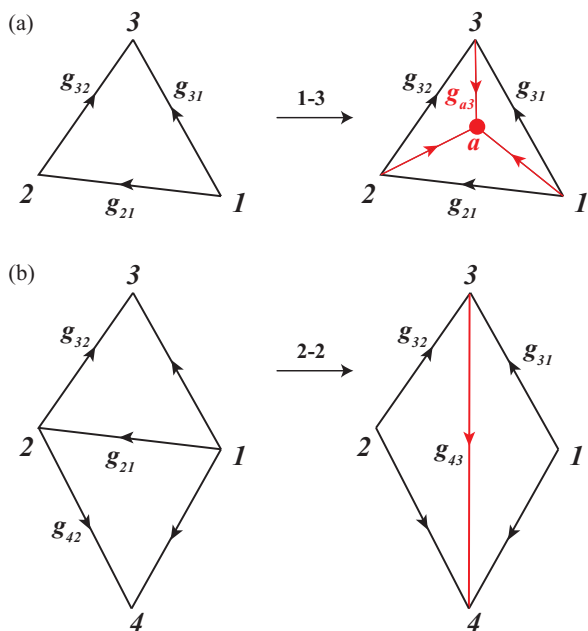


FIG. 8. (Color online) The 1-3 and 2-2 moves (in two dimensions) change triangulation but not total product of phases  $\prod_I W(\sigma_I)^{\epsilon_I}$  of 2-simplices  $\sigma_I$ . (a) The 1-3 move. (Left) The initial triangle is assigned the phase  $W_0 \equiv \omega(g_{32}, g_{21})$  (see Fig. 7). (Right) The vertex  $a$  is added, and we choose the ordering such that  $1 \rightarrow 2 \rightarrow 3 \rightarrow a$  [obvious from chosen orientations of new (red) edges]. There are now three smaller triangles, with phases 1, triangle  $1 \rightarrow 2 \rightarrow a$ ,  $W_1 \equiv \omega(g_{a2}, g_{21})$ ; 2, triangle  $2 \rightarrow 3 \rightarrow a$ ,  $W_2 \equiv \omega(g_{a3}, g_{32})$ ; 3, triangle  $1 \rightarrow 3 \rightarrow a$ :  $W_3 \equiv \omega(g_{a3}, g_{31})^{-1}$ . The 2-cocycle condition, Eq. (6), says the total phase does not change by the move:  $W_0 = W_1 W_2 W_3$ . Note that only one independent new group element is introduced (we marked the  $g_{a3}$ ), and from zero-flux rule  $g_{a2} = g_{a3} \cdot g_{32}$ . Changing our choice of ordering for  $a$  relative to 1, 2, 3 would lead to an equivalent 2-cocycle condition. (b) The 2-2 move. (Left) Two initial triangles, 123 and 124, are assigned the total phase  $W_0 \equiv \omega(g_{32}, g_{21})\omega(g_{42}, g_{21})^{-1}$ . (Right) The area is divided into two triangles by the other possible edge (red), and we choose the ordering  $3 \rightarrow 4$ . The phases of new triangles: 1, triangle  $1 \rightarrow 3 \rightarrow 4$ ,  $W_1 \equiv \omega(g_{43}, g_{31})^{-1}$ ; 2, triangle  $2 \rightarrow 3 \rightarrow 4$ ,  $W_2 \equiv \omega(g_{43}, g_{32})$ . The 2-cocycle condition gives  $W_0 = W_1 W_2$ . Note that the group element  $g_{43}$  is not independent; e.g.,  $g_{43} = g_{42} \cdot g_{32}^{-1}$ .

the product of the three new complex numbers equals the original one  $\omega(g_{32}, g_{21})^\epsilon$ .

Theorem 1 and Theorem 2 can also be generalized to 2-manifolds and 2-cocycles. For example, let us consider Theorem 2. For a 2-manifold  $M$  with boundary  $\partial M$ , one first chooses a triangulation (using 1-simplices, i.e., line segments), an ordering of vertices, and a coloring on  $\partial M$ , which we denote by  $\tau$ . Note that now there are no zero-flux rule constraints for  $\tau$ , because there is no triangle in a 1-simplex. Then one can extend the triangulation, ordering, and coloring into the bulk of  $M$  (where the zero-flux rule holds). We denote the assigned complex number for a 2-simplex  $\sigma_I$  in  $M$  as  $W(\sigma_I, \varphi)^{\epsilon(\sigma_I)}$  as before, where  $\varphi$  denotes the bulk coloring. With a fixed bulk triangulation and ordering, there will be many possible colorings that are compatible with  $\tau$ . Theorem 2 for 2-manifolds and 2-cocycles states that Eq. (43) defines a complex number  $Z_M(\tau)$  which is independent of the

choice of bulk triangulation and ordering of vertices, as long as  $\tau$  is fixed.

Following the discussion from the previous section, Theorem 1 and Theorem 2 suggest that a cocycle  $\omega(x, y) \in H^2(G, U(1))$  may define a 2D TQFT. This is indeed true and was discussed in a mathematical context.<sup>66</sup> In  $2 + 1d$ , we know that different topological orders can be characterized by different TQFTs. One may ask: Does this mean that there are nontrivial topological orders in  $1 + 1d$ ? However, we also know from previous research that nontrivial topological orders do not exist in  $1 + 1d$ .<sup>67</sup> It turns out that the 2D TQFTs induced by 2-cocycles do not give rise to physically nontrivial topological order. This is because the ground-state degeneracy is not robust, as one can lift it by a local perturbation.<sup>68</sup>

*Geometric interpretation of a 4-cocycle*  $\omega(x, y, z, u) \in H^4(G, U(1))$ . Similarly to the  $n = 3$  case, for a given 4-simplex one can choose an ordering of its vertices  $1 \rightarrow 2 \rightarrow 3 \rightarrow 4 \rightarrow 5$ , color the edges following the zero-flux rule, and assign the complex number  $\omega(g_{54}, g_{43}, g_{32}, g_{21})^\epsilon$  to it. Here again  $\epsilon$  is determined by the chirality of the ordering of vertices. The 4-cocycle condition  $\delta\omega = 1$  in Eq. (2) when  $n = 4$  can be understood as the invariance of the product of the assigned complex numbers to 1-5, 2-4, and 3-3 moves. Theorem 1 and Theorem 2 also hold for 4-manifolds. For any fixed 4-cocycle  $\omega(x, y, z, u) \in H^4(G, U(1))$ , these theorems give rise to a 4D TQFT. Equivalent 4-cocycles induce the same TQFT. These 4D TQFTs characterize different topological orders in  $3 + 1d$ .

## B. Exactly solvable models

In this section we define our exactly solvable models. Although we discuss the generalization to other dimensions in Sec. VIA, from now on we constrain ourselves to the  $2 + 1$ -dimensional case. It will become clear that our models exhibit both a global symmetry forming a group  $SG$ , as well as topological order described by a discrete gauge group  $GG$ . We explain our models' relation to both the SPT models of Ref. 20 and the DW gauge theories of Ref. 52. Through these connections it also becomes clear that each inequivalent choice of 3-cocycle in our models leads to a model with specific topological and symmetry properties, as labeled by the classification in Sec. II.

We consider a triangular (two-dimensional) lattice with oriented edges (bonds), where these orientations are compatible with an ordering of lattice sites, i.e., each edge oriented from a lower to higher ordered site and no triangle edges form an oriented loop, just as we discussed in Sec. III A and Fig. 7. For concreteness, in Fig. 9 we show our choice of edge orientations on the triangular lattice. We next introduce the ‘‘coloring’’  $\varphi$  by assigning an element  $h_{ij} \in GG$  to each oriented edge  $j \rightarrow i$ , again as discussed in Sec. III A; however, we now also assign a group element  $u_i \in SG$  to each lattice site  $i$ .

Actually, we further introduce the group element

$$g_{ij} \equiv h_{ij} \cdot u_i \cdot u_j^{-1} \in G \quad (45)$$

as our variable on edge  $ij$ . This definition might seem somewhat redundant, since the  $u_i$  elements appear both on sites and on edges through  $g_{ij}$ . It has important meaning, however. As discussed in Sec. IIC, it is already known that some cohomology based classifications of phases with symmetry

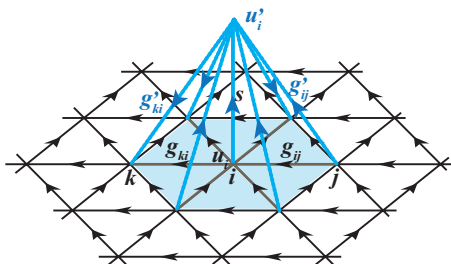


FIG. 9. (Color online) Action of the operator  $\hat{B}_p^s$ ,  $s = h_s \cdot \tilde{s}$ , with  $h_s \in GG$ ,  $\tilde{s} \in SG$ , on plaquette  $p$  centered on site  $i$ : For six elements  $h_{il} \in GG$  on edges  $il$  it resembles a local gauge transformation preserving zero flux through all triangles, e.g.,  $h'_{ij} = h_s \cdot h_{ij}$  and  $h'_{ki} = h_{ki} \cdot h_s^{-1}$ , while the on-site element transforms as  $u'_i = \tilde{s}u_i$ , leading to, e.g.,  $g'_{ij} = s \cdot g_{ij}$  and  $g'_{ki} = g_{ki} \cdot s^{-1}$ ; additionally, there is an overall phase factor which is the product of complex numbers assigned by the 3-cocycle  $\omega \in Z^3(SG \times GG, U(1))$  to the six 3-simplices (tetrahedrons) forming the “pyramid” [see Fig. 3 and Eq. (51)]. Note that fixing the initial and final state (i.e., the values  $u_i, u'_i$ , etc.) leads to a unique value of  $s$  for which the operator matrix element does not vanish. In that sense, this picture also describes the action of the plaquette operator  $\hat{B}_p$ .

and phases with topological order can be explicitly connected by duality. Due to the direct product structure of the group  $G = SG \times GG$  we consider here, it is simple to dualize either  $SG$  or  $GG$  (entire groups or their subgroups) without having to change the formalism. We, in fact, use dualization of  $SG$  explicitly when considering symmetry protected degeneracy in examples; see Sec. V G.

Let us then briefly consider how  $SG$  is dualized. The group variables  $u_i$  defined on lattice sites  $i$  are *replaced* by group variables  $u_{ij}$  living on oriented edges  $j \rightarrow i$  according to the rule<sup>79</sup>

$$u_{ij} \equiv u_i \cdot u_j^{-1}. \quad (46)$$

Due to importance of duality, we want to ensure that all gauge degrees of freedom present in a theory are treated equally. This is our motivation for using the edge variables  $g_{ij}$  defined in Eq. (45) as degrees of freedom on equal footing with  $h_{ij}$ .

An arbitrary quantum state in the Hilbert space  $\mathcal{H}$  of our model is therefore labeled by  $|i\rangle = |\{u_i\}, \{g_{ij}\}\rangle$ , or by  $|i\rangle = |\{u_i\}, \{h_{ij}\}\rangle$ .

The elementary building block for the theory is the operator  $\hat{B}_p^s$  labeled by a group element  $s \in G \equiv SG \times GG$ , and a plaquette  $p$  containing six triangles sharing a lattice site  $i$  at the center. The plaquette operator therefore acts on seven group elements, one at the site  $i$  and six on the edges that share this site. To define its action, we need an additional edge oriented vertically up into the third dimension at site  $i$ , to which we assign the element  $s \in G$  which can always be uniquely factored as

$$s = h_s \cdot \tilde{s}, \quad (47)$$

with  $h_s \in GG$ ,  $\tilde{s} \in SG$  (Fig. 9). The operator  $\hat{B}_p^s$  transforms the seven values of elements in the plaquette by  $s$ , preserving the orientation of edges, and these new values are represented on edges lifted above the original ones; see Fig. 9. With  $p$

centered on site  $i$ , we have

$$u_i \rightarrow \tilde{s} \cdot u_i, \quad h_{ij} \rightarrow h_s \cdot h_{ij}, \quad h_{ki} \rightarrow h_{ki} \cdot h_s^{-1}, \quad (48)$$

leading to

$$g_{ij} \rightarrow s \cdot g_{ij}, \quad g_{ki} \rightarrow g_{ki} \cdot s^{-1}. \quad (49)$$

Further, nonzero matrix elements of  $\hat{B}_p^s$ ,

$$B_p^s = \langle f(s) | \hat{B}_p^s | i \rangle, \quad (50)$$

are assigned the quantum amplitude

$$B_p^s \equiv \prod_{l=1}^6 W(\sigma_l, \varphi)^{\epsilon(\sigma_l)}, \quad (51)$$

where the six 3-simplices  $\sigma_l$  are built using the six triangles of the plaquette  $p$  (with the initial group element values assigned), the vertical edge (assigned the group element  $s$ ), and the six lifted edges [assigned the final element values according to Eq. (49)]. This action is shown in Fig. 9. The orientation of new (lifted) edges is chosen to match the orientation of original edges upon downward projection.

It is important to note that the zero-flux rule (discussed in Sec. III A) is by construction satisfied on all faces (triangles) of the six tetrahedra, *if it is satisfied* in the six triangles of the plaquette  $p$ . The zero-flux rule must hold on all faces of the tetrahedra for which we are calculating the phase  $W$ . The operator  $B_p^s$  is therefore defined only in a Hilbert subspace  $\mathcal{K}_p$  which consists of states having the zero-flux rule satisfied in all six triangles of the plaquette  $p$ . Finally, note that choosing a final state  $|f\rangle$  in a nonzero matrix element fixes a unique value of  $s$ .

We finally define the plaquette operators  $\hat{B}_p$  as having matrix elements

$$B_p = \frac{1}{|G|} \sum_{s \in G} B_p^s. \quad (52)$$

To explicitly illustrate the plaquette operator (as well as the full Hamiltonian defined below) through examples, in Appendix D we will consider the models for two  $Z_2$  topologically ordered phases, i.e., the well-known “toric code”<sup>65</sup> and “double-semion” theory.<sup>69</sup>

Returning to the most general case, our plaquette operators  $\hat{B}_p$  turn out to be projectors. Namely, using the properties of 3-cocycles, one finds that applying a  $\hat{B}_p^s$  operator twice at the same plaquette leads to a group multiplication in the amplitude,

$$\langle f | \hat{B}_p^s \hat{B}_p^{s'} | i \rangle = B_p^{s \cdot s'}. \quad (53)$$

Using the normalization in Eq. (52) it follows that

$$\langle f | \hat{B}_p \hat{B}_p | i \rangle = B_p \quad (54)$$

and also that  $\hat{B}_p$  is a projector.

Crucially, we show further below that the plaquette operators commute:

$$[B_p, B_{p'}] = 0, \quad \forall p, p'. \quad (55)$$

Let us next introduce the operator  $Q_t$ , which projects flux in a triangle  $t$  to zero; i.e., it enforces the zero-flux rule discussed in Sec. III A. In other words,  $Q_t$  is nonzero (and equal to 1) only when acting on a triangle  $t$  made out of lattice sites  $i, j, k$  such that

$$h_{ij} \cdot h_{jk} \cdot h_{ki} = \mathbb{1}_{GG}, \quad g_{ij} \cdot g_{jk} \cdot g_{ki} = \mathbb{1}, \quad (56)$$

where  $\mathbb{1}$  is the group identity in  $G$ , and the second equality follows directly from the definition Eq. (45).

We can at last define the Hamiltonian as

$$H = - \sum_t Q_t - \sum_p \hat{B}_p \prod_{t \in p} Q_t, \quad (57)$$

where the label  $t \in p$  enumerates the six triangles making up the plaquette  $p$ . As mentioned above, the factor  $\prod_{t \in p} Q_t$  is actually crucial to ensure that  $H$  is well-defined: It ensures that  $\hat{B}_p$  acts within the subspace  $\mathcal{K}_p$  on which it is defined [see discussion after Eq. (51)].

Further, it is easy to see that plaquette operator term  $\hat{B}_p \prod_{t \in p} Q_t$  actually commutes with the projectors  $Q_{t'}$ . Namely, the transformation rule by  $s$  in operator  $\hat{B}_p^s$ , as introduced above, preserves the product rule Eq. (56) on all triangle faces of simplices in Fig. 9, if it is satisfied in either the upper or the lower triangles, i.e., in either the  $|i\rangle$  or the  $|f\rangle$  state. Obviously, then the zero-flux rule enforced by action of  $Q_{t'}$  commutes with the action of  $\hat{B}_p \prod_{t \in p} Q_t$  even when  $t'$  belongs to the plaquette  $p$ .

Our model has the global symmetry group  $SG$ , following from the fact that the Hamiltonian commutes with the global symmetry operations,

$$u_i \rightarrow u_i \cdot \tilde{s}^{-1}, \quad \forall i, \quad (58)$$

and  $\tilde{s} \in SG$ . The symmetry operation obviously does not influence the zero-flux rule in Eq. (56) and therefore commutes with every  $Q_t$ . Considering a plaquette operator, the symmetry operation leaves the edge elements  $g_{ij}$  invariant, and also the final value of site elements  $u_i$  is the same no matter the order in which apply  $\hat{B}_p$  and  $\tilde{s}$ , due to the group property.

Next, our model  $H$  is exactly solvable: All terms in the Hamiltonian  $H$  commute with each other (we still have to prove the commutation of  $\hat{B}_p, \hat{B}_{p'}$ ), so the model is exactly solvable.

Let us now consider the ground-state manifold of our model. Since all the terms in  $H$  are also projectors, the ground-state manifold is the image of the projector  $P = \prod_p \hat{B}_p \prod_{t \in p} Q_t$ . Actually, it is also easy to see that  $\hat{B}_p^s \hat{B}_p = \hat{B}_p$  due to Eq. (53) and the group property. This means that for a ground state it also holds that  $\hat{B}_p^s = 1, \forall p, s$ .

First, let us consider the special cases in which  $SG = Z_1$  is trivial. In this case, the projector  $P = \prod_p \hat{B}_p \prod_{t \in p} Q_t$  is exactly the projector in the DW theory [Eq. (43)]. Namely, applying all  $\hat{B}_p$  operators in the plane creates a lifted copy of the plane, leaving the volume between them triangulated by tetrahedrons; the transition amplitude for this operation is equal to the product of  $\prod_{l=1}^6 W(\sigma_l, \varphi)^{\epsilon(\sigma_l)}$  phases contributed by all the  $\prod_p \hat{B}_p$ . The initial and final states fix the coloring  $\tau$  on the two planes, so the transition amplitude exactly equals the DW topological invariant  $Z_M(\tau)$  [Eq. (43)] evaluated on the manifold having the two planes as boundaries. [Note that there

are no vertices inside the volume, and the number of plaquettes  $p$  is equal to  $V_{\partial M}/2$  since there are two planes in  $\partial M$ , leading to correct prefactor from Eq. (43).] We can therefore conclude that when  $SG = Z_1$ , the ground-state sector of our model, to which  $P$  projects with eigenvalue 1, is also the ground-state sector of the DW TQFT<sup>52</sup> defined on the triangular plane. We generally study the topological order of our models in Appendix B.

On the other hand, we can consider the opposite situation where the gauge group is trivial  $GG = Z_1$ , so that  $G = SG$ . In that case, our models become equal to the exactly solvable models for SPT phases constructed by Chen *et al.* in Sec. II F of Ref. 20. Namely, since the only degrees of freedom on the edges are from  $SG$  [see Eq. (45)], the zero-flux rule is automatic so  $Q_t = 1$ . The Hamiltonian is just a sum of the  $\hat{B}_p$  plaquette operators, and these are obviously identical to the plaquette operators forming the Hamiltonian in Ref. 20. We can conclude, as claimed in the Introduction, that our exactly solvable models in the case of trivial gauge group  $GG$  become the models for SPT phases classified by  $H^3(SG, U(1))$ .

Our exactly solvable model is in-between these two extreme situations (the DW theory and the SPT model), and it can be understood as a partially dualized version of either of them.

In general, the ground states of our models do not break the physical symmetry  $SG$  so that they describe symmetric quantum phases. The simplest way to convince oneself of this is by noting that the  $\hat{B}_p^s$  operators in our models [see Eq. (50)] create/annihilate small domain walls in a quantum state when  $s \in SG$ . Since in a ground state it holds that  $\hat{B}_p^s = 1, \forall p$ , the ground state is a domain wall condensate, i.e., the symmetric phase.

Let us now prove Eq. (55) by using the DW topological invariant from Eq. (43). Consider the picture of action of two overlapping plaquette operators, described by matrix elements

$$BB_1 = \langle f | \hat{B}_p \hat{B}_{p'} | i \rangle, \quad (59)$$

and

$$BB_2 = \langle f | \hat{B}_{p'} \hat{B}_p | i \rangle, \quad (60)$$

where  $p$  and  $p'$ , the plaquettes centered on sites  $i, j$ , respectively, necessarily share two triangles, while only the  $ij$  edge is acted upon by both operators; see Fig. 10. The operator product  $\hat{B}_p \hat{B}_{p'}$  is obviously defined within the Hilbert subspace  $\mathcal{K}_{pp'} = \mathcal{K}_p \cap \mathcal{K}_{p'}$ .

First note that because the final state is the same in both  $BB_{1,2}$  cases [Figs. 10(a) and 10(b)], the final values on the  $ij$  bond,  $g''$  and  $\bar{g}''$ , respectively, have to be equal (the initial value is  $g \equiv g_{ij}$ ). Applying the rule Eq. (56) on triangular faces created by  $s, s', g$  edges shows that indeed  $g'' = \bar{g}'' = s \cdot g \cdot s'^{-1}$ , with conventions as in Figs. 9 and 10. Next, note that fixing the initial and final states amounts to choosing a coloring on the surface of the tent-shaped body formed on top of the  $p, p'$  plaquettes. The only unconstrained internal edges are  $s, s'$ . By construction of the model and the properties of the ground-state manifold, the edge orientations and the constraints on elements are consistent with a triangulation and coloring of the tent-shaped manifold as required in the definition [Eq. (43)] of  $Z_M(\tau)$ . The surface coloring  $\tau$  is fixed by the choice of initial and final states, while the sum over  $s, s'$  in the expressions for  $BB_1, BB_2$  is the sum over internal

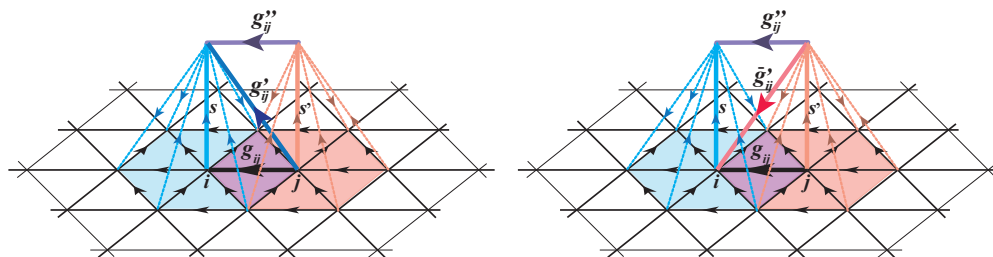


FIG. 10. (Color online) Overlapping plaquette operators commute. As in Fig. 9, the action and matrix elements of  $BB_1 = \langle f | \hat{B}_p \hat{B}_{p'} | i \rangle$  (right) and  $BB_2 = \langle f | \hat{B}_{p'} \hat{B}_p | i \rangle$  (left) are shown. Note that fixing  $|f\rangle$  and therefore  $g''_{ij}$  in both cases is consistent, giving  $g''_{ij} = s \cdot g_{ij} \cdot s'^{-1}$ . Concerning the overall phase factor due to the 3-cocycle factors in Eq. (51), the two images differ only in the choice of the single internal edge (dark blue on left, pink on right) of the triangulation of the tent-shaped object. The summation over elements  $s, s'$  inherent in the plaquette operators, Eq. (52), amounts to the sum over internal colorings, while  $|i\rangle, |f\rangle$  fix the surface coloring of the “tent.” The phase factor in both quantities  $BB_{1,2}$  becomes just the DW topological invariant [Eq. (43)] of the “tent” calculated with different triangulation choices, therefore having the same value.

colorings in the definition of  $Z_M(\tau)$ ; see Eq. (43). The  $BB_1$  and  $BB_2$  are therefore equal to the DW invariant  $Z_M(\tau)$  of the tentlike object in Fig. 10, and they differ from each other only in the choice of triangulation, i.e., the position of one internal edge (notice that the value of element on this edge is also different in the two cases, but in both consistent with general coloring demands from Sec. III A). According to the properties of the DW invariant expressed by Theorem 2 [Eq. (43)], this difference in triangulation does not change its value, meaning that  $BB_1 = BB_2$ .

#### IV. ELEMENTARY EXCITATIONS

In this section we introduce the low-energy excitations in our models, and study their general properties. We define ribbon operators which describe excitations at the ends of open strings in Sec. IV B, having first introduced the motivation for the definition in Sec. IV A. In Sec. IV C we use the algebra of ribbon operators (extended by some local operators) to study the general structure of these excitations. The 3-cocycles present in our models introduce a “twist” into this extended ribbon algebra and therefore play a key role.

Further, we explicitly show through examples in Sec. V that excitations in our models can have distinctive symmetry protected properties. Appendix B presents in detail the general braiding and fusion of quasiparticles based on the twisted extended algebra.

Up to now, the  $SG$  and the  $GG$  groups in our models were either Abelian or non-Abelian. From now on, for simplicity we assume both the  $SG$  and the  $GG$  to be Abelian.

##### A. Towards ribbons: Loop operators

We study closed-string (loop) operators in this section, which will motivate the subsequent expression for open-string (ribbon) operators. The loop operators we describe commute with the Hamiltonian in Eq. (57). The open-string operators will inherit this property locally along their string, except at the string ends, where the excitations are located.

To define a loop operator, let us consider a contiguous area  $A$  of the lattice. This area is bounded by a sequence of connected edges on the triangular lattice forming the lattice loop  $P$ . Next, if a lattice site  $i$  is inside the area  $A$ , or is lying on its boundary

$P$ , we define the plaquette  $p$  centered on  $i$  to be “inside  $A$ ”, i.e.,  $p \in A$ . Now, the loop operator is just a product of plaquette operators  $\hat{B}_p^s$  inside the area:

$$\hat{L}_P^s = \prod_{p \in A} \hat{B}_p^s, \quad (61)$$

where the ordering of the product is defined below, although it is physically irrelevant since the plaquette operators  $\hat{B}_p^s$  operators commute for  $p \neq p'$ . Obviously, the Hilbert subspace on which the loop operator is defined has the zero-flux rule obeyed in all triangles belonging to all plaquettes  $p \in A$ . This space is given by  $\mathcal{K}_{p_1} \cap \dots \cap \mathcal{K}_{p_a}$ , with  $p_1, \dots, p_a$  the plaquettes in  $A$ . For the purpose of this section, we can for simplicity consider only states which satisfy the zero-flux rule in all triangles of the lattice.

The loop operator will, for  $s \equiv h_s \tilde{s} \equiv h_s \cdot \mathbb{1}_{SG}$ ,  $h_s \in GG$ , have an action only on the boundary  $P$  of the area, and therefore we label  $\hat{L}_P^s$  by  $P$  only.

To prove this basic property of the loop operator, we start by considering the bulk of  $A$ , meaning the sites, edges, and triangles within  $A$  including its boundary  $P$ . We now need to fix the choice of ordering the operators  $\hat{B}_p^s$  in the product Eq. (61) according to their plaquettes  $p$ . A natural choice is according to the order of lattice sites  $i \equiv p$  on the lattice, putting highest  $p$  rightmost in the product. (As before,  $i \equiv p$  means the site  $i$  on which the plaquette  $p$  is centered.) This choice turns out to be the simplest and most convenient for calculations. The action of  $\hat{L}_P^s$  in the bulk of  $A$  is then given by the expressions presented in Fig. 11(a). The  $SG$  elements on the sites are unchanged due to  $\tilde{s} \equiv \mathbb{1}$ , while the  $GG$  elements on the edges get conjugated by  $s$  (contrast to Fig. 9). Since we focus on Abelian groups, the loop operator acts trivially on edges lying inside  $A$ , including its boundary  $P$ .

The nontrivial action of the loop operator is therefore limited to the edges which lie outside  $A$  but still share a site with the loop  $P$ , and this action is due to the  $\hat{B}_p^s$  operators having  $p$  centered on a site on the loop  $P$ ; see Fig. 11(b).

Returning to the contribution from the bulk of  $A$ , it reduces to the phase factors of 3-simplices (tetrahedrons) lying on top of the bulk of  $A$ , according to the action of operators  $\hat{B}_p^s$ . To evaluate these, we need to consider further the chosen ordering of  $p$ 's in the product. Consider an oriented edge  $j \rightarrow i$  inside  $A$



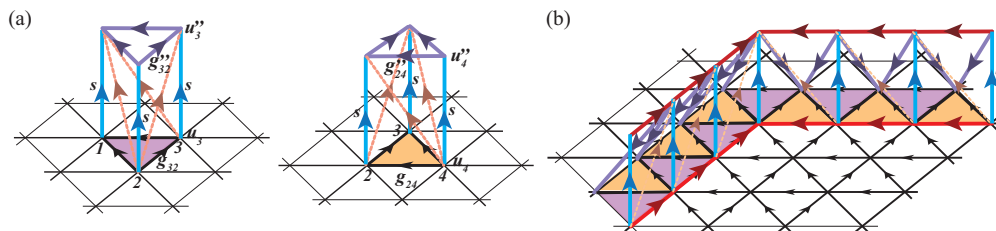


FIG. 11. (Color online) Creating a loop operator  $\hat{L}_P^s = \prod_{p \in A} \hat{B}_p^s$  by multiplying plaquette operators centered on sites within area  $A$  bounded by a lattice loop  $P$ . This leads to two types of phase factors in the bulk of  $A$ , coming from (a) left, down triangles; right, up triangles. The  $\hat{B}_p^s$ 's in the product are chosen to be ordered according to order of vertices  $i$  on which they are centered ( $p \equiv i$ ), with highest  $p$  being rightmost (i.e., applied first). For an Abelian group and the choice  $s \equiv h_s \cdot \mathbb{1}_{SG}$  the elements within  $A$  and  $P$  do not change, i.e.,  $u_4'' = u_4$ ,  $g_{32}'' = g_{32}$ , etc., and phase factors from all tetrahedrons cancel up to a total phase due to a 2-cocycle evaluated on edges along  $P$  [Eq. (70)]. (b) The loop operator only acts on triangle edges (thicker black) lying outside  $A$  but sharing one site with  $P$  (red edges).

(including  $P$ ), so that its arrow points towards  $i$ . By our choice  $\hat{B}_{p \equiv i}^s$  is applied before  $\hat{B}_{p \equiv j}^s$ . The action of  $\hat{B}_{p \equiv i}^s$  assigns the orientation  $j \rightarrow i$  to the lifted edge as in Fig. 9, so the lifted edge must have its arrow pointing “upwards” (towards the lifted  $i$  vertex). This property applies to all edges in the plane, so every lifted edge, connecting a vertex to a lifted vertex, will have its arrow pointing upwards, i.e., towards the lifted plane.

Having determined this fact, it is simple to determine the tetrahedrons formed by action of  $\hat{L}_P^s$  in bulk of  $A$ ; see Fig. 11(a). It becomes obvious that the bulk of the area is spanned by only two different types of triangles. For the up ( $\Delta$ ) and down ( $\nabla$ ) triangles on the lattice, as labeled in Fig. 11(a), the resulting phases are

$$\Phi_{\Delta}^s = c_s(g_{32}, g_{24}), \quad \Phi_{\nabla}^s = c_s^{-1}(g_{13}, g_{32}), \quad (62)$$

where using the 3-cocycle  $\omega$  we have introduced the function

$$c_s(g_1, g_2) \equiv \frac{\omega(s, g_1, g_2) \omega(g_1, g_2, s)}{\omega(g_1, s, g_2)}, \quad (63)$$

with  $g_1, g_2 \in G$ . The function  $c_s(g_1, g_2)$  is most generally parametrized by an arbitrary group element  $s \in G$ , even though here  $s \in GG$ , and it can be directly shown that this function satisfies the 2-cocycle condition introduced in Eq. (6).

On the other hand, the 2-cocycle ( $c_s$ ) value appearing in the phases Eq. (62) exactly corresponds to the phase assigned to the 2-simplices (i.e., triangles) on our ordered and colored lattice, according to the general considerations from Sec. III A. More precisely, just as in that section, a 2-simplex  $\sigma$  is defined

by a triangle with ordered vertices and group elements assigned to its edges. The 2-simplex is assigned the complex number

$$\Theta^s(\sigma, \varphi) = W(\sigma, \varphi)^{\epsilon(\sigma)}, \quad (64)$$

where  $W(\sigma, \varphi) \equiv c_s(g_{kj}, g_{ji})$  for a triangle with ordered vertices  $i \rightarrow j \rightarrow k$ . The sign  $\epsilon = \pm 1$  is given by the chirality; see Figs. 7 and 12.

The bulk of  $A$  is formed by the 2-simplices  $\sigma_I$ , so the total phase contributed by the bulk of  $A$  is

$$\Phi_A^s = \prod_{I \in A} \Theta^s(\sigma_I, \varphi), \quad (65)$$

which one can calculate by changing the triangulation of this area as in Fig. 12. (Recall that this retriangulation will not change the total phase due to the allowed “moves” from Fig. 8.) Namely, we make all the triangles share the vertex  $i = N \in P$ . Labeling the vertices  $i$  on the lattice loop in CW order  $P = \{i \mid i = 0, 1, \dots, N\}$  [see Fig. 12(c)], the phase  $\Phi_A^s \equiv \Theta_P^s$  becomes

$$\Theta_P^s = c_s(g_{N, N-1}, g_{N-1, N-2}) c_s(g_{N, N-1} \cdot g_{N-1, N-2}, g_{N-2, N-3}) \cdots c_s(g_{N, N-1} \cdots g_{21}, g_{10}), \quad (66)$$

where we took into account the zero-flux rule as well as  $g_{ij} = g_{ji}^{-1}$ . Equation (66) shows explicitly that the contribution of bulk of area  $A$  depends only on the edges along its boundary loop  $P$ .

This expression becomes useful for us later on, but let us now consider in more detail the case when the 2-cocycle  $c_s$  is

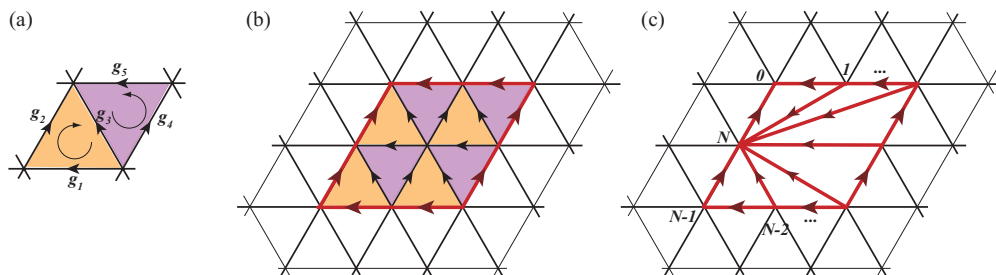


FIG. 12. (Color online) (a) The loop operator  $\hat{L}_P^s$ , with  $P$  the loop of lattice edges bounding area  $A$ , has total contribution from triangles within  $A$  which equals the product of 2-cocycle  $c_s$  [Eq. (67)] evaluated on the triangles as oriented 2-simplices (compare to Figs. 7 and 11). (b) An example loop  $P$  (red edges). (c) The phase can be calculated by retriangulating the area  $A$  inside the loop  $P$ . The resulting expression for the phase  $\Theta_P^s$ , Eq. (66), is given in terms of elements along edges on  $P$  with clockwise ordered vertices  $i = 0, \dots, N$ . The expression is used for the definition of an open string; see Sec. IV B.

trivial, which means that it can be rewritten in the form

$$c_s(g_1, g_2) = \frac{\varepsilon_s(g_1) \varepsilon_s(g_2)}{\varepsilon_s(g_1 \cdot g_2)}. \quad (67)$$

Because in expression Eq. (67) the three elements  $g_1, g_2, g_1 \cdot g_2$  belong to the three sides of the triangle, it is easy to check that contributions to  $\Theta^s$  from an edge shared by an up triangle and a down triangle cancel. The total phase then becomes a simple expression obtained by going around the loop:

$$\begin{aligned} \Theta_P^s &= \varepsilon_s(g_{N, N-1}) \varepsilon_s(g_{N-1, N-2}) \cdots \varepsilon_s(g_{20}) \varepsilon_s(g_{10}) \\ &= \prod_{\substack{i \in P \\ CW}} \varepsilon_s(g_{i+1, i}). \end{aligned} \quad (68)$$

Let us now return to the general case of arbitrary 2-cocycle  $c_s$ . Having dealt with the bulk contribution of  $A$ , the action of the loop operator is presented in Fig. 11(b), where a segment of the loop is marked by red edges, as in Fig. 12. Note again that along the loop  $i, i' \in P$ , elements  $u_i, g_{ii'}$  are unchanged between the initial and final states, just as they are not changed inside the loop.

### 1. Summary for loop operators

In summary, the loop operator  $\hat{L}_P^s$  only acts on two edges per triangle that has a vertex or edge on the loop  $P$ . This action follows from the action of  $\hat{B}_P^s$  [see Eq. (48)] with  $p$  centered on the loop  $P$ . [Such edges are marked thick black in Fig. 11(c).] Additionally, the loop operator has a phase factor contribution from the 3-cocycle of tetrahedrons  $\sigma_t$  on top of each such triangle [see shaded triangles in Fig. 11(c)], which we do not explicate as they cannot be simplified further; this phase factor we label succinctly by

$$\Psi_P^s \equiv \prod_{t \in P} W(\sigma_t)^{\varepsilon(\sigma_t)}. \quad (69)$$

Finally, there is the overall phase  $\Theta_P^s$ , giving the total amplitude for the loop operator:

$$\begin{aligned} L_P^s &= \Theta_P^s \Psi_P^s \\ &= \prod_{i=1}^{N-1} c_s \left( \prod_{j=i}^{N-1} g_{j+1, j}, g_{i, i-1} \right) \prod_{t \in P} W(\sigma_t)^{\varepsilon(\sigma_t)} \\ &= \prod_{\substack{i \in P \\ CW}} \varepsilon_s(g_{i+1, i}) \prod_{t \in P} W(\sigma_t)^{\varepsilon(\sigma_t)}, \end{aligned} \quad (70)$$

where the last line holds only for trivial 2-cocycles  $c_s$  and the CW loop  $P$  contains vertices  $P = \{i \mid i = 0, 1, \dots, N\}$ .

One can show, using a direct method as in Fig. 10, that the plaquette operator  $\hat{B}_P^s$  overlapping with the loop  $P$ , e.g.,  $p \in P$ , commutes with the loop operator.

The final expression Eq. (70) motivates a definition of an open-string operator, to which we now turn.

### B. Ribbon operator

In this section we introduce the open-string (ribbon) operators, which describe the low-energy excitations in our models.

Let us start by defining a geometric object: the open ribbon  $\Gamma$ . The ribbon has two ends, end  $A$  and end  $B$ , which we need to define first. Choosing two neighboring vertices on the triangular lattice, vertex  $i_A$  and vertex  $i'_A$ , there is a unique 2-simplex (triangle) formed by vertex  $i_A$  and vertex  $i'_A$  and another vertex that is *not* contained in  $\Gamma$ . We denote this 2-simplex by  $t_A$ . We then use the label  $A = (i_A, t_A)$ , the collection of the vertex  $i_A$  and the triangle  $t_A$ , to formally define the end  $A$  of the ribbon  $\Gamma$ . Similarly, we use  $B = (i_B, t_B)$  to define the end  $B$  of  $\Gamma$ . The 2-simplices  $t_A, t_B$  are *not* inside  $\Gamma$ . We also define the edges of ribbon  $\Gamma$  at the two ends: For end  $A$ , there is a single 1-simplex that is shared between  $\Gamma$  and  $t_A$ , which we denote as edge  $A$ . Similarly, we can define edge  $B$ .

Having defined its ends, the open ribbon  $\Gamma$  is finally specified by its two ‘‘ribbon edges.’’ Namely,  $\Gamma$  has an ‘‘inner edge,’’ which is a sequence of connected edges on the triangular lattice, going from the vertex  $i_A$  to the vertex  $i_B$ . Further,  $\Gamma$  also has an ‘‘outer edge,’’ running from the vertex  $i'_A$  to the vertex  $i'_B$ , which is displaced from the inner edge of  $\Gamma$  by one lattice spacing. (See Fig. 15 for an illustration of these definitions.) As a geometric object, the ribbon  $\Gamma$  contains all the vertices on the inner and outer edges, together with all 1-simplices and 2-simplices connecting these vertices (for these simplices, we say that they are *inside*  $\Gamma$ , or we write  $\in \Gamma$ ).

We now proceed to define the operator  $\hat{F}^{(h, g)}(\Gamma)$  for a given open ribbon  $\Gamma$ .

Let us define a Hilbert subspace  $\mathcal{K}(\Gamma) \subset \mathcal{H}$ , formed by those states which satisfy the zero-flux rule everywhere inside  $\Gamma$ . Namely,  $\forall |\psi\rangle \in \mathcal{K}(\Gamma)$  and  $\forall t \in \Gamma$ ,  $Q_t |\psi\rangle = |\psi\rangle$ . (Note that, however,  $|\psi\rangle$  may violate the zero-flux rule at  $t_A, t_B$ , for instance.) *For the purpose of this paper, we only define the operator  $\hat{F}^{(h, g)}(\Gamma)$  in the Hilbert subspace  $\mathcal{K}(\Gamma)$ .*

Based on the understanding of the loop operator from the previous section, we define the ribbon operator  $\hat{F}^{(h, g)}(\Gamma)$  such that it modifies the gauge degrees of freedom living on the lattice edges connecting the inner and outer ribbon edges of  $\Gamma$ , while leaving all degrees of freedom living elsewhere unchanged. In particular, for a lattice edge  $ij$  inside  $\Gamma$ , such that it connects the inner and outer ribbon edges, the group element  $h_{ij}$  living on it is changed into  $h'_{ij} = h \cdot h_{ij}$  [ $h'_{ij} = h_{ij} \cdot h^{-1}$ ] if the lattice edge is oriented to point towards the inner [outer] ribbon edge. The operator  $\hat{F}^{(h, g)}(\Gamma)$  therefore has nonzero matrix element only between states  $|\{u_i\}, \{h'_{ij}\}\rangle$  and  $|\{u_i\}, \{h_{ij}\}\rangle$ .

Finally, we need to define the nonzero matrix element of  $\hat{F}^{(h, g)}(\Gamma)$ . This matrix element has two factors: one chosen in accordance with the closed-loop operator and the other dependent on the degrees of freedom at the two ends of the open ribbon  $\Gamma$ . We define

$$\langle \{u_i\}, \{h'_{ij}\} | \hat{F}^{(h, g)}(\Gamma) | \{u_i\}, \{h_{ij}\} \rangle = f_A \cdot f_B \cdot f_{AB} \cdot w_h^\Gamma(g), \quad (71)$$

where (1)  $w_h^\Gamma(g)$  is motivated by the closed-loop operator and is presented shortly, and (2)  $f_A, f_B, f_{AB}$  are rather complicated phase factors depending only on the degrees of freedom living on ends of  $\Gamma$ , and we present them in Appendix B. To motivate the expression for  $w_h^\Gamma(g)$ , let us start from the expression for loop operator Eq. (70). Let the  $\Gamma$  ribbon's inner edge go

along the sequence of lattice sites  $\{i \mid i = 0, \dots, N\}$ , where now the sites  $i = 0$  and  $i = N$  are not nearest neighbors, but rather vertex  $i_B$  and vertex  $i_A$ , respectively. For convenience

(see Fig. 13 for the pictorial definition), we define the group elements  $a_n \in G, n = 1, \dots, N$  by  $a_i \equiv g_{i,i-1}$ . We then define the phase

$$\begin{aligned}
 w_h^\Gamma(g) &= \Psi_\Gamma^h \Theta_\Gamma^h \delta \left( \prod_{i=1}^N g_{i,i-1}, g \right) \\
 &\equiv \left( \prod_{t \in \Gamma} W(\sigma_t)^{\epsilon(\sigma_t)} \right) c_h(\mathbb{1}, a_N) c_h(a_N, a_{N-1}) c_h(a_N \cdot a_{N-1}, a_{N-2}) \cdots c_h(a_N \cdots a_2, a_1) \delta(a_1 \cdots a_N, g) \\
 &= \left( \prod_{t \in \Gamma} W(\sigma_t)^{\epsilon(\sigma_t)} \right) c_h(g \cdot a_1^{-1}, a_1) c_h(g \cdot a_1^{-1} \cdot a_2^{-1}, a_2) \cdots c_h(g \cdot a_1^{-1} \cdots a_{N-1}^{-1}, a_{N-1}) \\
 &\quad \times c_h(g \cdot a_1^{-1} \cdots a_N^{-1}, a_N) \delta(a_1 \cdots a_N, g),
 \end{aligned} \tag{72}$$

with  $\delta(g, g')$  the Kronecker  $\delta$  function, which we used in the second line to obtain a simple pictorial definition; see Fig. 13.

A way to understand the meaning of phase in Eq. (72) is to note that “cutting open” the loop to get an open string introduced the parameter  $g \in G$  which is related to the charge carried by the excitations at the string ends. We consider it in more detail below. [Compared to the loop, there is one extra factor  $c_h(\mathbb{1}, a_N)$ , which is inconsequential for canonical cocycles; see Eq. (87c).]

In accordance with the definition of the loop operator, the element  $h \in GG \subset G$ ; see after Eq. (61). Physically, the loop operator  $\hat{L}_p^h$  can be seen as a closed,  $P$  loop-shaped, domain wall inside which we acted using element  $h$  (through action of  $\hat{B}_p^h$ ). For a gauge element  $h \in GG$  there is actually no transformation inside the domain wall. It is further possible to create an “open domain wall” (i.e., open-string  $\Gamma$ ) in the gauge transformation  $h$ , and it defines gauge excitations at the ends of  $\Gamma$ . (On the other hand, one could define  $\hat{L}_p^{\tilde{h}}$  for a global symmetry operation  $\tilde{h} \in SG$ , which would create a closed domain wall inside which the transformation  $\tilde{h} \in SG$

is applied. However, it is physically unsound to try to define an open domain wall of such a transformation  $\tilde{h} \in SG$ .)

It is important to realize that the  $\delta$  function in the ribbon operator,  $\delta(a_1 \cdots a_N, g)$ , with  $a_i \equiv g_{i,i-1} = h_{i,i-1} \cdot u_i \cdot u_{i-1}^{-1}$ , has a different effect on the global symmetry and gauge parts of  $G = GG \times SG$ . Namely, given the factorization  $g = h_g \cdot \tilde{g}$ , the  $\delta$  function separates into

$$\delta(a_1 \cdots a_N, g) = \delta(h_{10} \cdots h_{N,N-1}, h_g) \delta(u_N u_0^{-1}, \tilde{g}). \tag{73}$$

The  $\delta$  function therefore constrains the product of gauge degrees of freedom along the inner edge of ribbon to the value  $h_g$ , while leaving *only one constraint on the undualized elements of  $SG$*  at the two ends of the ribbon:  $u_N = \tilde{g} \cdot u_0$ . (Recall that actually  $u_N$  is the element on site vertex  $i_A$ , while  $u_0$  is on vertex  $i_B$ .)

A special case that offers insight occurs when the 2-cocycle  $c_h$  is trivial. In that case, using the property Eq. (67) of trivial cocycles, we get

$$w_h^\Gamma(g) = \left( \prod_{t \in \Gamma} W(\sigma_t)^{\epsilon(\sigma_t)} \right) \delta(a_1 \cdots a_N, g) \varepsilon_h^{-1}(g) \prod_{i=1}^N \varepsilon_h(a_i), \tag{74}$$

where  $\varepsilon_h$  is a family of  $U(1)$  valued functions on  $G$  (i.e., a 1-cochain) parametrized by the element  $h$ .

We now show that away from its end points the ribbon operator  $F^{(s,g)}(\Gamma)$  commutes with  $\hat{B}_p^{s'}$  and, therefore, also with the Hamiltonian in Eq. (57). Obviously, the nontrivial situation occurs when the plaquette  $p$  is centered on a site  $i \in \Gamma$ , which is positioned on the inner edge of  $\Gamma$ ; see Fig. 14(a). Note that by definition of the operators, elements  $s \in GG$  and  $s' \in G$ . The product of the two operators is defined in the Hilbert subspace  $\mathcal{K}(\Gamma) \cap \mathcal{K}_p$ . Physically, we do not allow states with a flux-carrying excitation positioned on the ribbon  $\Gamma$  or inside the plaquette  $p$ , as we consider this commutator. We also choose  $p$  that does not overlap with  $i_A$  or  $i_B$ ; i.e., we consider the commutation away from ribbon ends.

It is clear that the final states of the system are the same no matter the order of applying the two operators, since  $G$  is Abelian. The two resulting quantum phases  $\langle f | F^{(s,g)}(\Gamma) \hat{B}_p^{s'} | i \rangle$

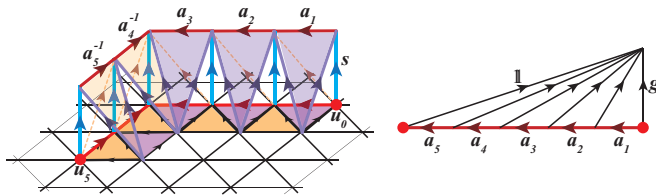


FIG. 13. (Color online) The phase contribution  $w_s^\Gamma(g) = \Psi_\Gamma^s \Theta_\Gamma^s \delta \left( \prod_{n=1}^N a_n, g \right)$  to matrix element of ribbon operator  $F^{(s,g)}(\Gamma)$ , with  $s \in GG$ , on a length  $N = 5$  example. (Left) The operator acts nontrivially only on elements adjacent to path  $\Gamma$  (thick black edges). Note that elements  $a_i \equiv g_{i,i-1} \equiv h_{i,i-1} u_i u_{i-1}^{-1}$  are defined to be directed along the path, so for  $n = 4, 5$  they are opposite to the standard definition, which is along the edge orientation. Elements at ends  $A, B$  of the ribbon  $\Gamma$ , i.e., vertex  $i_A$  and vertex  $i_B$ , are  $u_5 \in SG$  and  $u_0 \in SG$ , respectively. The phase factor  $\Psi_\Gamma^s$  is the product of 3-simplex phases  $W(\sigma_i)^{\epsilon(\sigma_i)}$  shown on top of shaded triangles. (Right) The phase  $\Theta_\Gamma^s$  is the product of 2-simplex phases  $W(\sigma_i)^{\epsilon(\sigma_i)}$  shown, where  $\mathbb{1}$  is the identity element, and the parameter  $g = a_1 \cdots a_N \in G$ .

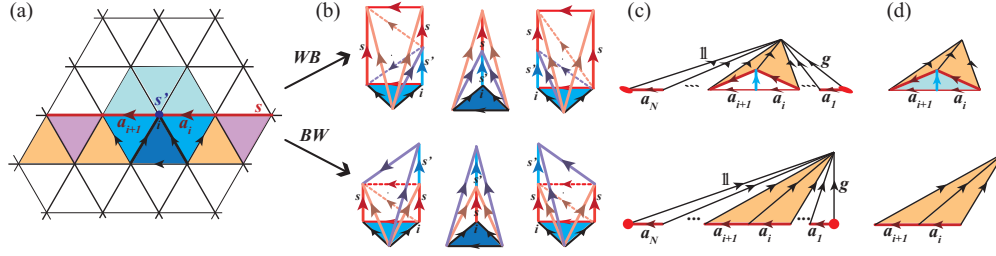


FIG. 14. (Color online) Inner segment of ribbon operator  $F^{(s,g)}(\Gamma)$ , with  $s \in GG$ , commutes with plaquette operator  $\hat{B}_p^{s'}$ , having  $p$  centered on inner edge of  $\Gamma$ , and therefore also with the Hamiltonian. (a) Only elements on two edges (thick black) are changed, but in the same way for  $F\hat{B}$  and  $\hat{B}F$  due to Abelian  $G$ . (b) Quantum phase for  $F\hat{B}$  (top row) and  $\hat{B}F$  (bottom row) differ only due to shown 3-simplices which are on top of three blue shaded triangles in (a). (c) The phase contribution due to string phase  $\Theta$  is shown. (d) The 3-simplices contribution to phase factor ratio  $WB/BW$  (from panel b) equals precisely the phase  $W(\sigma_i)^{\epsilon(\sigma_i)}$  due to two blue 2-simplices [see Eq. (78)]. The  $WB$  (top) and  $BW$  (bottom) cases are therefore graphically seen to be the same, as interior points of the polygon can be removed in a 1-3 move (Fig. 8).

and  $\langle f|\hat{B}_p^{s'}F^{(s,g)}(\Gamma)|i\rangle$  we label by  $wB$  and  $Bw$ , respectively, and we show that their ratio is 1.

The  $wB$  and  $Bw$  differ in their phase factor  $\Theta_\Gamma^s$  (which was defined in Fig. 13), and these are shown on the right of Fig. 14(b). Recalling that  $a_i \equiv g_{i,i-1} = h_{i,i-1} \cdot u_i \cdot u_{i-1}^{-1}$  and  $i = 1, \dots, N$ , the difference is due to operator  $\hat{B}_p^{s'}$  sending

$$\begin{aligned} a_i &\rightarrow s' \cdot a_i \\ a_{i+1} &\rightarrow a_{i+1} \cdot s'^{-1} \end{aligned} \quad (75)$$

[see the basic definition, Eq. (48)], and we remind the reader that  $p$  is centered on the site  $i$ . Due to the product structure in  $\Theta_\Gamma^s$ , there are only two factors affected by this change, and these are the shaded 2-simplices in Fig. 14(b)(right). The ratio of quantum amplitudes is

$$\begin{aligned} \frac{\Theta_{wB}}{\Theta_{Bw}} &= \frac{c_s(A \cdot s'^{-1} \cdot a_i^{-1}, s' \cdot a_i) c_s(A \cdot a_i^{-1} \cdot a_{i+1}^{-1}, a_{i+1} \cdot s'^{-1})}{c_s(A \cdot a_i^{-1}, a_i) c_s(A \cdot a_i^{-1} \cdot a_{i+1}^{-1}, a_{i+1})} \\ &= \frac{c_s(s'^{-1} \cdot a_{i+1}, s')}{c_s(s', a_i)}, \end{aligned} \quad (76)$$

where  $A$  is the product of  $a_{i' < i}$  elements, and we used the 2-cocycle condition [see Eq. (6)].

Further, it is obvious that the phase difference coming from 3-simplices is only due to ones stacked on top of three triangles that are shared by the ribbon and the plaquette, Fig. 14(a), and these simplices are presented in detail in Fig. 14(b). Grouping the phases according to the triangles from left to right, and using the definition of the 2-cocycle [Eq. (63)], we get

$$\begin{aligned} \frac{\Psi_{wB}^1}{\Psi_{Bw}^1} &= c_s(a_{i+1}, h) c_s^{-1}(s'^{-1} \cdot a_{i+1}, s' \cdot h) \omega^{-1}(s', h, s), \\ \frac{\Psi_{wB}^2}{\Psi_{Bw}^2} &= \omega(s', s, h) \omega^{-1}(s, s', h) \omega(s, s', a_i \cdot h) \omega(s', s, a_i \cdot h), \\ \frac{\Psi_{wB}^3}{\Psi_{Bw}^3} &= c_s(s', a_i) \omega(s', s, a_i \cdot h) \omega^{-1}(s, s', a_i \cdot h), \end{aligned} \quad (77)$$

where  $h$  is the element on the leftmost edge of left triangle in Fig. 14(a). The total phase due to 3-simplices becomes

$$\frac{\Psi_{wB}}{\Psi_{Bw}} = \frac{c_s(s', a_i)}{c_s(s'^{-1} \cdot a_{i+1}, s')}. \quad (78)$$

This phase ratio exactly cancels the contribution from the string of 2-cocycles in Eq. (76), completing the proof that the inner piece of ribbon operator commutes with plaquette operators.

We point out in the pictorial interpretation of the result that the 3-simplex contributions to the phase ratio, Eq. (78), are exactly equal to the phase of the two blue-shaded triangles in Fig. 14(c). The total phase ratio is then equal to the ratio of the upper and lower polygons in Fig. 14(c), which obviously equals 1 due to the rule that allows removal of internal points in polygons (rule from Fig. 8).

### C. Local symmetric operators and the twisted extended ribbon algebra

In this section we introduce local symmetric operators which have a nontrivial algebra with the ribbon operators. This will allow us to understand the general structure of excited states. The focus is on states with a single pair of excitations, or two pairs when discussing braiding. The obtained results will be directly relevant for studying examples in Sec. V. The fully general case of many quasiparticle pairs, including their braiding and fusion properties, are studied in detail in Appendix B by using the extended algebra.

Before giving the formal definitions, let us remark that given the positions of excitations, the “extended algebra” contains the set of ribbon operators  $F$  (with their strings connecting pairs of excitations), as well as a set of local operators  $D$  acting at the positions of excitations. However, the presence of the 3-cocycle  $\omega$  adds a twist in the algebra and crucially determines the resulting properties of excitations. It has been shown<sup>61</sup> that certain broken gauge theories with Chern-Simons terms lead to discrete (group  $\tilde{H}$ ) gauge theories having such twisted algebra describing their quasiparticles.<sup>61</sup> In that situation, the cocycle is generated by the Chern-Simons term, and the resulting discrete gauge theory can be classified using  $H^3(\tilde{H}, U(1))$ ,<sup>60</sup> making connection with discrete DW TQFTs. Importantly, a nontrivial cocycle twisting of the algebra can render the resulting theory non-Abelian even though its gauge group  $\tilde{H}$  is Abelian.<sup>62</sup> Our models inherit this interesting property, and we discuss this briefly concerning properties of multiple pairs of excitations in Sec. V G. In Appendix B we also show explicitly how the considered operators of our models form a Hopf algebra (more precisely, a quasitriangular quasi-Hopf

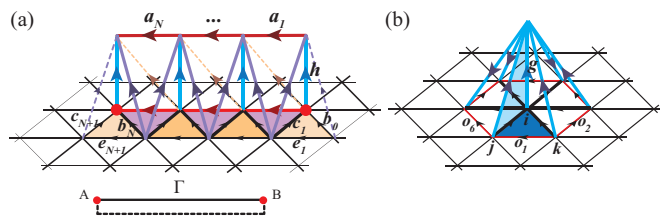


FIG. 15. (Color online) (a) Ribbon operator with both ends (red dots), shown schematically at the bottom. It only acts on the thick black edges, consistent with zero-flux rule on all 2-simplices above and within the ribbon. The transition amplitude of the ribbon is given in Fig. 13 without the phase factor  $f_A f_B f_{AB}$  local at the string ends;  $f$  is involved (Appendix B), but includes the edges of two triangles  $t_A, t_B$  at the ends (shaded light orange). Dashed violet lines indicate edge elements that are not acted on by the operator. (b) The local operator at position  $B \equiv (i, t)$ , with  $i$  the lattice site and triangle  $t$  (dark blue) having vertices  $i, j, k$  (shaded dark blue), has the transition amplitude  $\langle f| D_{(h,g)}(B) |i\rangle = \delta(g_{ij} \cdot g_{jk} \cdot g_{ki}, h) W_h W_6$ . It acts as the plaquette operator  $\hat{B}_p^g$  (Fig. 9) with plaquette  $p$  centered on  $i$  (changing only thick black edge elements), except that it also projects flux in  $t$  to value  $h$ , and also has an additional phase factor  $W_h$ , which is the phase of the 2-simplex (shaded light blue). [For operator  $D(A)$ , the triangle  $iki'$  is used instead.] The phase factor  $W_6$  depends on six drawn 3-simplices (tetrahedrons) having altered elements  $o$  (red edges) such that it is well defined even if the zero-flux rule is violated in the plane (as occurs at ribbon string ends); see after Eq. (79).

algebra due to the cocycle twist; see Refs. 61 and 70) and how they describe the braiding and fusion of excitations.<sup>71</sup>

It is important to emphasize that in the present context the local operators  $D$  are also crucial for determining the interplay of symmetry and topological order: After we explicitly construct the  $D$  operators, we show that they are symmetric, i.e., commute with transformations from  $SG$ , and further we expect them to span the algebra of all local symmetric operators.<sup>72</sup> Thereby the set  $D$  will provide us all symmetry-allowed local perturbations and therefore the possibility of calculating the symmetry protected degeneracy and other properties of excited states in Sec. V.

Let us briefly recall some relevant details about the ribbon operator  $F^{(h,g)}(\Gamma)$  from Sec. IV B; see Fig. 15. By definition, the element  $h \in GG$ , while  $g \in G$ . The operator definition demands that the zero-flux rule is satisfied for all triangles in ribbon  $\Gamma$ ; i.e., it acts within the Hilbert subspace  $\mathcal{K}(\Gamma)$ . The two ends of ribbon  $\Gamma$  we label by  $A, B$ . For this section it is important to recall the structure of the ribbon ends (Fig. 15), which are completely determined by a site and a lattice triangle  $A = (i_A, t_A)$ ,  $B = (i_B, t_B)$  ( $t_A, t_B$  are not considered to be within  $\Gamma$ ).

We next define the local operator  $D_{(h,g)}(B)$  positioned at  $B \equiv (i_B, t_B)$ ; see Fig. 15. [Operator  $D(A)$  is very similar, below.] Let the triangle  $t_B$  have ordered vertices  $k \rightarrow j \rightarrow i$  as in Fig. 15. The  $D_{(h,g)}(B)$  operator acts on the elements in the plaquette centered on  $i_B$  in the same way as the plaquette operator  $\hat{B}_{p=i_B}^g$ ; however,  $D_{(h,g)}(B)$  additionally projects the 2-simplex at  $t_B$  to having flux  $h \in GG$  and also has an additional phase factor. Actually, in contrast to  $\hat{B}_{p=i_B}^g$ , we define the operator  $D_{(h,g)}(B)$  in the entire Hilbert space  $\mathcal{H}$ , as will become clear soon. Let us first state the quantum amplitude

of the local operator:

$$\langle f| D_{(h,g)}(B) |i\rangle = \delta(g_{ij} \cdot g_{jk} \cdot g_{ki}, h) W_h W_6(i), \quad (79)$$

where  $W_h \equiv W_h(\sigma_{ij}, \varphi)^{\epsilon(\sigma_{ij})}$  is the phase of 2-simplex  $\sigma_{ij}$  (light blue shaded in Fig. 15) formed by edge  $ij$  and vertical edge  $g$ , so it equals  $c_h(g, g_{ij})$  (see Fig. 15). Of course, by the definition of group elements on edges, Eq. (45),  $\delta(g_{ij} \cdot g_{jk} \cdot g_{ki}, h) = \delta(h_{ij} \cdot h_{jk} \cdot h_{ki}, h)$  depends only on the elements of gauge group  $GG$ .

The phase  $W_6(i)$  is due to 3-simplices (tetrahedrons) on top of the plaquette; although analogous to the  $\hat{B}_p$  operator (Fig. 9), in this case operator  $D$  has to be well-defined even if the zero-flux rule is violated in the plane, as can occur at the  $t_A, t_B$  of the ribbon  $\Gamma$ . On the other hand, the 3-cocycle can assign a phase to a tetrahedron only if the zero-flux rule is satisfied on all its faces. Because of this, *just for the purpose of calculating the phase due to the six tetrahedrons*  $\prod_{l=1}^6 W(\sigma_l, \varphi)^{\epsilon(\sigma_l)}$ , we redefine the values  $o_1, \dots, o_6$  of elements on six outer edges of the plaquette [red in Fig. 15(b)] such that the zero-flux rule is satisfied in all six triangles of the plaquette in the plane. The six internal edge elements of the plaquette in the plane are considered unchanged from their value in  $|i\rangle$ , and they suffice to fix the redefined values  $o'_1, \dots, o'_6$  on the outer edges of the plaquette according to the zero-flux rule in all six triangles of the plaquette. Formally, this phase contribution is

$$W_6(i) = \langle o'_1, \dots, o'_6; f_1, \dots, f_6 | \hat{B}_p | o'_1, \dots, o'_6; i_1, \dots, i_6 \rangle, \quad (80)$$

with  $i_1, \dots, i_6$  the initial values of elements on six internal edges of plaquette, and  $f_1, \dots, f_6$  their final values. (Note that the redefined values on outer edges  $o'_1, \dots, o'_6$  have to stay the same in the initial and final state.)

It is now clear that operator  $D_{(h,g)}(B)$  is well defined in  $\mathcal{H}$ . Actually, it is also well-defined within the subspace  $\mathcal{K}(\Gamma)$  because it does not influence the flux in triangles belonging to ribbon  $\Gamma$  (recall that by definition  $t_B$  is not inside  $\Gamma$ ).

The definition and properties of the  $D(A)$  operator, relevant due to its action at the  $A$  end of a string, is almost identical to the  $D(B)$  case just described. The only difference is in the phase  $W_h$ , which in this case is not the phase of the 2-simplex  $iji'$  [light blue triangle in Fig. 15(b)], but the 2-simplex  $iki'$  instead.

Obviously, a nontrivial algebra between  $D(A), D(B)$  and  $F$  is due to their overlap at the triangles  $t_A, t_B$ . For concreteness, we presented ribbon ends of the form in Fig. 15, i.e.,  $t_A, t_B$  being the bottom up-pointing triangles, omitting versions rotated by multiples of  $60^\circ$ .

The local operators  $D_{(h,g)}(C)$ , with  $C = A, B$ , are symmetric. As noted before (see discussion of plaquette operator, Sec. III B), a global symmetry transformation  $\tilde{s} \in SG$  does not alter the elements on the edges, leaving the phases in Eq. (79) intact. Further, even though the local operator acts on the site  $i_C$  by the element  $\tilde{g} \in SG$ , where  $g = h_g \cdot \tilde{g}$ ,  $h_g \in GG$ , this action automatically commutes with the action of  $\tilde{s}$  since we have restricted  $G$  to be Abelian in the present analysis of elementary excitations in our models.

We emphasize again that for local operators  $D_{(h,g)}(C)$ , with  $C = A, B$ , by definition  $h \in GG$  while  $g \in G$ .

Having the definitions of ribbon  $\Gamma$  having ends  $C = A, B$ , the ribbon operator  $F(\Gamma)$ , and the local operators  $D(A)$ ,  $D(B)$  at hand, one can tediously but straightforwardly derive the following algebra:

$$D_{(h_2, g_2)}(C) D_{(h_1, g_1)}(C) = \delta_{h_1, h_2} c_{h_1}(g_2, g_1) D_{(h_1, g_1, g_2)}(C), \quad (81a)$$

$$F^{(h_2, g_2)}(\Gamma) F^{(h_1, g_1)}(\Gamma) = \delta_{g_1, g_2} c_{g_1}(h_2, h_1) F^{(h_2, h_1, g_1)}(\Gamma), \quad (81b)$$

$$F^{(h_1, g_2, g_1)}(\Gamma) D_{(h_2, h_1, g_2)}(A) = c_{g_2}(h_2, h_1) c_{h_1}(g_2, g_1) D_{(h_2, g_2)}(A) \times F^{(h_1, g_1)}(\Gamma), \quad (81c)$$

$$D_{(h_2, h_1, g_2)}(B) F^{(h_1, g_2, g_1)}(\Gamma) = c_{g_2}(h_1, h_2) c_{h_1}(g_1, g_2) F^{(h_1, g_1)}(\Gamma) \times D_{(h_2, g_2)}(B), \quad (81d)$$

where Eq. (81a) holds in the entire Hilbert space  $\mathcal{H}$  [and also within  $\mathcal{K}(\Gamma)$ ], while the three other relations hold within the subspace  $\mathcal{K}(\Gamma)$ , where the ribbon operators are well-defined.

To understand the implications of the operator algebra in Eqs. (81), we need to consider the precise form of the excited state. Starting from a two-particle excited state, having excitations at the two ends  $A, B$  of the string  $\Gamma$ , one would expect it to be given by the simple action of the ribbon operator on the ground state:

$$|\psi^{(h, g)}\rangle = F^{(h, g)}(\Gamma)|gs\rangle. \quad (82)$$

These states can be shown to be orthogonal. However, the space  $\mathcal{L}(A, B)$  spanned by these states needs to be specified further. Namely, as Eq. (73) shows, the ribbon operator puts only one constraint on the values of two elements at the lattice sites  $i_A, i_B$ , i.e.,  $u_{i_A} \cdot u_{i_B}^{-1} = \tilde{g} \in SG$ , with the factorization  $g = h_g \cdot \tilde{g}$ . We already know that the local operators transform these elements, e.g., under action of  $D_{(h, g_1)}(A)$ , the element  $u_{i_A} \rightarrow \tilde{g}_1 \cdot u_{i_A}$ , where  $g_1 = h_1 \cdot \tilde{g}_1$ ,  $h_1 \in GG$ ,  $\tilde{g}_1 \in SG$ . We therefore need to specify the value of one element (of either  $u_{i_A}$  or  $u_{i_B}$ ) in the excited state. By using the projectors

$$\hat{P}_u(A)|\{u_i\}, \{g_{ij}\}\rangle = \delta_{u_{i_A}, u} |\{u_i\}, \{g_{ij}\}\rangle, \quad (83)$$

we can consider the subspace  $\mathcal{L}_{u_A}(A, B)$  of the Hilbert space  $\mathcal{H}$  spanned by projected states:

$$|\psi_{u_A}^{(h, g)}\rangle \equiv \hat{P}_{u_A}(A)|\psi^{(h, g)}\rangle, \quad (84)$$

with a fixed element  $u_A \in SG$ . The value of  $u_{i_B}$  is then automatically fixed by the action of ribbon operator  $u_{i_B} = \tilde{g}^{-1} \cdot u_A$ .

Completely analogously we define the subspace  $\mathcal{L}_{u_B}(A, B)$  spanned by  $|\psi_{u_B}^{(h, g)}\rangle \equiv \hat{P}_{u_B}(B)|\psi^{(h, g)}\rangle$ , by using the projector  $\hat{P}_{u_B}(B)$  at the vertex  $i_B$ . Note that the projectors  $\hat{P}(A)$ ,  $\hat{P}(B)$  commute with the ribbon operator  $F(\Gamma)$ . It is also easy to check that  $D_{(h, g)}(C)\hat{P}_{u_C}(C) = \hat{P}_{\tilde{g} \cdot u_C}(C)D_{(h, g)}(C)$ , where  $C$  is either  $A$  or  $B$ , and the usual group element factorization is  $g = h_g \cdot \tilde{g}$ ,  $h_g \in GG$ ,  $\tilde{g} \in SG$ .

The subspaces  $\mathcal{L}_{u_C}(A, B)$  were introduced using the action of ribbon operators on the ground state. The end  $A$  and end  $B$  of ribbon  $\Gamma$ , in principle, carry excitations, and  $\mathcal{L}_{u_C}(A, B)$  does not depend on the particular shape of  $\Gamma$  (as long as  $\Gamma$  does not change topological class). It is, however, not trivial to prove that the subspace  $\mathcal{L}(A, B) = \bigoplus_{u_C \in SG} \mathcal{L}_{u_C}(A, B)$ , with  $C$  either  $A$  or  $B$ , actually exhausts all possible excited states with two

quasiparticles positioned at  $A$  and  $B$ . In Appendix E we prove that the space  $\mathcal{L}(A, B)$  indeed contains all such excited states. (We do not, however, have a proof that all multiparticle states having more than two particles are also given by the action of appropriate ribbon operators on the ground state.)

Now that we established the appropriate Hilbert space, it is easy to show that the local operators form a unitary projective representation of the group  $G$  within this two-particle Hilbert space. We give the precise definition and explicit proof of this fact in Appendix E.

Let us next show that the local operators, as well as the ribbon operators, form Hopf algebras. (The succinct notation we introduce here will be useful in Appendix E.) More precisely, let us denote the algebra formed by local operators  $D_{(h, g)}(A)$ , with  $h \in GG$ ,  $g \in G$ , by the symbol  $\mathbb{D}(A)$ . Analogously, the operators  $D_{(h, g)}(B)$  form the algebra  $\mathbb{D}(B)$ . Since  $\mathbb{D}(A)$  and  $\mathbb{D}(B)$  are formally algebraically the same, we use  $\mathbb{D}$  to denote this abstract algebra, keeping in mind that  $\mathbb{D}(A)$  and  $\mathbb{D}(B)$  act at physically different positions. The algebra of ribbon operators  $F^{(h, g)}$ ,  $h \in GG$ ,  $g \in G$ , having ribbon  $\Gamma$ , will be denoted by  $\mathbb{F}$ . We now consider the subspace  $\mathcal{K}(\Gamma)$  of Hilbert space, so that all these operators are simultaneously well-defined, and Eqs. (81) holds.

To start with, the operator relations in Eqs. (81) can be rewritten succinctly using double index notation: The Latin indices  $i, j, k, \dots, r$  are shorthand for group element pairs  $i \equiv (h_i, g_i)$ ,  $j \equiv (h_j, g_j)$ , etc., with  $h_i, h_j, \dots \in GG$  and  $g_i, g_j, \dots \in G$ . We can then write

$$D_m(C) D_n(C) = \Omega_{mn}^k D_k(C), \quad (85a)$$

$$F^m(\Gamma) F^n(\Gamma) = \Lambda_k^{mn} F^k(\Gamma), \quad (85b)$$

$$F^m(\Gamma) D_i(A) = \Lambda_i^{jk} \Omega_{kl}^m D_j(A) F^l(\Gamma), \quad (85c)$$

$$D_i(B) F^m(\Gamma) = \Lambda_i^{kj} \Omega_{lk}^m F^l(\Gamma) D_j(B), \quad (85d)$$

where we defined the tensors

$$\Omega_{ij}^k \equiv \delta_{h_i, h_j} \delta_{h_k, h_i} \delta_{g_k, g_i g_j} c_{h_k}(g_i, g_j), \quad (86a)$$

$$\Lambda_k^{ij} \equiv \delta_{g_i, g_j} \delta_{g_k, g_i} \delta_{h_k, h_i h_j} c_{g_k}(h_i, h_j), \quad (86b)$$

and summation over repeated double indices is understood as, e.g.,  $\sum_i \equiv \sum_{h_i \in GG, g_i \in G}$ .

The tensors in Eqs. (86) contain the twist due to the cocycle  $\omega$  present in our models. Similar realizations of twisted algebra, but describing broken gauge theories, are analyzed in, e.g., Ref. 71. We also note that only when the cocycle is trivial,  $\omega(g_1, g_2, g_3) \equiv 1 \Rightarrow c_g(g', g'') = 1$ , do these tensors reduce to the form occurring in the generalization of toric code to arbitrary finite groups, as given in Ref. 65.

To derive the properties of this algebra, we have to use several properties of a 2-cocycle  $c$  derived from an arbitrary 3-cocycle  $\omega$  [Eq. (63)], listed here for convenience:

$$c_a(g, h) c_a(gh, s) = c_a(h, s) c_a(g, hs), \quad (87a)$$

$$c_a(g, h) c_b(g, h) c_g(a, b) c_h(a, b) = c_{gh}(a, b) c_{ab}(g, h), \quad (87b)$$

$$c_a(g, h) = 1, \text{ if any of } a, g, h \text{ equals } \mathbb{1}, \quad (87c)$$

$$c_a(g, g^{-1}) = c_a(g^{-1}, g). \quad (87d)$$

(We note that all these properties actually hold generally, i.e., for arbitrary elements  $a, b, g, h, s \in G$ .) The identity (87a) is the general condition for a 2-cocycle, Eq. (87b) can be derived directly using the definition Eq. (63), identity (87c) follows from our choice to use only canonical cocycles  $\omega$  ( $\mathbb{1}$  is the identity group element), and finally the useful relation (87d) follows from Eqs. (87a) and (87c).

Using these identities we can prove that the ribbon and local operators form Hopf algebras.

A basic axiom of Hopf algebra is the associativity of multiplication with identity, which holds for  $F$  and  $D$  algebras, as shown by the following two relations, respectively:

$$\Lambda_i^{lm} \Lambda_k^{in} = \Lambda_k^{lj} \Lambda_j^{mn}, \quad \epsilon_i \Lambda_k^{im} = \epsilon_j \Lambda_k^{mj} = \delta_k^m, \quad (88a)$$

$$\Omega_{lm}^i \Omega_{in}^k = \Omega_{lj}^k \Omega_{mn}^j, \quad e^i \Omega_{im}^k = e^j \Omega_{mj}^k = \delta_m^k, \quad (88b)$$

where for double indices the Kronecker  $\delta$  function  $\delta_j^i \equiv \delta_{h_i, h_j} \delta_{g_i, g_j}$  and the functions  $\epsilon_i \equiv \delta_{h_i, \mathbb{1}}$ ,  $e^i \equiv \delta_{g_i, \mathbb{1}}$  define the unit and counit of the algebras,  $\mathbb{1}_{\mathbb{F}} = \epsilon_k F^k$ ,  $\mathbb{1}_{\mathbb{D}} = e^k D_k$ ,  $\hat{e}(F^k) = e^k$ , and  $\hat{\epsilon}(D_k) = \epsilon_k$ . Both Eqs. (88a) and (88b) hold due to Eqs. (87a) and (87c).

The comultiplication in the Hopf algebra is physically related to fusion, and instead of presenting a formal definition here, we show in Sec. IV D and Appendix B that the braiding and fusion properties of excitations are consistent and contain the twist by the 3-cocycle characteristic of a quasi-Hopf algebra first introduced in Ref. 70.

Having established the Hopf algebra relations in Eqs. (88a) and (88b), we are in a position to prove that all two-particle excited states in our models are indeed within the Hilbert subspace  $\mathcal{L}(A, B)$  we defined in this section. The proof is presented in Appendix E and is based on a derivation given in Ref. 65. This Hilbert space for an excitation pair is especially important here since it will be studied explicitly for several example groups in Sec. V.

In summary, the local operators are the set of nontrivial operators acting on excitations, and they are also symmetric and form a projective representation of the group. We use these properties to study the symmetry protected properties of our models in Sec. V.

We close this subsection by briefly introducing the Hilbert space of many-particle excitations. (It is studied in more detail in Appendix B.) Let us consider a system having  $n$  quasiparticles at positions  $A_1, \dots, A_n$ , and one quasiparticle at position  $B$ , and no other excitations. Such a system is described by the Hilbert space  $\tilde{\mathcal{L}}(A_1, \dots, A_n, B)$ . To study these states, we consider a space  $\mathcal{L}(A_1, \dots, A_n, B)$  spanned by the action of ribbon operators, as described in the following. Let us connect each position  $A_i$  through a ribbon  $\Gamma_i$  having end- $A_i$  to the common isolated position  $B$ . Therefore, all ribbons' end  $B_i$  coincide, and all are equal to  $B$ . (For further discussion and lattice realization, see Appendix B.) Focusing on the subspace  $\mathcal{K}(\Gamma_1, \dots, \Gamma_n)$  in which all ribbon operators having ribbons  $\Gamma_i$  are simultaneously well-defined (i.e., zero-flux rule obeyed inside all ribbons), we can now define its subspaces  $\mathcal{L}_{u_B}(A_1, \dots, A_n, B)$  spanned by states of the form

$$|\psi_{u_B}^{k_1, \dots, k_n}\rangle = \hat{P}_{u_B}(B) F^{k_1}(\Gamma_1) \dots F^{k_n}(\Gamma_n) |g_S\rangle. \quad (89)$$

The states in Eq. (89) form the subspaces with  $u_B$  fixed. We actually expect that the space  $\tilde{\mathcal{L}}(A_1, \dots, A_n, B)$  coincides with

the space  $\mathcal{L}(A_1, \dots, A_n, B) = \bigoplus_{u_B \in SG} \mathcal{L}_{u_B}(A_1, \dots, A_n, B)$ . [We have a proof of this only in the two-particle case (see Appendix E), but, as mentioned, this is hard to prove in general.]

At the same time, the extended algebra of each given ribbon  $F(\Gamma_i)$  contains the local operators  $D_k^{(i)} \equiv D_k(B)$  which we define to affect only that (i.e., the  $i$ th) ribbon. These operators, being local at  $B$ , commute with all local operators  $D_m(A_j)$ ,  $j = 1, \dots, n$  at the excitations  $A_j$ . The  $D_k^{(i)}$  operators therefore act, in view of Eq. (85d), as

$$D_{j_1}^{(1)} \otimes \dots \otimes D_{j_n}^{(n)} |\psi_{u_B}^{k_1, \dots, k_n}\rangle = \Omega_{m_1 j_1}^{k_1} \dots \Omega_{m_n j_n}^{k_n} |\psi_{u_B}^{m_1, \dots, m_n}\rangle. \quad (90)$$

In this definition we constrain the elements in  $D(B)$  strictly to  $GG$ , e.g., the double index  $j = (h_j, h_{g_j}) \in GG$ . This constraint to  $GG$  elements is exactly encountered when describing braiding in the next section.

Because the  $D_k^{(i)}$  operators are nonlocal with respect to the excitations at  $A_i$  while commuting with  $\mathbb{D}(A_i)$  they are called "topological operators."<sup>65</sup>

Topological operators and braiding in many-particle states are analyzed in detail in Appendix B.

## D. Braiding matrix

In this section we calculate the braiding matrix of two quasiparticles, restricting ourselves to a system that has quasiparticles at most at three positions,  $A_1, A_2, B$  (see previous section). An alternative and more explicit way to obtain the braiding properties of quasiparticles is by considering ribbons of strings that cross, but this approach is applicable to Abelian quasiparticles only; we present it in Appendix C and show there that the results of the two approaches agree for Abelian quasiparticles. The braiding as well as fusion in states with many quasiparticles introduce additional subtleties, and this situation is presented in detail in Appendix B. Here we focus only on braiding of two particles and show that the braiding properties are entirely determined by the topological order, i.e., the gauge group  $GG$ . The effects of interplay of topological order and symmetry are revealed in the concrete examples in Sec. V.

Recall that we define the ribbon operator matrix element [see Eq. (71)] such that the operator algebra in Sec. IV C is obtained. (The matrix element is fully presented in Appendix B.) That definition also leads to the following algebra for two ribbon operators having strings  $\Gamma_1, \Gamma_2$  which share their  $B$  end:

$$\begin{aligned} & F^{(h_2, g_2)}(\Gamma_2) F^{(h_1, g_1)}(\Gamma_1) \\ &= c_{h_1}(g_1 h_2^{-1}, h_2) F^{(h_1, g_1 h_2^{-1})}(\Gamma_1) F^{(h_2, g_2)}(\Gamma_2) \frac{\omega(h_2, h_1, h_B)}{\omega(h_1, h_2, h_B)}, \end{aligned} \quad (91)$$

where  $h_B$  is the value of flux in triangle  $t_B$ . Equation (91) is well-defined only in the subspace  $\mathcal{K}(\Gamma_1, \Gamma_2)$  of the Hilbert space, i.e., when zero-flux is obeyed in every triangle inside  $\Gamma_1$  or  $\Gamma_2$  (note that  $t_B$  is outside both ribbons). Figure 16(a) sketches this situation, which will enable us to determine the braiding of the two quasiparticles at the end  $A_1$  and end  $A_2$ . (Appendix B considers in detail the case when the end  $A$  is shared by the ribbons.)

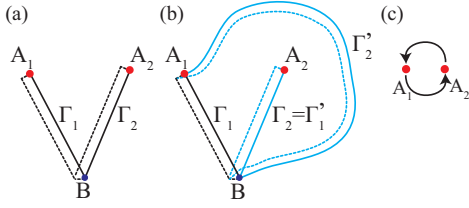


FIG. 16. (Color online) (a) Ribbon operators for two-particle excited state and braiding two excitations at  $A_1, A_2$  (see also Fig. 15). The common end point  $B$  contains no excitation, but “topological” operators of  $i$ th ribbon  $D^{(i)}(B)$ ,  $i = 1, 2$ , local at  $B$ , can be used to represent braiding. (b) Applying different ribbons (blue) than in original state shown in (a) leads to a braided state (see Sec. IV D). (c) The resulting counterclockwise braid of particles 1 and 2.

The 3-cocycle factor on the right-hand side of Eq. (91) has to be considered with care in a many-particle situation, as is done in Appendix B; in this section we, however, focus on a system with only the two ribbons  $\Gamma_1, \Gamma_2$ . Because of this, a product of two ribbon operators, such as appearing on both sides of Eq. (91), can only act on the ground state; i.e., there are no other excitations in the system. Because of this, the value of flux in triangle  $t_B$  on the right-hand side of Eq. (91) is necessarily zero, which means that the element  $h_B = \mathbb{1}$  (see also Appendix B). Due to our choice of canonical cocycles, the two  $\omega$  factors on the right of Eq. (91) therefore disappear.

Let us now formally introduce the braiding matrix relevant for ribbons sharing their end  $B$  by rewriting Eq. (91) in a compact form,

$$F^j(\Gamma_2) F^l(\Gamma_1) = R^{qr} \Omega_{mr}^l \Omega_{nq}^j F^m(\Gamma_1) F^n(\Gamma_2), \quad (92)$$

where according to Eq. (91), the  $R$  matrix of our model equals  $R^{ik} = \delta_{h_i, g_k} \delta_{g_i, \mathbb{1}}$ .

We now calculate the operator  $\mathcal{R}_{CC}$  describing the counterclockwise braiding operation by  $180^\circ$  of the two excitations positioned at  $A_1$  and  $A_2$ . This operator is defined by setting  $|\psi^{ab}\rangle_{\text{braid}} = \mathcal{R}_{CC} |\psi^{ab}\rangle$ . We consider the original state, Fig. 16(a), and the one where excitations are exchanged [Fig. 16(b)] by braiding particle 2 counterclockwise around particle 1:

$$|\psi_{u_B}^{ab}\rangle = \hat{P}_{u_B}(B) F^a(\Gamma_1) F^b(\Gamma_2) |gs\rangle \quad (93)$$

$$|\psi_{u_B}^{ab}\rangle_{\text{braid}} = \hat{P}_{u_B}(B) \mathcal{R}_{CC} |\psi^{ab}\rangle \quad (94)$$

$$= \hat{P}_{u_B}(B) F^a(\Gamma'_1) F^b(\Gamma'_2) |gs\rangle, \quad (95)$$

where we used the double index notation, i.e.,  $a \equiv (h_a, g_a), b \equiv (h_b, g_b)$ . Note that we choose to project the states by fixing the value of  $u_{i_B}$  equal to  $u_B$ ; the ribbon operators then determine the values of  $u_{i_{A_1}}, u_{i_{A_2}}$  [see the definition in Eq. (84)].

According to the definition of states in Eq. (89), the order of applying ribbon operators reflects the order of particles, while the new strings  $\Gamma'_1, \Gamma'_2$  compared to original ones  $\Gamma_1, \Gamma_2$  represent the braiding movement. Figures 16(a) and 16(b) illustrate this. We see that the new string of particle 1 coincides with the old string of particle 2,  $\Gamma'_1 = \Gamma_2$ , while the new string  $\Gamma'_2$  is topologically equivalent (and the operator therefore the same) to  $\Gamma_1$  only if there is no particle at original position of 2 at the time these two strings are compared; see Fig. 16(b).

Therefore, the new ribbon operator on  $\Gamma'_2$  is the same as a ribbon on  $\Gamma_1$  if it is applied before the new  $\Gamma'_1$ . This is actually true in Eq. (94), and we therefore have

$$F^a(\Gamma'_1) F^b(\Gamma'_2) = F^a(\Gamma_2) F^b(\Gamma_1). \quad (96)$$

We now only need to commute the ribbon operators to make a comparison to Eq. (93). The commutation relation in Eq. (92) directly gives

$$\hat{P}_{u_B}(B) \mathcal{R}_{CC} |\psi^{ab}\rangle = R^{qr} \Omega_{mr}^b \Omega_{nq}^a |\psi_{u_B}^{mn}\rangle \quad (97)$$

$$= R^{qr} D_r^{(1)} \otimes D_q^{(2)} |\psi_{u_B}^{ba}\rangle. \quad (98)$$

We note that the  $R^{qr}$  matrix in this expression constrains the group elements in  $D^{(1,2)}$  to be strictly in  $GG$ , e.g.,  $r \equiv (h_r, h'_r \cdot \tilde{g}_r)$ ,  $h_r, h'_r \in GG$ , is constrained to  $\tilde{g}_r = \mathbb{1}_{SG}$ ; this implies that the site element  $u_{i_B}$  is not changed from its value  $u_B$  by the action of  $D^{(1)}, D^{(2)}$ . The explicit form of the braiding operation is therefore

$$\mathcal{R}_{CC} |\psi_{u_B}^{ab}\rangle = c_{h_b}(g_b h_a^{-1}, h_a) |\psi_{u_B}^{(h_b, g_b h_a^{-1})(h_a, g_a)}\rangle, \quad (99)$$

which one can of course obtain directly using the commutation in Eq. (91), without first defining the  $R^{ik}$  matrix. The result nontrivially involves the cocycle  $\omega$  of our model.

Applying  $\mathcal{R}_{CC}$  twice, we obtain for the  $360^\circ$  braiding

$$\mathcal{R}_{CC}^2 |\psi_{u_B}^{ab}\rangle = c_{h_a}(g_a h_b^{-1}, h_b) c_{h_b}(g_b h_a^{-1}, h_a) |\psi_{u_B}^{(h_a, g_a h_b^{-1})(h_b, g_b h_a^{-1})}\rangle \\ = D_{(h_a, h_b)}^{(1)} \otimes D_{(h_b, h_a)}^{(2)} |\psi_{u_B}^{ab}\rangle, \quad (100)$$

where we remind that  $D_g^{(i)} \equiv D_g(B)$  is acting on the  $i$ th ribbon operator in the product state Eq. (89).

The case when the braided quasiparticles are positioned at  $B$  ends of their ribbons which share the end  $A$ , is similar and discussed in detail in Appendix B. Here we just quote the result for the  $2\pi$  braiding of particles at end  $B_1$  and end  $B_2$ :

$$\bar{\mathcal{R}}_{CC}^2 |\bar{\psi}_{u_A}^{ab}\rangle = D_{(h_a^{-1}, h_b^{-1})}^{(1)} \otimes D_{(h_b^{-1}, h_a^{-1})}^{(2)} |\bar{\psi}_{u_A}^{ab}\rangle, \quad (101)$$

where we use the bar over symbols to signify that the state and braiding concern particles at end  $B$ 's of strings.

Equations (100) and (101) explicitly show that the braiding of quasiparticles is described by the action of “topological operators” [see Eq. (90)], which act only on the gauge degrees of freedom, obviously since they are labeled only by elements  $h_a, h_b \in GG$ . This fact means that the braiding properties follow directly from the topological order in our models, which is described by the gauge group  $GG$ . In Appendix B we show explicitly that the topological operators form an algebra called “quasi-quantum double,”<sup>70,71</sup> which is mathematically a realization of a quasi-Hopf algebra. The prefix “quasi” denotes the presence of the twist by cocycle  $\omega$ , which is here restricted to elements of  $GG$ . Appendix B also clarifies how representations of the quasiquantum double label the quasiparticle species, while the multiplication and comultiplication operations in the algebra directly determine the braiding and fusion of quasiparticles.

The quasiquantum double construction, i.e., the presence of a cocycle twist in the algebra of braiding and fusion operators, appeared in the description of excitations in gauge theories broken to a discrete subgroup.<sup>61</sup> This is to be expected since



both those theories and our models describe topological order classified by DW TQFTs.<sup>52,61</sup>

In Appendix B we also discuss in detail the situation with an arbitrary number of quasiparticles (either end- $A$  or end- $B$  ones), describing their braiding and fusion as well as the quasi-quantum double mathematical structure.

## V. EXAMPLES

As will become clear through this section, the gauge charge and gauge flux quasiparticles in our theories do not behave in the same way regarding the phenomena of symmetry fractionalization. We therefore focus on the gauge fluxes, which have nontrivial properties, while leaving the case of gauge charges, which behave trivially, to Sec. VF.

At the end of this section, we also discuss the degeneracy of states with multiple quasiparticle pairs by considering the dualization of the global symmetry  $SG$ .

### A. Hilbert space for a pair of gauge fluxes

We now analyze the properties of excitations in our exactly solvable models, as announced in Sec. II. We later study in detail examples where the groups  $SG$  and  $GG$  are products of  $Z_2$ . In general, we study a pair of gauge fluxes positioned at the ends  $A$  and  $B$  (which also label the lattice sites there) of a string  $\Gamma$ , created by the action of a ribbon operator,

$$|h_v, g; u_A\rangle \equiv |\psi_{u_A}^{(h_v, g)}\rangle = \hat{P}_{u_A}(A)F^{(h_v, g)}(\Gamma)|g_S\rangle, \quad (102)$$

where we introduced more succinct notation. These projected states span  $\mathcal{L}(A, B, h_v)$ . According to the general definition of ribbon operators,  $h_v \in GG$  and  $g \in G = SG \times GG$ , and we label the unique factors of the latter element as  $g = h_g \cdot \tilde{g}$ , with  $h_g \in GG$ ,  $\tilde{g} \in SG$ . The value of  $u_B$  is automatically fixed by the action of ribbon operator  $u_B = \tilde{g}^{-1} \cdot u_A$ , with  $u_A, u_B \in SG$ . We focus on a pair of gauge fluxes, so that  $h_v$  is chosen as a fixed nontrivial element of  $GG$ . (In  $Z_2$  gauge theory, such a flux quasiparticle is called ‘‘vison’’.)

Recalling the discussion in Sec. IV C,  $D_{(h_v, g)}(A)\hat{P}_{u_A}(A) = \hat{P}_{\tilde{g} \cdot u_A}(A)D_{(h_v, g)}(A)$  because the local operators transform these elements, e.g.,  $u_A \rightarrow \tilde{g} \cdot u_A$  with  $g = h \cdot \tilde{g}$ ,  $h \in GG$ ,  $\tilde{g} \in SG$ . The action of local operators on the Hilbert space of the gauge flux pair having flux  $h_v$  is therefore given by

$$\begin{aligned} D_{[g_1]}(A)|h_v, g; u_A\rangle &= c_{g_1}^{-1}(h_v, h_v^{-1})c_{h_v}(g_1, g)|h_v, g_1 \cdot g; \tilde{g}_1 \cdot u_A\rangle, \\ D_{[g_1]}(B)|h_v, g; u_A\rangle &= c_{h_v}(g_1^{-1} \cdot g, g_1)|h_v, g_1^{-1} \cdot g; u_A\rangle, \end{aligned} \quad (103)$$

where we remind the reader that  $g_1 = h_1 \cdot \tilde{g}_1$ ,  $h_1 \in GG$ ,  $\tilde{g}_1 \in SG$ , and since the flux  $h_v$  is fixed we introduced the shorthand notation  $D_{[g]}(A) \equiv D_{(h_v^{-1}, g)}(A)$  and  $D_{[g]}(B) \equiv D_{(h_v, g)}(B)$ . Our analysis of the examples will use Eqs. (103) to explicitly construct the matrices of local operators in this basis.

### B. Construction of local symmetry operators in symmetry-fractionalized models

Let us now, from a general viewpoint, consider the possibility of symmetry fractionalization in our models. According

to Eq. (20), we seek to factorize the global symmetry transformation  $U(\tilde{g} \in SG)$ , when acting in the flux-quasiparticle Hilbert space  $\mathcal{L}(A, B, h_v)$ , into two local factors:

$$U(\tilde{g}) = U_{\tilde{g}}(A) \cdot U_{\tilde{g}}(B), \quad \tilde{g} \in SG. \quad (104)$$

First of all, we observe that the global symmetry transformation  $\tilde{g}$  acts by transforming elements on each lattice site  $i$  by sending  $u_i \rightarrow u_i \cdot \tilde{g}^{-1}$ , while the operators  $D$  perform a similar operation on a single site, i.e., *locally*, for example  $D_{(h, g)}(A) : u_{iA} \rightarrow \tilde{g} \cdot u_{iA}$ , where  $g = h_g \cdot \tilde{g}$ ,  $h_g \in GG$ ,  $\tilde{g} \in SG$ . (Recall that we deal with Abelian groups  $G$  here.) This is reasonable, since for any local operator in  $\mathcal{L}(A, B, h_v)$ , such as the tentative  $U_{\tilde{g}}(C)$ , we expect that it is representable in terms of the local operators  $D(C)$ .

We therefore see that whenever symmetry fractionalization occurs, it should be possible to find a local phase  $\varphi$  such that  $U_{\tilde{g}}(C) = e^{i\varphi(h_v, \tilde{g}, C)}D_{(h, \tilde{g}^{-1})}(C)$ , where  $\tilde{g} \in SG$  and  $C = A, B$ . [Note that although the phase  $\varphi(C)$  can depend on local variables at  $C$ , e.g., on  $u_C$ , the functional form cannot depend on the position  $C$ , since the local symmetry operation cannot depend on the spatial position at which it is applied.] We now show under which conditions (i.e., for what kind of 3-cocycle  $\omega$ ) it is possible to find such a phase  $\varphi$ .

We can effectively use the demand on the global symmetry transformation  $U(\sigma)$  which says that  $U(\sigma)$  commutes with the ribbon operator creating the quasiparticles; more precisely, only  $u_A, u_B$  of the projected basis vectors [Eq. (102)] in  $\mathcal{L}(A, B, h_v)$  are transformed by  $u_C \rightarrow \sigma^{-1} \cdot u_C$ . Tentatively writing  $U_\sigma(A) = D_{(h_v^{-1}, \sigma^{-1})}(A)$ ,  $U_\sigma(B) = D_{(h_v, \sigma^{-1})}(B)$  (note that the gauge fluxes at end  $A$  and end  $B$  are  $h_v^{-1}$  and  $h_v$ , respectively), with  $\sigma \in SG$ , we get

$$\begin{aligned} U_\sigma(A)U_\sigma(B)|h_v, g; u_A, u_B\rangle &= \epsilon_{h_v, \sigma^{-1}, g} c_{\sigma^{-1}}^{-1}(h_v, h_v^{-1})|h_v, g; \sigma^{-1} \cdot u_A, \sigma^{-1} \cdot u_B\rangle, \end{aligned} \quad (105)$$

where we have introduced the 1-cocycle

$$\epsilon_{x, y, z} \equiv \frac{c_x(z, y)}{c_x(y, z)}, \quad x, y, z \in G. \quad (106)$$

Obviously, with this choice of  $U(C)$ , the quasiparticle state is properly transformed only up to a phase, but we can proceed to absorb the resulting phase by a nontrivial  $\varphi(C)$ . We need some useful properties of the introduced 1-cocycle:

$$\begin{aligned} \epsilon_{x, y, z \cdot w} &= \epsilon_{x, y, z} \epsilon_{x, y, w}, \\ \epsilon_{x, y, z} &= \epsilon_{y, z, x} = \epsilon_{z, x, y} = \epsilon_{y, x, z}^{-1} = \epsilon_{x, z, y}^{-1} = \epsilon_{z, y, x}^{-1}, \\ \epsilon_{x, y, z} &= \epsilon_{x, y, z}^{-1}. \end{aligned} \quad (107)$$

Using the fact that  $g = h_g \cdot u_A u_B^{-1}$  and the listed properties of  $\epsilon$ , we can define a valid phase  $\varphi$  by

$$\begin{aligned} U_\sigma(A) &\equiv \sqrt{c_{\sigma^{-1}}(h, h^{-1})} \epsilon_{h, \sigma^{-1}, u_A} D_{(h, \sigma^{-1})}(A), \\ U_\sigma(B) &\equiv \sqrt{c_{\sigma^{-1}}(h, h^{-1})} \epsilon_{h, \sigma^{-1}, u_B} D_{(h, \sigma^{-1})}(B). \end{aligned} \quad (108)$$

Note that the  $h$  in  $U_\sigma(A)$  ( $U_\sigma(B)$ ) is defined to be the gauge flux at the end  $A$  (end  $B$ ), which can be measured locally. This

leads to

$$\begin{aligned} U_\sigma(A)U_\sigma(B)|h_v, g; u_A, u_B\rangle \\ = \epsilon_{h_v, \sigma^{-1}, h_g} |h_v, g; \sigma^{-1} \cdot u_A, \sigma^{-1} \cdot u_B\rangle \\ = \epsilon_{h_v, \sigma^{-1}, h_g} U(\sigma) |h_v, g; u_A, u_B\rangle. \end{aligned} \quad (109)$$

Symmetry fractionalization  $U(\sigma) = U_\sigma(A)U_\sigma(B)$  can therefore occur if

$$\epsilon_{h_v, \sigma, h_g} = 1, \quad \forall h_v, h_g \in GG, \quad \sigma \in SG. \quad (110)$$

It is not physical to absorb this phase factor into the local operators  $U_\sigma(C)$ . The reason is that the phase depends on the element value  $h_g$  carried by the quasiparticles (recall the definition of ribbon operators Eq. (73):  $h_g = h_{1,0} \cdots h_{N,N-1} \in GG$  for a ribbon on lattice sites  $0, \dots, N$ ), while, on the other hand, the symmetry transformation should not depend on such specific properties of the quasiparticles. The presented argument at least gives an indication when symmetry fractionalization should be impossible. We will see that for  $GG = Z_2 \times Z_2$  and  $SG = Z_2$  there is one 3-cocycle,  $\omega^{(123)}$  (see Table III), for which Eq. (110) is violated, in accordance with our claim about a single  $Z_2$  index beyond SFC (see example “3” at the end of Sec. IIC). For that example, we additionally show that global symmetry *exchanges* the two species of excitations, thus giving a strong physical argument against the possibility of representing symmetry by local operators.

In Appendix F we show that this construction of fractionalized symmetry operators is generally correct for multiple quasiparticles in the examples below.

Returning to the present single-ribbon case, let us for a moment assume that symmetry fractionalization is explicitly possible in a given model, i.e., Eq. (110) is satisfied. We can then give general formulas for the transformation of a single quasiparticle at position  $C$  under fractionalized symmetry transformations  $U_\sigma(C)$ , where again  $C = A, B$  is either end of ribbon. The fractionalized symmetry transformations physically only need to be projective, as discussed in Sec. IIB. In the examples of the following sections, these general expressions will be used to check whether the symmetry group generators obey the SFC relations shown at the end of Sec. IIB. [The results will be corroborated by explicit constructions of  $U_\sigma(C)$ ]. Because our examples will be based on the group  $Z_2$  and on direct products of the group  $Z_2$ , we can make some simplifications. Namely, we can set  $h_v^{-1} = h_v$ . Further, considering arbitrary symmetry operations  $\tilde{g}_0, \tilde{g}_1, \tilde{g}_2 \in SG$ , we have that  $\tilde{g}_0^2 = \tilde{g}_1^2 = \tilde{g}_2^2 = \mathbb{1}$ , with  $\mathbb{1}$  the group identity element. Finally, for such groups the inequivalent cocycles  $\omega$  can be chosen to only take values  $\pm 1$ , see Tables I and III. Now, using Eqs. (103) and (108), as well as properties of the 2-cocycle [see Eqs. (87a)–(87d)], it is easy to show that in the Hilbert space of a  $h_v$  flux pair:

$$U_{\tilde{g}_2}(C)U_{\tilde{g}_1}(C) = \epsilon_{h_v, \tilde{g}_2, \tilde{g}_1} U_{\tilde{g}_1}(C)U_{\tilde{g}_2}(C), \quad (111)$$

$$U_{\tilde{g}_0}(A)^2 = c_{h_v}(\tilde{g}_0, \tilde{g}_0) c_{\tilde{g}_0}(h_v, h_v), \quad (112)$$

$$D_{[\tilde{g}_0]}(A)^2 = c_{h_v}(\tilde{g}_0, \tilde{g}_0), \quad (113)$$

where the fluxes are positioned at ribbon ends  $C = A, B$ . In Eq. (113) we show the result for the standard local operator  $D$ , to contrast it with the fractionalized symmetry operator in

TABLE I. Inequivalent basic 3-cocycles  $\omega^{(l)}$  for  $G \equiv GG \times SG = Z_2 \times Z_2$ , which label classes in  $H^3(G, U(1)) = Z_2^3$ . A cocycle  $\omega(x, y, z)$  has value 1, *except* when the group elements  $x, y, z \in G$  take the special values shown in the table, in which case  $\omega(x, y, z)$  is equal to  $-1$ . The element notation  $x = (g_1, g_2)$  signifies the direct product factorization, i.e.,  $g_1 \in GG$  and  $g_2 \in SG$ , and the elements of  $Z_2$  are 0, 1 (additive group action). The star symbol  $*$  stands for “any value of element.”

$\omega(x, y, z) = -1$	$x, y, z$
$\omega^{(1)}$	$(1, *, (1, *), (1, *))$
$\omega^{(2)}$	$(*, 1), (*, 1), (*, 1)$
$\omega^{(12)}$	$(1, *), (*, 1), (*, 1)$

Eq. (112) (in both cases the operator on the right-hand side is just the identity operator).

Equipped with this formalism, we can proceed to solve the instructive examples introduced in Secs. IIB and IIC.

### C. The simplest example with symmetry fractionalization (PSG): Vison pair in $GG = Z_2$ and $SG = Z_2$

Let us from now on use the additive notation for our groups, i.e., any element  $g \in Z_2$  takes values  $g = 0, 1$ , with 0 the identity element, and the group product becomes addition  $g_1 \cdot g_2 \equiv g_1 + g_2 \pmod{2}$ .

The different classes of phases described by our models are classified by the inequivalent 3-cocycles  $\omega$ . An explicit expression for all representatives of inequivalent 3-cocycles in the case where the group is a product of  $Z_n$  factors is given in Ref. 60, and the result for the case  $G = Z_2 \times Z_2$  is shown in Table I. This means that there are three indices  $p_1, p_2, p_3 \in Z_2$ , labeling the elements of  $H^3(SG \times GG, U(1)) = Z_2^3$ . The trivial phase has  $p_1 = p_2 = p_3 = 0$  and can be described by the trivial cocycle  $\omega(x, y, z) = 1, \forall x, y, z \in G$ . When an index  $p_I$  is 1, the representative 3-cocycle  $\omega \in H^3(SG \times GG, U(1))$  of that phase is chosen to satisfy the property described in the definition of  $\omega^{(l)}$ ; when the index  $p_I$  is 0, this index does not affect the value of cocycle. In other words, the elementary cocycle properties  $\omega^{(l)}$  in Table I generate all representative cocycles that are elements of  $H^3$ : The three basic 3-cocycles  $\omega^{(l)}$  generate a total of  $2^3$  3-cocycles in  $H^3(SG \times GG, U(1)) = Z_2^3$ , each of them leading to a physically different model, as stated at the end of Sec. IIC.

Let us now consider a pair of visons  $h_v = 1 \in GG \equiv (1, 0) \in G$ , which are the only flux quasiparticles for this group  $G$ .

Since the value of  $h_v$  is fixed, we omit it from the label of local operators; i.e., we use the labels  $D_{[g=(h, \tilde{g})]}$  with  $h \in GG, \tilde{g} \in SG$  [this notation was introduced after Eq. (103)]. Let us introduce Pauli matrices  $\mu_i, \rho_i, \tau_i$  acting in the Hilbert space of the visons on the basis  $|h_v = 1, g; u_A\rangle \equiv |(h_g, \tilde{g}); u_A\rangle$  from Eq. (102), with the usual  $g \in G \equiv (h_g \in GG, \tilde{g} \in SG)$ . The action of the matrices is naturally defined through setting  $\mu_z$  as  $(-1)^{\tilde{g}}$ ,  $\rho_z$  as  $(-1)^{h_g}$ , and finally  $\tau_z$  as  $(-1)^{u_A}$ . The local operators, Eq. (103), together with the global and

TABLE II. The values of local operators and fractionalized symmetries for  $GG = Z_2$ ,  $SG = Z_2$  for (the only possible) vison pair  $h_v = (1,0) = 1 \in GG$ .  $D$  and  $D'$  are shorthand for  $D(A)$  and  $D(B)$ , respectively. The cocycle  $\omega^{(12)}$  is the only one leading to nontrivial projective realization of local symmetry,  $U_\sigma(C)^2 = -1$ , and is therefore identified as the cocycle in  $H^3(G, U(1))$  which generates the nontrivial symmetry fractionalization classes; i.e., the index  $p_{12}$  labels the  $SFC(Z_2 \times Z_2, U(1)) = Z_2$ . (The action of the matrices in the vison pair Hilbert space is given in the text.)

	$D_{[(0,0)]}$	$D_{[(0,1)]}$	$D_{[(1,0)]}$	$D_{[(1,1)]}$	$D'_{[(0,0)]}$	$D'_{[(0,1)]}$	$D'_{[(1,0)]}$	$D'_{[(1,1)]}$	$U_\sigma(A)$	$U_\sigma(B)$	$U(\sigma)$
$\omega^{(1)}$	$\mathbb{1}$	$\mu_x \tau_x$	$i \rho_y$	$\mu_x i \rho_y \tau_x$	$\mathbb{1}$	$\mu_x$	$i \rho_y$	$\mu_x i \rho_y$	$\mu_x \tau_x$	$\mu_x$	$\tau_x$
$\omega^{(2)}$	$\mathbb{1}$	$\mu_x \tau_x$	$\rho_x$	$\mu_x \rho_x \tau_x$	$\mathbb{1}$	$\mu_x$	$\rho_x$	$\mu_x \rho_x$	$\mu_x \tau_x$	$\mu_x$	$\tau_x$
$\omega^{(12)}$	$\mathbb{1}$	$-i \mu_y \tau_x$	$\rho_x$	$-i \mu_y \rho_x \tau_x$	$\mathbb{1}$	$i \mu_y$	$\rho_x$	$i \mu_y \rho_x$	$-i \mu_y \tau_x$	$i \mu_y$	$\tau_x$

fractionalized symmetry operators, Eq. (108), are presented in Table II for all basic 3-cocycles  $\omega^{(I)}$ .

We can see that the global symmetry  $U(\sigma \equiv 1 \in SG)$ , which sends  $u_C \rightarrow u_C + 1$  is in this basis equal to  $\tau_x$  and, as expected, commutes with all local operators, for any choice of cocycle.

The phase in the definition of fractionalized symmetry, Eq. (108), is for all cocycles trivial (note that the cocycle  $\epsilon_{x,y,z}$  contains one factor of  $\omega$  for each permutation of  $x, y, z$ ). The fractionalized symmetry is then just equal to the local operator  $U_\sigma(C) = D_{[(0,1)]}(C)$ , and clearly for each cocycle it is true that  $U(\sigma) = U_\sigma(A)U_\sigma(B) = D_{[(0,1)]}(A)D_{[(0,1)]}(B) = \tau_x$ .

There is a nontrivial symmetry-fractionalized phase in case of  $\omega^{(12)}$ , since  $U_\sigma(C)^2 = -1$ . [One can also confirm this from the general expression Eq. (112).] That means precisely that the index  $p_{12}$  labels a nontrivial realization of symmetry fractionalization, where the local symmetry operation on a single vison at position  $C$  is projectively realized  $U_\sigma(C)^2 = (-1)^{p_{12}} \mathbb{1}$ , exactly as claimed in Eq. (25). The index  $p_{12}$  is obviously the only index classifying the SFC,  $SFC(Z_2 \times Z_2, U(1)) = Z_2$ , as presented in Eq. (37).

We can now consider the influence of interplay between global symmetry and topological order on the physical system with excitations. Let us assume that the excitations are a vison pair at  $A, B$ . The topological nature of the state must be robust against arbitrary local perturbations; i.e., we have to consider adding arbitrary local perturbation terms to the Hamiltonian [Eq. (57)]. The local perturbations, however, also have to be symmetric, i.e., commute with the global symmetries. The set of all local perturbation terms is formed by the local operators, i.e.,  $\tilde{D} = \{D(A), D(B)\}$ , so that

$$H_{\text{perturb}} = H + \sum_{\alpha} a_{\alpha} \tilde{D}^{\alpha}, \quad (114)$$

where the index  $\alpha$  labels all operators in the set  $\tilde{D}$ , and  $a_{\alpha}$  are arbitrary coefficients. The operators  $\tilde{D}$  are by construction symmetric, which is easily explicitly checked by showing that their matrices commute with the global symmetry operation  $\tau_x$ . For any fixed elementary cocycle in Table II, one can see that there are no other matrices that commute with the perturbations (except the global symmetries, of course). Further, all the local operators, for any fixed cocycle, commute with each other. Therefore, the algebra of conserved observables is trivial, and there are no degeneracies protected by symmetry. (This changes in the next examples.)

Physically, it is important to note that the eigenvalues of the local operator  $D_{[(1,0) \in GG]}$  are actually the values of gauge charge of the vison excitations [note that they act on the  $h_g$  element in the ribbon operators, where from Eq. (73):  $h_g = h_{1,0} \cdots h_{N,N-1} \in GG$  for a ribbon with inner edge on lattice sites  $0, \dots, N$ ]. These operators are indeed the same on both visons,  $D_{[(1,0) \in GG]}(A) = D_{[(1,0) \in GG]}(B)$ . The gauge charge value is an important quantity that will be nontrivial when the  $GG$  is enlarged in our third example.

#### D. Example with symmetry protected degeneracy: Vison pair in $GG = Z_2$ and $SG = Z_2 \times Z_2$

In this example, we again have only one type of vison,  $h_v = 1 \in GG$ , but two  $Z_2$  global symmetry generators,  $\sigma = (1,0) \in SG \equiv (0,1,0) \in G$  and  $\tau = (0,1) \in SG \equiv (0,0,1) \in G$ .

We use the elementary 3-cocycles for the group  $G = Z_2 \times Z_2 \times Z_2$  according to the results of Ref. 60 and present them in Table III. This means that there are seven indices  $p_I = 0, 1$ , labeling the elements of  $H^3(G, U(1)) = Z_2^7$ . The seven elementary 3-cocycles  $\omega^{(I)}$  generate a total of  $2^7$  cocycles in  $H^3(G, U(1)) = Z_2^7$ , each of them leading to a physically different model, as stated at the end of Sec. II C. However, the physical properties of the models will be very different depending on the particular choice of  $SG$  and  $GG$ , even though  $G$  is the same in this and the next example.

TABLE III. Inequivalent elementary 3-cocycles  $\omega^{(I)}$  for  $G \equiv GG \times SG = Z_2 \times Z_2 \times Z_2$ , which label classes in  $H^3(G, U(1)) = Z_2^7$ . A cocycle  $\omega(x, y, z)$  has value 1, *except* when the group elements  $x, y, z \in G$  take the special values shown in the table, in which case  $\omega(x, y, z)$  is equal to  $-1$ . The element notation  $x = (g_1, g_2, g_3)$  signifies the direct product factorization, and so in the example  $GG = Z_2, SG = Z_2 \times Z_2, g_1 \in GG$ , while in the example  $GG = Z_2 \times Z_2, SG = Z_2, g_3 \in SG$ . The elements of  $Z_2$  are 0, 1 (additive group action). The star symbol  $*$  stands for ‘‘any value of element.’’

$\omega(x, y, z) = -1$	$x, y, z$
$\omega^{(1)}$	$(1, *, *), (1, *, *), (1, *, *)$
$\omega^{(2)}$	$(*, 1, *), (*, 1, *), (*, 1, *)$
$\omega^{(3)}$	$(*, *, 1), (*, *, 1), (*, *, 1)$
$\omega^{(12)}$	$(1, *, *), (*, 1, *), (*, 1, *)$
$\omega^{(23)}$	$(*, 1, *), (*, *, 1), (*, *, 1)$
$\omega^{(13)}$	$(1, *, *), (*, *, 1), (*, *, 1)$
$\omega^{(123)}$	$(1, *, *), (*, 1, *), (*, *, 1)$

TABLE IV. Relevant local operators and fractionalized symmetries for  $GG = Z_2$ ,  $SG = Z_2 \times Z_2$ , for (the only possible) vison pair  $h_v = (1,0,0) \equiv 1 \in GG$  located at  $A, B$ . The symmetry generators are  $\sigma = (1,0) \in SG$ ,  $\tau = (0,1) \in SG$ , and they act as  $U(\sigma) = v_x$  and  $U(\tau) = \rho_x$ . There is symmetry fractionalization  $U(s) = U_s(A)U_s(B)$ , nontrivial (projective) for cocycles  $\omega^{(12)}$ ,  $\omega^{(13)}$ , and  $\omega^{(123)}$ , which “mix”  $GG$  with  $SG$  (Table III). The fractionalized symmetries differ (by a local operation) from local operators  $D_{[\sigma]}$ ,  $D_{[\tau]}$  only for the  $\omega^{(123)}$  cocycle [see Eq. (108)]. The definitions of all matrices in the vison pair Hilbert space are given in the text.

$\sigma = (0,1,0)$ $\tau = (0,0,1)$	$\omega^{(1)}$	$\omega^{(2)}$	$\omega^{(3)}$	$\omega^{(12)}$	$\omega^{(23)}$	$\omega^{(13)}$	$\omega^{(123)}$
$D_{[\tau]}(A)$	$\sigma_x \rho_x$	$\sigma_x \rho_x$	$\sigma_x \rho_x$	$\sigma_x \rho_x$	$\sigma_x \rho_x$	$-i\sigma_y \rho_x$	$\sigma_x \rho_x$
$U_\tau(A)$	$\sigma_x \rho_x$	$\sigma_x \rho_x$	$\sigma_x \rho_x$	$\sigma_x \rho_x$	$\sigma_x \rho_x$	$-i\sigma_y \rho_x$	$\sigma_x v_z \rho_x$
$D_{[\tau]}(B)$	$\sigma_x$	$\sigma_x$	$\sigma_x$	$\sigma_x$	$\sigma_x$	$i\sigma_y$	$\mu_z \sigma_x$
$U_\tau(B)$	$\sigma_x$	$\sigma_x$	$\sigma_x$	$\sigma_x$	$\sigma_x$	$i\sigma_y$	$\sigma_x v_z$
$D_{[\sigma]}(A)$	$\mu_x v_x$	$\mu_x v_x$	$\mu_x v_x$	$i\mu_y v_x$	$\mu_x v_x$	$\mu_x v_x$	$\mu_x \sigma_z v_x$
$U_\sigma(A)$	$\mu_x v_x$	$\mu_x v_x$	$\mu_x v_x$	$i\mu_y v_x$	$\mu_x v_x$	$\mu_x v_x$	$\mu_x \sigma_z v_x \rho_z$
$D_{[\sigma]}(B)$	$\mu_x$	$\mu_x$	$\mu_x$	$i\mu_y$	$\mu_x$	$\mu_x$	$\mu_x$
$U_\sigma(B)$	$\mu_x$	$\mu_x$	$\mu_x$	$i\mu_y$	$\mu_x$	$\mu_x$	$\mu_x \sigma_z \rho_z$
$D_{[(1,0,0)]}(A)$	$i\tau_y$	$\tau_x$	$\tau_x$	$\tau_x$	$\tau_x$	$\tau_x$	$\tau_x$
$D_{[(1,0,0)]}(B)$	$i\tau_y$	$\tau_x$	$\tau_x$	$\tau_x$	$\tau_x$	$\tau_x$	$\tau_x$

After fixing  $h_v$ , it is straightforward to construct the matrices for all local operators by using Eqs. (103), as well as to construct the fractionalized symmetry operators using their definition, Eq. (108), for each cocycle in Table III. We use the tensor product of Pauli matrices which are defined through setting  $\tau_z$  as  $(-1)^{h_s}$ ,  $\mu_z$  as  $(-1)^{\tilde{g}_1}$ ,  $\sigma_z$  as  $(-1)^{\tilde{g}_2}$ ,  $v_z$  as  $(-1)^{u_{A1}}$ , and  $\rho_z$  as  $(-1)^{u_{A2}}$  in our standard basis  $|h_g, \tilde{g}; u_A\rangle \equiv |h_g \times \tilde{g}_1 \times \tilde{g}_2; u_{A1} \times u_{A2}\rangle$ , with  $h_g \in GG$ ,  $(\tilde{g}_1, \tilde{g}_2) \in SG$ ,  $(u_{A1}, u_{A2}) \in SG$ .

Direct inspection of the obtained matrices, which are presented in Table IV, reveals the results quoted in Secs. II B and II C. Namely, for all cocycles one indeed finds that both global symmetries,  $U(\sigma) = v_x$  and  $U(\tau) = \rho_x$ , are fractionalized:  $U(s) = U_s(A)U_s(B)$ . Although  $U(\sigma)^2 = U(\tau)^2 = \mathbb{1}$  and  $U(\sigma)U(\tau) = U(\tau)U(\sigma)$ , the fractionalized symmetry can be realized projectively:

- (i) for cocycle  $\omega^{(12)}$  (which “mixes” the  $GG$  and the first  $Z_2$  of  $SG$ ), one finds the only nontrivial case  $U_\sigma(A)^2 = U_\sigma(B)^2 = -\mathbb{1}$ ;
- (ii) for cocycle  $\omega^{(13)}$  (which “mixes” the  $GG$  and the second  $Z_2$  of  $SG$ ), one finds the only nontrivial case  $U_\tau(A)^2 = U_\tau(B)^2 = -\mathbb{1}$ ;
- (iii) for cocycle  $\omega^{(123)}$  (which “mixes” all three subgroups), one finds the only nontrivial case  $U_\sigma(C)U_\tau(C) = -U_\tau(C)U_\sigma(C)$ , for both  $C = A, B$ .

One should note that only in the case  $\omega^{(123)}$  the local operators had to be modified to obtain the fractionalized symmetry operators, as clearly seen in the last column of Table IV. We can directly confirm that these are local redefinitions by noticing that the operators  $(-1)^{u_{A1}} = v_z$ ,  $(-1)^{u_{A2}} = \rho_z$  are local at  $A$ , while operators  $(-1)^{u_{B2}} = \sigma_z \rho_z$ ,  $(-1)^{u_{B1}} = \mu_z v_z$  are local at  $B$ .

We can now consider the influence of interplay between global symmetry and topological order on the physical system with excitations by repeating the analysis of local symmetric perturbations as in the previous example. [In this example it is also easy to explicitly check that the local, symmetric perturbation terms  $\tilde{D} = \{D(A), D(B)\}$  indeed commute with the global symmetry operations  $v_x, \rho_x$ .]

We can now ask: What operators can be used to label this state? Let us for concreteness consider the state having the cocycle  $\omega^{(123)}$ . The matrices that commute with the entire  $\tilde{D}$  algebra (which includes  $D_{[g \in G]}$  operators not shown explicitly in Table IV), and therefore with the arbitrarily locally perturbed Hamiltonian [Eq. (114)], are

- (i)  $\rho_x$  and  $v_x$ , which are just the global symmetries;
- (ii)  $\tau_x$ , which measures the gauge charge, as is explained further below;
- (iii)  $\sigma_x v_z$ ,  $\mu_x \sigma_z \rho_z$ ,  $\sigma_x \rho_x v_z$ , and  $\mu_x \sigma_z v_x \rho_z$ , which are just the fractionalized symmetries  $U_\tau(B)$ ,  $U_\sigma(B)$ ,  $U_\tau(A)$ , and  $U_\sigma(A)$ , respectively. [Note that these operators are not symmetric themselves, as a consequence of  $U_\sigma(C)U_\tau(C) = -U_\tau(C)U_\sigma(C)$ .]

In the algebra formed from these conserved operators, there are exactly two disjunct pairs,  $U_\tau(B), U_\sigma(B)$  and  $U_\tau(A), U_\sigma(A)$ , respectively, which anticommute, as we already learned through the symmetry fractionalization for  $\omega^{(123)}$ . Each anticommuting pair, acting on one of the visons, forces a twofold degeneracy on the state. [We checked this degeneracy numerically by considering an arbitrary perturbation term from Eq. (114).] We arrive at the physical signature of this phase, which is as follows.

*The symmetry protects a twofold degeneracy per vison of the pair in the  $p_{123} = 1$  phase of  $GG = Z_2$ ,  $SG = Z_2 \times Z_2$  model.* The degeneracy due to a vison at  $C$  is labeled by the fractionalized symmetry operators  $U_\sigma(C), U_\tau(C)$ .

Let us now discuss the gauge charge observables  $\tau_x$ . These are just the local operators  $D_{[1 \in GG]}$ , listed in Table IV. Physically, the operators  $D_{[1 \in GG]}(B)$  appear in the braiding matrix  $\mathcal{R}_{CC}^2$ , Eq. (100), describing the braiding of two visons at  $A$  ends of two ribbons which share a  $B$  end; see Fig. 16, Sec. IV D, and Appendix B.

Finally, let us emphasize that, at least in the case when  $G$  is a product of simple  $Z_2$  factors, there is no need to explicitly construct all the matrices as was done here. One can directly resort to Eqs. (109) and (111)–(113) to test whether a cocycle allows SF, and then whether this SF is nontrivial. For this purpose, we note that the cocycle  $\epsilon$  is easy to use since it

TABLE V. Relevant local operators for  $GG = Z_2 \times Z_2$ ,  $SG = Z_2$ : (top half) for a vison pair  $h_v = (1,0,0) \equiv (1,0) \in GG$  located at  $A, B$ ; (bottom half) for a vison pair  $h_v = (0,1,0) \equiv (0,1) \in GG$  located at  $A, B$ . The only global symmetry generator is  $\sigma = (0,0,1) \equiv 1 \in SG$ , acting as  $U(\sigma) = \rho_x$ . Except for  $\omega^{(123)}$ , there are fractionalized symmetry operators  $U_\sigma(C) \equiv D_{[\sigma]}(C)$ , with  $C = A, B$  [see Eq. (108)], such that  $U(\sigma) = U_\sigma(A)U_\sigma(B)$ . The fractionalized symmetries are nontrivial (projective) for cocycles  $\omega^{(13)}$  and  $\omega^{(23)}$ , which “mix”  $GG$  with  $SG$  (Table III). Phase having  $\omega^{(123)}$  is beyond SFC, since for it  $D_{[\sigma]}^{h_v=(010)}(A)D_{[\sigma]}^{h_v=(010)}(B) = \tau_z \rho_x$ ,  $D_{[\sigma]}^{h_v=(100)}(A)D_{[\sigma]}^{h_v=(100)}(B) = \mu_z \rho_x$ , and no local redefinition of  $D_{[\sigma]}$  can remove the  $\tau_z, \mu_z$  factors. The definitions of all matrices are given in the text.

$\sigma = (0,0,1)$	$\omega^{(1)}$	$\omega^{(2)}$	$\omega^{(3)}$	$\omega^{(12)}$	$\omega^{(23)}$	$\omega^{(13)}$	$\omega^{(123)}$
Vison pair: $h_v = (1,0,0)$							
$D_{[\sigma]}(A)$	$\sigma_x \rho_x$	$\sigma_x \rho_x$	$\sigma_x \rho_x$	$\sigma_x \rho_x$	$\sigma_x \rho_x$	$-i\sigma_y \rho_x$	$\sigma_x \rho_x$
$D_{[\sigma]}(B)$	$\sigma_x$	$\sigma_x$	$\sigma_x$	$\sigma_x$	$\sigma_x$	$i\sigma_y$	$\mu_z \sigma_x$
$D_{[(1,0,0)]}(A)$	$i\tau_y$	$\tau_x$	$\tau_x$	$\tau_x$	$\tau_x$	$\tau_x$	$\tau_x$
$D_{[(1,0,0)]}(B)$	$i\tau_y$	$\tau_x$	$\tau_x$	$\tau_x$	$\tau_x$	$\tau_x$	$\tau_x$
$D_{[(0,1,0)]}(A)$	$\mu_x$	$\mu_x$	$\mu_x$	$-i\mu_y$	$\mu_x$	$\mu_x$	$\mu_x \sigma_z$
$D_{[(0,1,0)]}(B)$	$\mu_x$	$\mu_x$	$\mu_x$	$i\mu_y$	$\mu_x$	$\mu_x$	$\mu_x$
Vison pair: $h_v = (0,1,0)$							
$D_{[\sigma]}(A)$	$\sigma_x \rho_x$	$\sigma_x \rho_x$	$\sigma_x \rho_x$	$\sigma_x \rho_x$	$-i\sigma_y \rho_x$	$\sigma_x \rho_x$	$\sigma_x \rho_x$
$D_{[\sigma]}(B)$	$\sigma_x$	$\sigma_x$	$\sigma_x$	$\sigma_x$	$i\sigma_y$	$\sigma_x$	$\tau_z \sigma_x$
$D_{[(0,1,0)]}(A)$	$\mu_x$	$i\mu_y$	$\mu_x$	$\mu_x$	$\mu_x$	$\mu_x$	$\mu_x$
$D_{[(0,1,0)]}(B)$	$\mu_x$	$i\mu_y$	$\mu_x$	$\mu_x$	$\mu_x$	$\mu_x$	$\mu_x$
$D_{[(1,0,0)]}(A)$	$\tau_x$	$\tau_x$	$\tau_x$	$-\tau_x$	$\tau_x$	$\tau_x$	$\tau_x \sigma_z$
$D_{[(1,0,0)]}(B)$	$\tau_x$	$\tau_x$	$\tau_x$	$\tau_x$	$\tau_x$	$\tau_x$	$\tau_x$

contains six factors of  $\omega(x,y,z)$ , such that each permutation of  $x,y,z$  appears exactly once; importantly, when  $G$  has only  $Z_2$  factors, the generating 3-cocycles in  $H^3(G,U(1))$  (Ref. 60) can only take values  $\pm 1$ , as is the case in Tables I and III.

### E. The simplest example beyond symmetry fractionalization: Vison pairs in $GG = Z_2 \times Z_2$ and $SG = Z_2$

In this example there are two fundamental vison types. We consider in parallel a pair of  $h_v = (1,0) \in GG \equiv (1,0,0) \in G$  visons and a pair of  $h_v = (0,1) \in GG \equiv (0,1,0) \in G$  visons.

We again construct the matrices of all local operators by using Eqs. (103). Before proceeding, one should notice that the condition stated in Eq. (110) is violated for the cocycle  $\omega^{(123)}$ : Only in that case does  $\epsilon_{h_v, \sigma, h_g} = -1$  become possible since  $h_v$  and  $h_g$  can differ while both being nontrivial elements of  $GG$ . According to Eq. (109), we then expect that in that case the symmetry fractionalization will fail.

Let us nevertheless continue with the explicit construction of fractionalized symmetry operators. Using their definition, Eq. (108), for each cocycle in Table III including  $\omega^{(123)}$ , each fractionalized symmetry operator is just equal to its corresponding local operator  $D$ . We therefore avoid repetition in Table V, and one should keep in mind that  $U_\sigma(C) \equiv D_{[\sigma]}(C)$ , where the only global symmetry generator is  $\sigma = 1 \in SG$ .

The Pauli matrices are here defined through setting  $\tau_x$  as  $(-1)^{h_{g1}}$ ,  $\mu_z$  as  $(-1)^{h_{g2}}$ ,  $\sigma_z$  as  $(-1)^{\tilde{g}}$ , and  $\rho_z$  as  $(-1)^{u_A}$  in our standard basis  $|h_g, \tilde{g}; u_A\rangle \equiv |h_{g1} \times h_{g2} \times \tilde{g}; u_A\rangle$ , with  $(h_{g1}, h_{g2}) \in GG$ ,  $\tilde{g} \in SG$ ,  $u_A \in SG$ .

Direct inspection reveals that the global symmetry, represented by  $U(\sigma) = \rho_x$ , is fractionalized for both visons, i.e.,  $U(\sigma) = U_\sigma^{h_v}(A)U_\sigma^{h_v}(B) = \rho_x$ , except for the cocycle  $\omega^{(123)}$ . In the case of this cocycle, we get

$$\begin{aligned} U_\sigma^{h_v=(1,0)}(A)U_\sigma^{h_v=(1,0)}(B) &= \mu_z \rho_x \\ U_\sigma^{h_v=(0,1)}(A)U_\sigma^{h_v=(0,1)}(B) &= \tau_z \rho_x \end{aligned} \quad (\text{cocycle } \omega^{(123)}), \quad (115)$$

for the vison pairs  $h_v = (1,0)$  and  $h_v = (0,1)$ , respectively. We discuss this further below.

Considering all the cocycles (except  $\omega^{(123)}$ ), we find phases with nontrivial SF, i.e. where the fractionalized symmetry is realized projectively:

(i) for cocycle  $\omega^{(13)}$  (which “mixes” the first  $Z_2$  in  $GG$  with  $SG$ ), one finds the only nontrivial case  $U_\sigma^{h_v=(1,0)}(A)^2 = U_\sigma^{h_v=(1,0)}(B)^2 = -\mathbb{1}$ ;

(ii) For cocycle  $\omega^{(23)}$  (which “mixes” the second  $Z_2$  in  $GG$  with  $SG$ ), one finds the only nontrivial case  $U_\sigma^{h_v=(0,1)}(A)^2 = U_\sigma^{h_v=(0,1)}(B)^2 = -\mathbb{1}$ .

These results match the claims in Sec. II B. There are obviously two symmetry-fractionalization  $Z_2$  indices,  $p_{13}$  and  $p_{23}$ , in accordance with the general results:  $H^2(SG, GG) = Z_2^2$  and, for this group,  $SFC(SG, GG) = H^2(SG, GG)$  (see Sec. II C).

We can try to use our explicit matrix expressions to “force” symmetry fractionalization in the case of cocycle  $\omega^{(123)}$ . This attempt will fail, as expected from general arguments above, and therefore this state is beyond SFC, with the index  $p_{123}$  labeling the *EXTRA*( $SG, GG$ ) class. What we would need to achieve is the removal of  $\mu_z$  and  $\tau_z$  factors in Eq. (115). Inspecting the operators

$$(-1)^{u_A} = \rho_z, \quad (-1)^{u_B} = \sigma_z \rho_z, \quad (116)$$

the first being local at  $A$  and the second local at  $B$ , we see that there is no hope in manipulating the  $\mu$  and  $\tau$  subspaces. Physically,  $\mu_z$  and  $\tau_z$  measure the  $GG$  degrees of freedom, and these are connected to the vison gauge charge, which is nonlocal.

The local operators  $D_{[h_v]}$  (which we use to measure the gauge charge shortly) by definition change this group element (i.e.,  $\tau_x$ ) and cannot provide us with  $\tau_z, \mu_z$ .

We next ask: Which operators can be used to physically label this state? Let us consider the especially interesting

cocycle  $\omega^{(123)}$ . As explained in the previous example, we need to find matrices that commute with the entire  $\tilde{D}$  algebra (which includes all  $D_{[g \in G]}$  operators). These are:

- (i)  $\rho_x$ , which is just the global symmetry;
- (ii)  $\hat{e}_1, \hat{e}_2$ , which measure the two  $Z_2$  gauge charges in  $GG$ , as we explain further below. [For the  $h_v = (1,0)$  vison pair,  $\hat{e}_1 \equiv \tau_x, \hat{e}_2 \equiv \mu_x \sigma_z \rho_z$ , while for  $h_v = (0,1)$  vison pair,  $\hat{e}_1 \equiv \tau_x \sigma_z \rho_z, \hat{e}_2 \equiv \mu_x$ .]

In the algebra of these conserved operators, exactly one pair anticommutes: The global symmetry anticommutes with the gauge charge of  $Z_2$  complementary to the visons' flux  $h_v$ . For example, considering a vison pair with flux set by  $h_v = (1,0) \in GG$ , the *second*  $Z_2$  gauge charge of  $GG$  ( $\hat{e}_2$ ) anticommutes with the global symmetry. A signature of this phase is then as follows.

*The symmetry protects a twofold degeneracy of a single vison pair in the  $p_{123} = 1$  phase of  $GG = Z_2 \times Z_2, SG = Z_2$  model.*

This result for the cocycle  $\omega^{(123)}$  reveals its physical interpretation. To understand it better, we need to explicitly consider the consequences of anticommutation between symmetry and gauge charge. Let us proceed with that goal and leave for later the detailed explanation of why  $\hat{e}_1, \hat{e}_2$  can indeed be understood as gauge charge operators.

The quasiparticles of this theory are labeled by the values of flux and charge, and we consider the elementary ones: (1) Flux particle  $m_1 = 1[m_2 = 1]$  has flux in the first[second]  $Z_2$  of  $GG$ , which is set by the values of  $h_v = (*,0)[h_v = (0,*)]$ , and no gauge charge; (2) charge particle  $e_1 = 1[e_2 = 1]$  has charge in the first[second]  $Z_2$  of  $GG$ , which is set by the values of  $h_g = (*,0)[h_g = (0,*)]$ , and has no flux. A general quasiparticle will have arbitrary values (0 or 1) for these four numbers, so we label it  $(e_1, e_2, m_1, m_2)$ . For instance,  $(1, 1, 0, 0)$  is the particle bound state of charge and flux in the first  $Z_2$  of  $GG$ . When symmetry anticommutes with  $\hat{e}$ , that means it switches the two eigenvalues of  $\hat{e}$ , and therefore switches the particles'  $\hat{e}$  number between trivial (0) and nontrivial (1). As we established, symmetry anticommutes with  $\hat{e}_1$  when the particle pair in question is  $m_2$ , while it anticommutes with  $\hat{e}_2$  when the particle pair is  $m_1$ . This leads to the following transformation of elementary quasiparticles under the action of symmetry:

$$(e_1, m_1, e_2, m_2) \xrightarrow{\sigma} (e_1 + m_2, m_1, e_2 + m_1, m_2), \quad (117)$$

where (mod 2) algebra is understood. As expected, the symmetry changes the charges of particles, but we can further assign a deeper meaning to this transformation. Namely, in  $Z_2$  theories the charge and flux are physically equivalent: They are dual to each other, and we can rename them at will without changing the physics (e.g., the braiding properties) of particles. We therefore assign new fluxes  $\tilde{m}$  and charges  $\tilde{e}$  according to the rules:  $(\tilde{e}_1, \tilde{m}_1, \tilde{e}_2, \tilde{m}_2) \equiv (e_1 + m_2, m_1, e_2 + m_1)$ . Note that the quasiparticle statistics is indeed conserved, i.e., bosonic except between  $e_i$  and  $m_i$ , when it is fermionic. This leads to the elegant transformation rule,

$$(\tilde{e}_1, \tilde{m}_1, \tilde{e}_2, \tilde{m}_2) \xrightarrow{\sigma} (\tilde{e}_2, \tilde{m}_2, \tilde{e}_1, \tilde{m}_1), \quad (118)$$

so that the global symmetry transformation only exchanges the particle types 1 and 2. (We note that this physical interpretation

might carry on to higher dimensions. For instance in  $3d$ , charge excitations are pointlike while fluxes are stringlike, so they cannot be interchanged among each other; however, it is still well defined to change their type, e.g.,  $1 \leftrightarrow 2$ .)

We have therefore found the physical nature of this state: *The global symmetry operation exchanges the two quasi-particle types in  $p_{123} = 1$  phase of  $GG = Z_2 \times Z_2, SG = Z_2$  model.* This shows that symmetry performs a nonlocal transformation on the excitation pair, and the state is beyond symmetry fractionalization classification.

Let us now discuss in detail the gauge charge observables  $\hat{e}_1, \hat{e}_2$ , as promised above. We focus on a particular vison pair  $h_v$ . As in the previous example, one naively expects the gauge charge observables to just equal the appropriate local operators:  $D_{[(1,0) \in GG \equiv (1,0,0)]}$  and  $D_{[(0,1) \in GG \equiv (0,1,0)]}$ , which are listed in Table V. Focusing on the cocycle  $\omega^{(123)}$ , we however see that these local operators differ at the two quasiparticles, e.g.,  $D_{[(1,0,0)]}(A) \neq D_{[(1,0,0)]}(B)$ , which would mean that measuring the gauge charge of a vison and antivison in the pair would give differing answers. This is physically wrong, but it is easy to resolve the problem. Namely, the physical operators  $\hat{e}_1, \hat{e}_2$  differ from the corresponding local operators  $D$  by a simple local operation. Using the local transformations in Eq. (116), one immediately obtains that

- (i) for vison pair  $h_v = (1,0)$ ,

$$\begin{aligned} \hat{e}_1 &= D_{[(1,0,0)]}(A) = D_{[(1,0,0)]}(B) = \tau_x, \\ \hat{e}_2 &= (-1)^{u_A} D_{[(0,1,0)]}(A) = (-1)^{u_B} D_{[(0,1,0)]}(B) = \mu_x \sigma_z \rho_z; \end{aligned} \quad (119)$$

- (ii) for vison pair  $h_v = (0,1)$ ,

$$\begin{aligned} \hat{e}_1 &= (-1)^{u_A} D_{[(1,0,0)]}(A) = (-1)^{u_B} D_{[(1,0,0)]}(B) = \tau_x \sigma_z \rho_z, \\ \hat{e}_2 &= D_{[(0,1,0)]}(A) = D_{[(0,1,0)]}(B) = \mu_x. \end{aligned} \quad (120)$$

These  $\hat{e}_1, \hat{e}_2$  operators exactly match the ones we found to commute with the entire local  $\tilde{D}$  algebra.

We already know that the local operators  $D_{[h_g]}(B)$  appear in the braiding matrix  $\mathcal{R}_{CC}^2$ , Eq. (100), describing the braiding of two visons at  $A$  ends of two ribbons which share a  $B$  end; see Fig. 16. Physically, we expect these local operators to equal the gauge charge operators and thereby transparently provide the braiding rules of anyons in  $Z_2$  topologically ordered theory. A question that arises then is: If we *redefine* the local operators so that they become exactly equal to the gauge charge operators [following Eqs. (119) and (120)], do the braiding properties change? The answer is negative. Namely, if we choose to braid to visons of same type  $h_v^1 = h_v^2 \equiv h_v$ , the braiding operator [Eq. (100)] will apply the same  $D_{(h_v, h_v)}(B)$  on both visons, and these local operators are not even redefined. When we braid two differing vison types, e.g.,  $h_v^1 = (1,0), h_v^2 = (0,1)$ , the braiding will apply  $D_{(h_v^1, h_v^2)}$  and  $D_{(h_v^2, h_v^1)}$ , both of which are redefined by  $(-1)^{u_B}$  according to Eqs. (119) and (120). As pointed out earlier, our analysis of vison Hilbert space revealed that such braiding operations should be considered after choosing, and keeping fixed, some value of  $u_B$ . Since the two ribbons share the end at  $B$ , the  $(-1)^{u_B}$  operation applied on both braided quasiparticles cancels. Therefore, we can freely redefine the considered local operators to be equal to the physical gauge charge operators  $\hat{e}_1, \hat{e}_2$ .

**F. Gauge charges**

In the previous subsections we considered in detail pairs of gauge fluxes, i.e., visons. The other fundamental type of excitations is a pair of gauge charge excitations, which is created by the ribbon operator:

$$|g\rangle \equiv F^{(h=\mathbb{1},g)}(\Gamma) |gs\rangle, \tag{121}$$

i.e., the special case of the flux  $h \in GG$  being trivial. As always,  $g \in G = SG \times GG$  uniquely factorizes as  $g = h_g \cdot \tilde{g}$ , with  $h_g \in GG$  being related to the gauge charge of the excitations, and  $\tilde{g} \in SG$ . [Recall again the definition of ribbon operators Eq. (73):  $h_g = h_{1,0} \cdots h_{N,N-1} \in GG$  for a ribbon on lattice sites  $0, \dots, N$ .]

Recall that in this paper we use “canonical” 3-cocycles  $\omega$ , meaning that  $\omega(g_1, g_2, g_3) = 1$  if any of  $g_1, g_2, g_3$  is equal to  $\mathbb{1}$ . Specifically, the elementary cocycles for a group  $G$  which is a product of  $Z_n$  factors are written in Ref. 60, and are all canonical.

Since  $h_v = \mathbb{1}$  for gauge charges, it then follows immediately from Eqs. (111), (112), and (108) that for these excitations the symmetry fractionalization is always trivial. Further, Eq. (99) shows that the braiding matrix between various gauge charges is also trivial in our models.

As a particular demonstration, let us consider the examples from the previous subsections. Equation (103) reveals that the action of local operators  $D$  in our basis of the excitation pair Hilbert space  $\mathcal{L}(A, B)$  does not involve any phase factors. It is as if the chosen cocycle is always the trivial one,  $\omega = 1$ . To avoid repetition in writing explicitly the local operators in the present case of a gauge charge pair, we refer the reader to just look at the cases of  $\omega^{(2)}$  for the  $GG = Z_2, SG = Z_2$  model;  $\omega^{(2)}$  for the  $GG = Z_2, SG = Z_2 \times Z_2$  model; and finally  $\omega^{(3)}$  for the  $GG = Z_2 \times Z_2, SG = Z_2$  model. The lack of nontrivial phase factors in the action of local operators leads to a trivial algebra: Repeating the analysis from above, one finds that in all three examples all the  $D$  operators commute, and the only matrices commuting with them are the global symmetry operations, which, of course, commute among each other in these direct product groups. Therefore, there are no symmetry protected degeneracies for the gauge charges in our present examples, in sharp contrast to the case of fluxes.

**G. Multiple vison pairs and dualization**

Let us briefly consider a system with multiple vison pairs. For simplicity, we focus on the case where all these quasiparticles are of the same type. Since the calculation even for this case becomes very complicated, we try to give general arguments and speculate about the symmetry protected degeneracy of a general state with  $N$  pairs of visons.

One way to analyze this situation is to consider the dualization of  $SG$ . By this we mean the standard replacement of lattice site degrees of freedom  $u_i$  with edge degrees of freedom  $u_{ij} \equiv u_i \cdot u_j^{-1}$ , as we also mentioned in Sec. III B. The total group becomes a pure gauge group,  $G = GG \times \tilde{SG} \equiv \tilde{G}$ , where  $\tilde{SG}$  denotes the gauge group  $SG$ . The visons in the  $G$  model are mapped to gauge flux particles in the  $\tilde{G}$  model. Let us denote the protected degeneracy of  $N$ -particle-pair state by  $\text{VDEG}_G(N)$  and  $\text{VDEG}_{\tilde{G}}(N)$  for the models with  $SG$  and the dualized  $\tilde{SG}$ , respectively.

One should note that this is a many-to-one mapping, in the sense that  $|SG|$  states obtained by multiplying all  $u_i$  by an arbitrary element  $s \in SG$  (in the  $G$  theory) get mapped to a single state (in the dualized  $\tilde{G}$  theory). In general, therefore, we expect that the state with visons can only have the same or smaller degeneracy upon dualization to  $\tilde{G}$ :

$$\text{VDEG}_G(N) \geq \text{VDEG}_{\tilde{G}}(N). \tag{122}$$

Particularly, the mentioned many-to-one nature of the mapping indicates that the change in degeneracy (from  $G$  to  $\tilde{G}$ ) might involve the factor  $|SG|$ .

In fact, we can recall that the Hilbert space  $\mathcal{L}(A, B)$  of an excitation pair in the  $SG$  description (Sec. V A) had to be specified by keeping track of value of the element  $u_A$ , or  $u_B$ , which belong to  $SG$ . In the most general description of the  $2N$  visons, one connects all their ribbons to a common point on the lattice  $x_0$ , which contains no excitation (see discussion in Sec. IV D). We then have to keep track of  $u_{x_0}$ , which takes  $|SG|$  different values. Since this degree of freedom becomes obsolete upon dualization to  $\tilde{G}$ , one is again led to the assumption that the degeneracy of the  $2N$ -vison state in the dualized theory ( $\tilde{G}$ ) is reduced by a factor of  $|SG|$ .

Let us test these assumptions on the results of Sec. V. In our first example,  $SG = Z_2, GG = Z_2$ , a single vison pair had no symmetry protected degeneracy. Upon dualization, this model becomes the gauge theory  $\tilde{G} = Z_2 \times Z_2$ . This is an Abelian theory, which implies that its excitations are anyons with quantum dimension equal to 1. (The quantum dimension is defined as the degeneracy per excitation in the limit of infinite number of excitations.) In this case, there is no degeneracy. Therefore, the inequality (122) is saturated, and there is no factor  $|SG| = 2$ .

The Abelian case, having nondegenerate anyon states, might be a too special case for our general considerations. Let us instead focus on the examples with  $G = Z_2^3$ , and the especially interesting cocycle  $\omega^{(123)}$ . In those cases we found that a single vison pair has degeneracy 4 and 2, in the  $SG = Z_2 \times Z_2$  and  $SG = Z_2$  examples, respectively. The topological order described upon dualization of either of these example groups becomes very interesting due to the presence of the cocycle  $\omega^{(123)}$ . Namely, the topological order realized in that way can be described by the *non-Abelian* theory having the gauge group  $\tilde{G}_{nA} = D_4$  and no twist by a cocycle.<sup>62</sup> It is known that the  $D_4$  theory has no degeneracy for a single excitation pair, i.e.,  $\text{VDEG}_{D_4}(1) = 1$ .

For a single excitation pair and the case where the topological order in the dual theory is described by  $\tilde{G}_{nA} = D_4$ , we therefore established the anticipated

$$\begin{aligned} \text{VDEG}_G(N) &= |SG| \cdot \text{VDEG}_{\tilde{G}_{nA}}(N) \quad (\text{for } \tilde{G}_{nA} = D_4, N = 1). \end{aligned} \tag{123}$$

Let us proceed to the case of multiple pairs of particles, still all being of the same type. The excitations of the  $D_4$  gauge theory have quantum dimension 2; therefore, for large  $N$  one has the scaling  $\text{VDEG}_{D_4}(N \gg 1) \sim 4^N$ . Since for  $N = 1$  we already discussed that  $\text{VDEG}_{D_4}(1) \sim 4^0$ , we expect that an interpolation formula  $\text{VDEG}_{D_4}(N) \sim 4^{(N-1)}$  should hold for all  $N$ . Combining this expectation with the result in Eq. (123)

leads us to conjecture

$$\begin{aligned} \text{VDEG}_G(N) \\ = |SG| \cdot \text{VDEG}_{\tilde{G}_{n_A}}(N) \quad (\text{non-Abelian } \tilde{G}_{n_A}, N \geq 1). \end{aligned} \quad (124)$$

In this conjecture we also anticipate that the key property which ensured Eq. (123) is that  $D_4$  is non-Abelian, since in the previous paragraphs we established that Eq. (123) does not hold (even though  $N = 1$ ) when  $\tilde{G}$  described an Abelian topological order (i.e.,  $Z_2 \times Z_2$ ).

We leave further study of these questions for future research.

## VI. DISCUSSION AND CONCLUSIONS

In this paper, we present a classification of topologically ordered phases in the presence of an on-site global symmetry, equipped with local bosonic exactly solvable models. The discussion in Sec. II C and the solutions of our models in some examples allow us to reveal the physical meaning of this classification, which is given in Eqs. (31) and (32). Basically, the classification  $H^3(SG \times GG, U(1))$  is a direct product of many finite Abelian groups, and each group has a clear physical meaning. Among them  $H^3(SG, U(1))$  is the index for SPT phases,  $H^3(GG, U(1))$  is the index for DW topological orders, and  $SET(SG, GG)$  in Eq. (31) is the index labeling the possible interplays between the global symmetry and the topological order (SET phases).

$SET(SG, GG)$  can be further understood. It is a direct product of two Abelian groups,  $SFC(SG, GG)$  and  $EXTRA(SG, GG)$ .  $SFC(SG, GG)$  is labeling different possible ways to fractionalize the global symmetry by the topological order, while  $EXTRA(SG, GG)$  is labeling the phenomena that the global symmetry transformation could interchange quasiparticle species, which is beyond the symmetry fractionalization scheme.

Some measurable consequences of the SET phases are discussed. In particular, we show that under certain conditions, SET phases have nontrivial symmetry protected degeneracy for excited states. For instance, in one striking example beyond the symmetry fractionalization scheme, we show that symmetry protects a twofold degeneracy for a single pair of gauge flux quasiparticles, which cannot be locally associated with either quasiparticle. This degeneracy of excited states can be used to detect the SET phases in numerics/experiments. However, we leave the most general diagnosis of SET phases for future investigation. In any case, the exactly solvable models constructed in the current work can be very useful tools for this purpose.

The SPT phases are known to host gapless edge states, topologically protected by the global symmetry. We have not studied the possible gapless edge states due to SET topological indices in this paper. We also leave this issue as a subject of future investigations.

Below we discuss the generalization and limitations of our classification.

### A. Generalization to higher dimensions

Although we have been focusing on  $2 + 1$  dimensions, where the classification is given by  $H^3(SG \times GG, U(1))$ ,

this can be easily generalized to  $H^{d+1}(SG \times GG, U(1))$  in general  $d + 1$  dimensions ( $d \geq 2$ ). One way to understand this generalization is to dualize  $GG$  to be part of global symmetry, after which the system has an on-site global symmetry  $\tilde{S}G = SG \times GG$ . According to Ref. 20, the SPT phases in  $d + 1$  dimensions are classified by  $H^{d+1}(\tilde{S}G, U(1))$ , and it is natural to expect that these phases may still be different before the duality. (In fact, this point of view is not completely correct, which we discuss shortly in Sec. VI C.)

The higher dimension classification is also equipped with local bosonic exactly solvable models. For instance, in  $3 + 1d$ , one can also construct the exactly solvable models on a three-dimensional lattice which triangulates the three-dimensional space. The  $GG$  degrees of freedom live on the edges and the  $SG$  degrees of freedom live on the vertices. Similar to the  $2 + 1d$  case, the Hamiltonian of the model is a sum of local projectors. Theorem 1 and Theorem 2 (see Sec. III A2) in  $3 + 1d$  dictate that these local projectors mutually commute and the model is exactly solvable. We leave the complete solution of such  $3 + 1d$  models (i.e., the excited states) as a subject of future investigations.

However, at this moment it is still possible to explore the physical meaning of the  $3 + 1d$  classification using  $H^4(SG \times GG, U(1))$ . A Künneth expansion immediately gives

$$\begin{aligned} H^4(SG \times GG, U(1)) = H^4(SG, U(1)) \times H^4(GG, U(1)) \\ \times SET^4(SG, GG). \end{aligned} \quad (125)$$

Here clearly, the index  $H^4(SG, U(1))$  is labeling the SPT phases, while  $H^4(GG, U(1))$  is labeling the different  $3 + 1d$  topological orders described by the gauge group  $GG$ . Note that  $H^4(GG, U(1))$  is labeling the direct generalization of the DW discrete gauge theories in  $3 + 1$  dimension. Further,  $SET^4(SG, GG)$ , as explicated below, is labeling the different possible interplays between the global symmetry and the topological order in  $3 + 1d$ .

Let us use  $SET^3(SG, GG)$  to denote the symmetry enriched indices  $SET(SG, GG)$  in Eq. (32), emphasizing that it is for  $2 + 1$  dimensions.  $SET^4(SG, GG)$  contains a rather different mathematical structure than  $SET^3(SG, GG)$ :

$$\begin{aligned} SET^4(SG, GG) = [H^3(SG, Z) \otimes H^2(GG, Z)] \\ \times [H^2(SG, Z) \otimes H^3(GG, Z)] \\ \times \text{Tor}[H^4(SG, Z), H^2(GG, Z)] \\ \times \text{Tor}[H^2(SG, Z), H^4(GG, Z)] \\ \times \text{Tor}[H^3(SG, Z), H^3(GG, Z)]. \end{aligned} \quad (126)$$

One can anticipate the possible nontrivial interplay between the global symmetry and the topological order in  $3 + 1d$ . First, let us consider the generalization to  $3 + 1d$  of  $EXTRA(SG, GG)$ , a part of  $SET^3(SG, GG)$ . In  $2 + 1d$ ,  $EXTRA(SG, GG)$  is describing the interchange of quasiparticle species by  $SG$  action. We expect that in  $3 + 1d$ , part of  $SET^4(SG, GG)$  also describes the interchange of excitation species. Note that in  $3 + 1d$ , the topological excitations can be either pointlike gauge charges or looplike gauge fluxes. More precisely, this part of  $SET^4(SG, GG)$  should describe the species interchange of gauge fluxes and of gauge charges by the global symmetry (but not interchange of gauge flux and gauge charge).



Next, we consider the generalization to  $3 + 1d$  of the other part of  $SET^3(SG, GG): SFC(SG, GG)$ . One may wonder: Does part of  $SET^4(SG, GG)$  label the symmetry fractionalization phenomena in  $3 + 1d$ ? Naively, if we consider the symmetry fractionalization classes of pointlike gauge charges, we should have a similar mathematical structure as in  $2 + 1d$  [see Eq. (33)]. In particular, when  $GG$  is Abelian, we should have  $H^2(SG, GG) = [H^2(SG, Z) \otimes H^2(GG, Z)] \times \text{Tor}[H^3(SG, Z), H^2(GG, Z)]$  indices labeling the different projective representations of the symmetry group. However, this mathematical structure is missing in  $SET^4(SG, GG)$  above.

In fact, we know that symmetry fractionalization classes of gauge charges are actually missing from  $SET^3(SG, GG)$  in  $2 + 1d$ , as discussed in Sec. V F (see also Sec. II C). It is not surprising that  $SET^4(SG, GG)$  is also missing those indices. However, we know that the symmetry fractionalization classes of gauge fluxes are completely contained in  $SET^3(SG, GG)$ . We expect that  $SET^4(SG, GG)$  also contains the generalized “symmetry fractionalization classes” of gauge fluxes, the topological loop excitations in  $3 + 1d$ . Therefore, a part of  $SET^4(SG, GG)$  should describe the nontrivial action of global symmetry on gauge flux loops, *without changing their species*. However, because gauge flux loops are extended objects, the action of global symmetry on them can no longer be implemented by local operators. So, to be precise, we should not call this phenomenon symmetry fractionalization, as it is discussed in Sec. II B. We call it the *extended symmetry fractionalization*.

Although the full understanding of the extended symmetry fractionalization is beyond the scope of this paper, we can intuitively guess the underlying mathematical structure. When  $GG$  is Abelian, a direct generalization of  $H^2(SG, GG)$  to one higher dimension is  $H^3(SG, GG)$ . By the universal coefficients theorem, we have

$$H^3(SG, GG) = [H^3(SG, Z) \otimes H^2(GG, Z)] \times \text{Tor}[H^4(SG, Z), H^2(GG, Z)], \quad (127)$$

where we used  $H^2(GG, Z) = GG$  for finite Abelian group  $GG$ . These two terms indeed appear in Eq. (126) (the first and the third term). We propose that  $H^3(SG, GG)$  is at least part of the mathematical structure describing the extended symmetry fractionalization classes when  $GG$  is Abelian.

### B. Generalization to continuous groups, and/or antiunitary symmetry groups

Our discussion has been limited to the case in which both  $SG$  and  $GG$  are finite groups, and  $SG$  is assumed to be unitary (i.e., does not contain time reversal). These constraints are introduced here for simplicity rather than due to difficulty of principle.

First, it is quite straightforward to consider an on-site symmetry group  $SG$  containing the antiunitary time-reversal transformation  $\mathcal{T}$ . In the work by Xie *et al.* on SPT phases,<sup>20</sup> when  $SG$  contains  $\mathcal{T}$ , the classification is given by  $M^{d+1}(SG, U_T(1))$ . Here  $U_T(1)$  means that  $\mathcal{T}$  acts nontrivially on the  $U(1)$  group; in particular,  $\mathcal{T}$  sends the phase  $e^{i\theta} \in U(1)$  to its complex conjugate  $e^{-i\theta}$ . [For the detailed definition and discussion of  $H^{d+1}(SG, U_T(1))$ , see Ref. 20]. We expect that the classification of gapped bosonic quantum phases with

topological order described by a  $GG$  gauge group, and in the presence of an on-site global symmetry group  $SG$  containing  $\mathcal{T}$ , is given by  $H^{d+1}(SG \times GG, U_T(1))$ , in which only the  $SG$  part of the cross product acts nontrivially on  $U_T(1)$ .

Further, Ref. 20 considered the classification of SPT phases with a continuous on-site symmetry group  $SG$ , in which case the Borel group cohomology was used. It appears to us that the inclusion of a continuous  $SG$  results in an appropriate (but may be subtle) mathematical generalization of  $H^{d+1}(G, U(1))$  for a finite group  $G$ . We, in principle, do not expect that this generalization is hindered by difficulties.

### C. About the completeness of the classification

Finally, we comment on the issue of completeness of the classification by  $H^{d+1}(SG \times GG, U(1))$ . *Is the classification complete, incomplete, or overcomplete?*

First, we want to comment on the following question: Do distinct elements in  $H^{d+1}(SG \times GG, U(1))$  necessarily correspond to distinct quantum phases? We believe that the answer is negative, and the classification is generally overcomplete in this sense. One can understand this claim by considering a simple example  $SG = Z_1$  and  $GG = Z_2 \times Z_2$  in  $2 + 1$  dimensions. According to  $H^3(GG, U(1)) = Z_2^3$ , it appears that there are eight different topological orders. However, this is overcomplete. Among these three  $Z_2$  indices, the first (second)  $Z_2$  is labeling the toric-code/double-semion topological order in the first (second)  $Z_2$  gauge group, and the third  $Z_2$  is labeling a certain extra twist of the topological order involving both  $Z_2$  gauge groups. Let us consider two phases labeled by  $(1, 0, 0)$  and  $(0, 1, 0)$ , where we group the three  $Z_2$  indices into a vector. Clearly,  $(1, 0, 0)$  and  $(0, 1, 0)$  physically correspond to the same phase; they just differ by an ordering of the gauge group. This is analogous to the  $K$ -matrix classification of Abelian quantum Hall states. For instance,  $K = \begin{pmatrix} 1 & 0 \\ 0 & 2 \end{pmatrix}$  and  $K = \begin{pmatrix} 2 & 0 \\ 0 & 1 \end{pmatrix}$  are labeling the same physical phase.

The  $SET(SG, GG)$  classification of SET phases is also overcomplete in this sense. For instance, the symmetry fractionalization classes when  $SG = Z_2$  and  $GG = Z_2 \times Z_2$  are given by  $SFC(SG, GG) = H^2(SG, GG) = H^2(SG, Z_2) \times H^2(SG, Z_2) = Z_2 \times Z_2$ , using the universal coefficients theorem. If we use  $(a, b)$ , with  $a, b = 0, 1 \in Z_2$ , to represent this index, then  $(1, 0)$  [(0, 1)] simply means that there is nontrivial symmetry fractionalization in the first [second]  $Z_2$  gauge sector, and these are physically the same situation.

Second, our classification is certainly *not* a full classification of all possible gapped bosonic quantum phases with both global symmetry and topological order. There are certainly topological orders that cannot be described by discrete gauge theories, for instance, the chiral fractional quantum Hall states. Even for nonchiral topological orders, there are phases realized by the string-net models<sup>69</sup> in which quasiparticle quantum dimensions are not integers, which again cannot be described by discrete gauge theories, where quasiparticle quantum dimensions must be integers.

So let us ask, under the constraint that the topological order is indeed described by a discrete gauge theory, is the classification complete? However, we must first specify the condition: What exactly do we mean by “topological order described by a discrete gauge theory”? We actually

mean nothing but phases characterized by  $H^{d+1}(GG, U(1))$ . Unfortunately, this sounds like a circular argument, but we do not know how to translate it into a more physical statement. For example,  $H^4(Z_2, U(1)) = Z_1$ , meaning that there is only one  $Z_2$  gauge theory in  $3 + 1d$  in our context. However, the string-net models in  $3 + 1d$  allow one to construct two topological phases, both of which look like  $Z_2$  gauge theories. The difference is that in one phase the  $Z_2$  gauge charge is a boson, while in the other phase it is a fermion. In our classification, the second phase is not included.

Even under this condition, namely the topological order given by  $H^{d+1}(GG, U(1))$ , it seems that the classification may still be incomplete. For instance, we already mentioned that the gauge charges always have trivial symmetry fractionalization in our classification. Maybe it is better to ask: Is the classification complete under additional physical conditions? And if yes, what are these additional physical conditions? These are difficult questions and we currently do not know the answers. Nevertheless, we can make some comments. Below we address two aspects of these issues.

*Is the classification of symmetry fractionalization classes complete?* We want to further comment on the *missing* symmetry fractionalization classes for gauge charges. Let us focus on  $2 + 1d$ , where the gauge charges and gauge fluxes are dual to each other, at least for Abelian  $GG$ . In this case, we can reinterpret the symmetry fractionalization classes for gauge fluxes as those for gauge charges, after performing the duality. So the real missing part should be those phases with nontrivial symmetry fractionalization for both gauge charges and gauge fluxes.

Naively one may think that it is possible to construct such a phase by coupling two phases together. For instance, consider  $GG = Z_2$ . Our models can be used to construct two phases: phase a (phase b) in which gauge fluxes  $m_a$  (charges  $e_b$ ) have nontrivial symmetry fractionalization (i.e., transform under  $SG$  as a nontrivial projective representation), while  $e_a$  ( $m_b$ ) transform trivially under  $SG$ . (Phase b can be constructed by performing  $e \rightarrow m$  duality from phase a.) We can couple these two phases together. When the coupling is weak the topological order is  $Z_2 \times Z_2$ . After a phase transition of condensing  $m_a m_b$  bound states (or the  $e_a e_b$ ), the topological order will reduce from a  $Z_2 \times Z_2$  gauge theory to a  $Z_2$  gauge theory. However, the condensed  $m_a m_b$  (or  $e_a e_b$ ) quasiparticles actually transform nontrivially under  $SG$ . Consequently, the new  $Z_2$  topologically ordered phase breaks  $SG$ .

However, it seems possible to construct an effective lattice gauge theory for the phases with nontrivial symmetry fractionalization (for on-site  $SG$ ) for both gauge charges and gauge fluxes. So it is feasible to expect that these phases do exist. However, the above discussion signals that these phases may not be adjacent to the phases classified by  $H^{d+1}(SG \times GG, U(1))$  in some sense. The reason that we miss those phases in  $H^{d+1}(SG \times GG, U(1))$  may be because they cannot be described by exactly solvable models.

*Is the classification of the interplay between  $SG$  and  $GG$  beyond symmetry fractionalization complete?* Let us consider the classes indexed by nontrivial elements in  $EXTRA(SG, GG)$  in  $2 + 1d$ . We show that in the example of  $GG = Z_2 \times Z_2$  and  $SG = Z_2$ , the minimal model for a nontrivial  $EXTRA(SG, GG)$ , such a phase means that  $SG$

can interchange the species of quasiparticles. However, we know that in  $2 + 1d$ , even for the usual toric code topological order with  $GG = Z_2$ , it is fine to imagine that  $SG = Z_2$  could interchange  $e$  and  $m$  quasiparticles, leaving the fusion and braiding algebra invariant. In fact, the translational symmetry (not an on-site symmetry) along the  $45^\circ$  axis of a square-lattice toric code model indeed interchanges  $e$  and  $m$ . Such an  $e$  and  $m$  interchange induced by  $SG$  is also missing from  $H^3(GG, U(1))$ . It is, however, actually reasonable that such phenomena are missing in our classification. That is because our classification can be generalized to arbitrary higher dimensions, while the  $e$ - $m$  interchange can only occur in  $2 + 1d$ . For instance, in  $3 + 1d$   $e$  is pointlike and  $m$  is looplike, so they can never be interchanged.

*Note added.* Recently, we noticed the recent work by Hung and Wen,<sup>73</sup> which discusses the general duality between SPT phases and the DW TQFTs. Another recent work, by Essin and Hermele,<sup>74</sup> classifies the general symmetry fractionalization of gapped  $Z_2$  QSLs. Also, Hu, Wan, and Wu<sup>75</sup> have very recently analyzed in detail the topological phases described by models similar to ours in absence of global symmetries.

## ACKNOWLEDGMENTS

Y.R. thanks helpful discussions with Fa Wang and especially Michael Hermele. This work is supported by the Alfred P. Sloan foundation and National Science Foundation under Grant No. DMR-1151440.

## APPENDIX A: PROJECTIVE SYMMETRY GROUP IN PARTON CONSTRUCTION

Parton construction is a convenient way to obtain quantum states with topological order. The basic idea is to write a topologically ordered state directly using the anyonic quasiparticle degrees of freedom. For example, in the Schwinger-fermion representation of QSLs with  $Z_2$  topological order, fermionic quasiparticles are used to represent a physical spin- $\frac{1}{2}$ :  $\vec{S}_i = 1/2 f_{i\alpha}^\dagger \vec{\sigma}_{\alpha\beta} f_{i\beta}$ , where  $i$  labels sites and  $\alpha, \beta$  label spins. Note that this construction enlarges the Hilbert space from 2 to 4 per site, and one eventually needs to remove the unphysical states (empty and doubly-occupied sites) to obtain a physical spin- $\frac{1}{2}$  wave function. This removal of unphysical states can be accomplished by the so-called Gutzwiller projection:  $P_G \equiv \prod_i n_i(2 - n_i)$ , where  $n_i = f_{i\alpha}^\dagger f_{i\alpha}$  is the fermion number on site  $i$ .

In this approach, on the mean-field level, a  $Z_2$  QSL can be represented as a free fermion state  $|\psi_{\text{MF}}\rangle$  of  $f_{i\alpha}$  fermions, which is the ground state of a spin-singlet mean-field Hamiltonian:

$$H_{\text{MF}} = \sum_{ij} \chi_{ij} f_{i\alpha}^\dagger f_{j\alpha} + \Delta_{ij\epsilon\alpha\beta} f_{i\alpha}^\dagger f_{j\beta}^\dagger + \text{H.c.} \quad (\text{A1})$$

$H_{\text{MF}}$  has both hopping and pairing terms on a lattice ( $\epsilon_{\alpha\beta}$  term is the spin singlet pairing). The physical spin- $\frac{1}{2}$  wave function of the  $Z_2$  QSL can be obtained by Gutzwiller projection:  $|\psi_{\text{QSL}}\rangle = P_G |\psi_{\text{MF}}\rangle$ . Here the  $Z_2$  gauge fluctuations emerge exactly because of this projection: two mean-field states differing by a gauge transformation  $\chi_{ij} \rightarrow \epsilon_i \chi_{ij} \epsilon_j, \Delta_{ij} \rightarrow \epsilon_i \Delta_{ij} \epsilon_j$  ( $\epsilon_i = \pm 1$ ) give exactly the same spin wave function. Therefore,

such local  $Z_2$  fluctuations correspond to redundancies in the formulation and are gauge fluctuations. The  $f_{i\alpha}$  fermions are the quasiparticles carrying the  $Z_2$  gauge charge. The low-energy effective theory of the state  $|\psi_{\text{QSL}}\rangle$  is described by  $Z_2$  gauge charges  $f_{i\alpha}$  coupled with a dynamical  $Z_2$  gauge field.

How can we make sure that the QSL wave function  $|\psi_{\text{QSL}}\rangle$  is symmetric under a symmetry group  $SG$ , such as lattice translations? Naively, one would require the mean-field Hamiltonian  $H_{\text{MF}}$  to be invariant under  $SG$  transformations. In fact, this is not required. Because two mean-field states differing by a  $Z_2$  gauge transformation label exactly the same physical state, one only requires  $H_{\text{MF}}$  to be “projectively symmetric.” Namely,  $H_{\text{MF}}$  before and after an  $SG$  transformation can differ by a  $Z_2$  gauge transformation. This is the key observation underlying the  $PSG$ .

For any element  $g$  in  $SG$ , there will be a certain  $Z_2$  gauge transformation  $G_g$  associated with the  $g$  such that the combination  $G_g \cdot g$  leaves the mean-field Hamiltonian  $H_{\text{MF}}$  or the state  $|\psi_{\text{MF}}\rangle$  invariant. The collection of all such combinations form a group, which is defined to be  $PSG$ :  $PSG \equiv \{G_g \cdot g : G_g \cdot g \text{ leaves } H_{\text{MF}} \text{ invariant}, \forall g \in SG\}$ .

Let us look at the mean-field Hamiltonian Eq. (A1) again. Clearly, one can do a global gauge transformation:  $\epsilon_i = -1, \forall i$  and  $H_{\text{MF}}$  is invariant, which is also the only nontrivial gauge transformation which leaves  $H_{\text{MF}}$  invariant. This means that in  $PSG$ , there will be two elements corresponding to the identity element in  $SG$ : either  $\epsilon_i = 1, \forall i$ , or  $\epsilon_i = -1, \forall i$ . In general, for any element  $g \in SG$  there will be two elements,  $G_g \cdot g$  and  $\tilde{G}_g \cdot g$  in  $PSG$  corresponding to it. The gauge transformations  $G_g$  and  $\tilde{G}_g$  differ by the global  $Z_2$  gauge transformation. Mathematically, the algebraic relation between  $PSG$  and  $SG$  is given by<sup>56</sup>:

$$PSG/IGG = SG. \quad (\text{A2})$$

Here  $IGG = Z_2$ , the group of global gauge transformations.

Equation (A2) is the key mathematical structure underlying  $PSG$ . It indicates that  $PSG$  is a group extension of the group  $SG$  by  $IGG$ . When  $IGG$  is Abelian, which is true in the  $Z_2$  case, we know that  $IGG$  is in the center of  $PSG$ , because global gauge transformations obviously commute with any  $PSG$  element. In this case, a  $PSG$  is a central extension of  $SG$  by  $IGG$ . Further, the classification of all different  $PSGs$  becomes the classification of all possible central extensions. There is a nice mathematical theorem on central extensions of groups stating that all such central extensions are classified by  $H^2(SG, IGG)$  (see, for example, Ref. 57).

At this moment, it appears that  $PSG$  is a feature of the parton mean-field states only. Whether  $PSG$  is physical or not beyond the mean-field formulation is not completely clear. To see the physical meaning of  $PSG$  and  $H^2(SG, IGG)$  beyond the mean-field formulation, we need to consider the low-energy effective theory, which is discussed in the main text.

## APPENDIX B: THE OPERATOR REALIZATION OF TWISTED EXTENDED RIBBON ALGEBRA AND THE QUASI-QUANTUM DOUBLE

In this section we write the explicit forms of the ribbon operators  $F^{(h,g)}(\Gamma)$  and the operators acting on ends of ribbons

$D_{(h,g)}(A), D_{(h,g)}(B)$  and demonstrate the algebra satisfied by these operators. As in the main text, we also only consider an Abelian group  $SG \times GG$ . These operators are defined for  $h \in GG, g \in SG \times GG$ . In addition, we study the braiding and fusion properties of the quasiparticles created by these ribbon operators and show that they are mathematically described by the quasi-quantum double.<sup>61,70</sup>

### 1. The operator realization of the twisted extended ribbon algebra

Let us start by noting that the definition and some properties of ribbon operators were presented in Sec. IV B. Here we start by recalling the form of the nonzero matrix element of the ribbon operator  $F^{(h,g)}(\Gamma)$ :

$$\langle \text{fin} | F^{(h,g)}(\Gamma) | \text{i} \rangle = f_A \cdot f_B \cdot f_{AB} \cdot w_h^\Gamma(g), \quad (\text{B1})$$

where  $w_h^\Gamma(g)$  is defined in Eq. (72), and the relation between the initial and final states,  $|\text{i}\rangle, |\text{fin}\rangle$ , is explained in Eq. (71); the  $f_A, f_B, f_{AB}$  are rather complicated phase factors depending only on the degrees of freedom living on ends of  $\Gamma$ , which we here explicitly define:

$$\begin{aligned} f_A &= \frac{\omega(h_A h^{-1}, h, b_N) \omega(b_N, h, h_A h^{-1}) \omega(e_{N+1}^{-1}, b_N c_{N+1}^{-1}, h)}{\omega(c_{N+1}, b_N c_{N+1}^{-1}, h) \omega(h_A h^{-1}, h, h_A^{-1}) \omega(h_A^{-1}, h, h_A h^{-1})}, \\ f_B &= \frac{c_{h_B}(h, h_B) c_{hh_B}(c_1, h)}{c_{hh_B}(h_B, h) c_{c_1}(h, h_B)} \\ &\quad \times \frac{\omega(h, h^{-1} c_1^{-1} b_0, e_1^{-1}) \omega(c_1, h, h^{-1} c_1^{-1} b_0)}{\omega(h_B, h, h_B^{-1} h^{-1})}, \\ f_{AB} &= \omega^{-1}(h, h_A^{-1}, h_A h_B). \end{aligned} \quad (\text{B2})$$

Here the flux in  $t_A$  is  $h_A = b_N^{-1} c_{N+1} e_{N+1}$  and the flux in  $t_B$  is  $h_B = b_0^{-1} c_1 e_1$  in the initial state  $|\{u_i\}, \{\tilde{g}_{ij}\}\rangle$  (see Fig. 15 for the definitions of  $b_0, b_N, \dots$ , degrees of freedom living of the ends of  $\Gamma$ ). Although here we use the specific geometric configuration of the ribbon  $\Gamma$  in Fig. 15, the definitions of  $F^{(h,g)}(\Gamma)$  and  $D_{(h,g)}(A)$  ( $D_{(h,g)}(B)$ ) below can be easily generalized to any geometric configuration of  $\Gamma$ .

Next, we define the operator  $D_{(h,g)}(A)$  ( $D_{(h,g)}(B)$ ) explicitly on end  $A$  (end  $B$ ) (also mentioned in the main text), where  $h \in GG, g \in SG \times GG$ . They are defined as an operator in the whole Hilbert space  $\mathcal{H}$  [in fact, they are also well-defined in  $\mathcal{K}(\Gamma)$ , because  $D_{(h,g)}(A), D_{(h,g)}(B)$  do not change the flux of a 2-simplex inside  $\Gamma$ ], via the matrix elements,

$$\begin{aligned} \langle f | D_{(h,g)}(A) | i \rangle &= \delta_{h_A, h} \cdot c_h(g, b_N) W_6(i), \\ \langle f | D_{(h,g)}(B) | i \rangle &= \delta_{h_B, h} \cdot c_h(g, c_1) W_6(i), \end{aligned} \quad (\text{B3})$$

where the phase factor  $W_6(i)$  is defined in the main text in Eq. (80).

With these definitions, after straightforward but complicated algebra, one can show that, in both the Hilbert space  $\mathcal{H}$  and its subspace  $\mathcal{K}(\Gamma)$ ,

$$\begin{aligned} D_{(h_2, g_2)}(A) \cdot D_{(h_1, g_1)}(A) &= \delta_{h_1, h_2} \cdot c_{h_1}(g_2, g_1) D_{(h_1, g_2 g_1)}(A), \\ D_{(h_2, g_2)}(B) \cdot D_{(h_1, g_1)}(B) &= \delta_{h_1, h_2} \cdot c_{h_1}(g_2, g_1) D_{(h_1, g_2 g_1)}(B). \end{aligned} \quad (\text{B4})$$

In the sub-Hilbert space  $\mathcal{K}(\Gamma)$ , we have more identities:

$$F^{(h_1, g_2 g_1)}(\Gamma) D_{(h_2, h_1, g_2)}(A) = c_{g_2}(h_2, h_1) c_{h_1}(g_2, g_1) D_{(h_2, g_2)}(A) F^{(h_1, g_1)}(\Gamma), \quad (\text{B5})$$

$$D_{(h_1, h_2, g_2)}(B) F^{(h_1, g_1, g_2)}(\Gamma) = c_{g_2}(h_1, h_2) c_{h_1}(g_1, g_2) F^{(h_1, g_1)}(\Gamma) D_{(h_2, g_2)}(B), \quad (\text{B6})$$

and

$$F^{(h_2, g_2)}(\Gamma) F^{(h_1, g_1)}(\Gamma) = \delta_{g_1, g_2} \cdot c_{g_1}(h_2, h_1) F^{(h_2, h_1, g_1)}(\Gamma). \quad (\text{B7})$$

Equations (B4)–(B7) are summarized in Eqs. (81a), (81c), (81d), and (81b) in the main text.

In addition, it can be easily shown that  $D_{(h, g)}(A)$ ,  $D_{(h, g)}(B)$  and  $F^{(h, g)}(\Gamma)$  operators all commute with the global symmetry transformations in  $SG$ .

## 2. Braiding

### a. Braiding between the quasiparticles at end $A$ 's

Next, we describe the braiding and fusion properties of the quasiparticles created by the  $F^{h, g}(\Gamma)$  operators when applied on the ground state  $|gs\rangle$ . For these purposes, we must consider multiple ribbons. Starting from multiple ribbons  $\Gamma_1, \Gamma_2, \dots, \Gamma_N$ , we define a sub-Hilbert space  $\mathcal{K}(\Gamma_1, \Gamma_2, \dots, \Gamma_N) \subset \mathcal{H}$  to be the one spanned by those states satisfying zero-flux rule everywhere inside  $\Gamma_1, \Gamma_2, \dots, \Gamma_N$ . Now all the operators  $F^{(h, g)}(\Gamma_n)$ ,  $D_{(h, g)}(A_n)$ ,  $D_{(h, g)}(B_n)$ ,  $n = 1, 2, \dots, N$  are all well-defined in  $\mathcal{K}(\Gamma_1, \Gamma_2, \dots, \Gamma_N)$ . ( $A_n$  and  $B_n$  are the two ends of the ribbon  $\Gamma_n$ .)

In order to make the braiding and fusion algebra of the quasiparticles at both the  $A_n$  and  $B_n$  ends on the same footing, it is convenient to introduce a slightly modified ribbon operator:

$$\tilde{F}^{(h, g)}(\Gamma) \equiv F^{(h, g)}(\Gamma) f_{AB}^{-1}, \quad (\text{B8})$$

where the phase factor  $f_{AB}$  is given in Eq. (B2).  $\tilde{F}^{(h, g)}(\Gamma)$  also commutes with the global symmetry and satisfies the same operator algebra as  $F^{(h, g)}(\Gamma)$  with  $D(A), D(B)$  operators [see Eqs. (B5) and (B6)]. [However, the algebra in Eq. (B7) is no longer satisfied by  $\tilde{F}^{(h, g)}(\Gamma)$ .] We can then construct an excited state using multiple ribbons  $\Gamma_1, \dots, \Gamma_N$  that all share the same end  $B$ , but end  $A_n$  are all different from each other. Here by “sharing the same end  $B$ ”, we require that the vertices  $i_{B_n}$ , the triangles  $t_{B_n}$ , and the edge  $B_n$ 's are all the same:  $B_1 = B_2 = \dots = B_N \equiv B$ , edge  $B_1 = \text{edge } B_2 = \dots = \text{edge } B_N \equiv \text{edge } B$ . Let us only consider the case that  $\Gamma_1, \dots, \Gamma_N$  do not overlap/intersect with each other except over a finite length starting from end  $B$ , which is enough for our purposes. We can choose an ordering of the ribbons:  $\Gamma_n$  is on the counterclockwise side of  $\Gamma_{n+1}$ ,  $\forall n$ . [See Fig. 17(a) for a geometric illustration.] An excited state is given by

$$|\psi_{u_B}^{k_1, \dots, k_N}\rangle = \hat{P}_{u_B}(B) \tilde{F}^{k_1}(\Gamma_1) \tilde{F}^{k_2}(\Gamma_2), \dots, \tilde{F}^{k_N}(\Gamma_N) |gs\rangle, \quad (\text{B9})$$

where we have used  $k_1 = (h_1, g_1), \dots, k_N = (h_N, g_N)$  to save notation.  $\hat{P}_{u_B}(B)$  is a projection operator that enforces  $u_{i_B} = u_B \in SG$  at end  $B$ , which commutes with all the  $\tilde{F}$  operators.  $|\psi_{u_B}^{k_1, \dots, k_N}\rangle$  only contains quasiparticles at end  $A_n$  and end  $B$  and will be very useful to understand the braiding and fusion

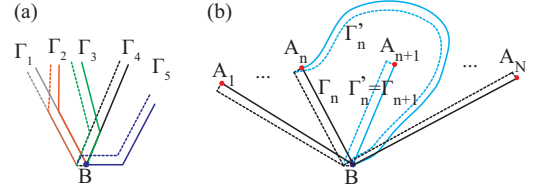


FIG. 17. (Color online) Multiple ribbons sharing end  $B$ , describing quasiparticles at their end  $A$ 's. (a) Example of ordering multiple (five) ribbons, with strings  $\Gamma_1, \dots, \Gamma_5$ , in a “counterclockwise sense.” The ribbons are allowed to have overlaps only over a finite length starting from end  $B$ . The figure shows a realization possible on a triangular lattice. (b) The counterclockwise  $180^\circ$  braiding of particles  $A_n$  and  $A_{n+1}$  in an  $N$ -particle state, a generalization of Fig. 16. The (blue) strings  $\Gamma'$  apply to the braided state.

algebra. We denote the sub-Hilbert space spanned by all the states  $|\psi_{u_B}^{k_1, \dots, k_N}\rangle$  with a fixed  $u_B$  as  $\mathcal{L}_{u_B}(A_1, A_2, \dots, A_N, B)$ , because one can show that this sub-Hilbert space only depends on the ribbons' ends, but does not depend on the paths of the ribbons.

We will soon study the braiding and fusion operations of the quasiparticles at the end  $A_n$ 's in  $\mathcal{L}_{u_B}(A_1, A_2, \dots, A_N, B)$ . These operations only act within the sub-Hilbert space  $\mathcal{L}_{u_B}(A_1, A_2, \dots, A_N, B)$  for a fixed  $u_B$ , because  $u_B$  is always unchanged in them. In fact, we show that the braiding and fusion algebra (or, the superselection sectors of end  $A_n$  quasiparticles) only involve  $D_{(h_1, h_2)}(B)$ , with  $h_1, h_2 \in GG$ .

However, when a general  $D_{(h, g)}(B)$  operator ( $g = h_g \cdot \tilde{g}$ ,  $h_g \in GG$  and  $\tilde{g} \in SG$ ) acts on a state in  $\mathcal{L}_{u_B}(A_1, A_2, \dots, A_N, B)$ , it will send the state to a different sub-Hilbert space  $\mathcal{L}_{\tilde{g} \cdot u_B}(A_1, A_2, \dots, A_N, B)$ . In addition, the global symmetry transformation of  $\tilde{g}$  also sends  $\mathcal{L}_{u_B}(A_1, A_2, \dots, A_N, B)$  to  $\mathcal{L}_{\tilde{g}^{-1} \cdot u_B}(A_1, A_2, \dots, A_N, B)$ . Therefore, if one wants to study the general  $D_{(h, g)}(B)$  operators and the global symmetry transformations, one should consider a larger sub-Hilbert space:  $\mathcal{L}(A_1, A_2, \dots, A_N, B) \equiv \bigoplus_{u_B \in SG} \mathcal{L}_{u_B}(A_1, A_2, \dots, A_N, B)$ . Although we do not have a proof, we believe that  $\mathcal{L}(A_1, A_2, \dots, A_N, B)$  contains all possible excited states at end  $A_n$ 's and the end  $B$ . (For single-ribbon states  $|\psi_{u_B}^k\rangle$ , we do have a proof in the main text that they span all possible excited states at the end  $A$  and the end  $B$ .)

Note that because  $h_{A_n} = \mathbb{1}$  in  $|gs\rangle$ ,  $f_{AB} = 1$  due to the canonical form of 3-cocycle. Therefore,  $|\psi_{u_B}^{k_1, \dots, k_N}\rangle$  can be equally created by the original  $F^{(h, g)}(\Gamma)$  ribbon operator:

$$|\psi_{u_B}^{k_1, \dots, k_N}\rangle = \hat{P}_{u_B}(B) F^{k_1}(\Gamma_1) F^{k_2}(\Gamma_2) \dots F^{k_N}(\Gamma_N) |gs\rangle, \quad (\text{B10})$$

which is given in Eq. (89) in the main text. In fact, to study the braiding and fusion operations of the end- $A_n$  quasiparticles, it does not matter whether  $F^{(h, g)}(\Gamma)$  or  $\tilde{F}^{(h, g)}(\Gamma)$  is used, because they give the same algebra. This is why we only use  $F^{(h, g)}(\Gamma)$  operators in the main text for simplicity.

The geometric illustration of the braiding process between an end  $A_n$  and an end  $A_{n+1}$  has been discussed in the main text, but is also shown in Fig. 17(b). The following operator identity is crucial to compute the braiding algebra: When  $\Gamma_1$  and  $\Gamma_2$  share the same end  $B$  but have different end  $A$ 's, and

$\Gamma_1$  is on the counterclockwise side of  $\Gamma_2$ ,

$$\begin{aligned} & \tilde{F}^{(h_1, g_1)}(\Gamma_2) \tilde{F}^{(h_2, g_2)}(\Gamma_1) \\ &= c_{h_2}(g_2 h_1^{-1}, h_1) \tilde{F}^{(h_2, g_2 h_1^{-1})}(\Gamma_1) \tilde{F}^{(h_1, g_1)}(\Gamma_2) \frac{\omega(h_1, h_2, h_B)}{\omega(h_2, h_1, h_B)}. \end{aligned} \quad (\text{B11})$$

$$\begin{aligned} & \hat{R}_{CC}^{n, n+1} | \psi_{u_B}^{k_1, \dots, (h_n, g_n), (h_{n+1}, g_{n+1}), \dots, k_N} \rangle \\ &= \hat{R}_{CC}^{n, n+1} \hat{P}_{u_B}(B) \tilde{F}^{k_1}(\Gamma_1) \dots \tilde{F}^{(h_n, g_n)}(\Gamma_n) \tilde{F}^{(h_{n+1}, g_{n+1})}(\Gamma_{n+1}) \dots \tilde{F}^{k_N}(\Gamma_N) | g_S \rangle \\ &= \hat{P}_{u_B}(B) \tilde{F}^{k_1}(\Gamma_1) \dots \tilde{F}^{(h_n, g_n)}(\Gamma_{n+1}) \tilde{F}^{(h_{n+1}, g_{n+1})}(\Gamma_n) \dots \tilde{F}^{k_N}(\Gamma_N) | g_S \rangle \\ &= \frac{\omega(h_n, h_{n+1}, h_{n+2} h_{n+3}, \dots, h_N)}{\omega(h_{n+1}, h_n, h_{n+2} h_{n+3}, \dots, h_N)} c_{h_{n+1}}(g_{n+1} h_n^{-1}, h_n) \hat{P}_{u_B}(B) \tilde{F}^{k_1}(\Gamma_1) \dots \tilde{F}^{(h_{n+1}, g_{n+1} h_n^{-1})}(\Gamma_n) \tilde{F}^{(h_n, g_n)}(\Gamma_{n+1}) \dots \tilde{F}^{k_N}(\Gamma_N) | g_S \rangle \\ &= \frac{\omega(h_n, h_{n+1}, h_{n+2} h_{n+3}, \dots, h_N)}{\omega(h_{n+1}, h_n, h_{n+2} h_{n+3}, \dots, h_N)} c_{h_{n+1}}(g_{n+1} h_n^{-1}, h_n) | \psi_{u_B}^{k_1, \dots, (h_{n+1}, g_{n+1} h_n^{-1}), (h_n, g_n), \dots, k_N} \rangle. \end{aligned} \quad (\text{B12})$$

Here the  $h_B$  in Eq. (B11) picks up the accumulated flux in  $t_B$ :  $h_{n+2} h_{n+3}, \dots, h_N$ .

Although everything about braiding can be understood from Eq. (B12), the  $\omega$  factor in it is not convenient. Can we get rid of this phase factor and find the underlying algebraic structure satisfied by  $\hat{R}_{CC}^{n, n+1}$ ?

When acting on the ground state,  $h_B = \mathbb{1}$ , and the  $\omega$  term in Eq. (B11) is 1 due to the canonical form of a 3-cocycle. In this particular case Eq. (B11) becomes Eq. (99). The braiding of an excited state with only two ribbons  $\Gamma_1, \Gamma_2$  is indeed described by Eq. (97). Let us define a formal braiding operator  $R_{CC}^{1,2}$  which implements the physical braiding  $\hat{R}_{CC}^{1,2}$  in  $|\psi_{u_B}^{k_1, k_2}\rangle$ :

$$\begin{aligned} R_{CC}^{1,2} &= R^{qr} D_r^{(1)}(B) \otimes D_q^{(2)}(B) \cdot \sigma \\ &= \sigma \cdot R^{rq} D_r^{(1)}(B) \otimes D_q^{(2)}(B) \\ &= \sigma \cdot \sum_{h_1, h_2 \in GG} D_{(h_1, \mathbb{1})}^{(1)}(B) \otimes D_{(h_2, h_1)}^{(2)}(B), \end{aligned} \quad (\text{B13})$$

where  $\sigma$  is the permutation operator:  $\sigma |\psi_{u_B}^{k_1, k_2}\rangle = |\psi_{u_B}^{k_2, k_1}\rangle$ , the tensor  $R^{(h_1, g_1), (h_2, g_2)} = \delta_{h_1, g_2} \delta_{g_1, \mathbb{1}}$  is also defined in the main text, and  $D_{(h_n, p_n)}^{(n)}(B)$  with  $h_n, p_n \in GG$  is defined to be a formal operator that only transforms the  $\Gamma_n$  operator  $\tilde{F}^{(h, g)}(\Gamma_n)$  as if we are in a single-ribbon state [see Eq. (B6)]. More precisely, because

$$D_{(h_1, p_1)}(B) | \psi_{u_B}^{(\tilde{h}_1, \tilde{g}_1)} \rangle = \delta_{h_1, \tilde{h}_1} \cdot c_{\tilde{h}_1}(\tilde{g}_1 p_1^{-1}, p_1) | \psi_{u_B}^{(\tilde{h}_1, \tilde{g}_1 p_1^{-1})} \rangle, \quad (\text{B14})$$

we have

$$\begin{aligned} & D_{(h_1, p_1)}^{(1)}(B) \otimes D_{(h_2, p_2)}^{(2)}(B) | \psi_{u_B}^{(\tilde{h}_1, \tilde{g}_1), (\tilde{h}_2, \tilde{g}_2)} \rangle \\ &= \delta_{h_1, \tilde{h}_1} \cdot \delta_{h_2, \tilde{h}_2} \cdot c_{\tilde{h}_1}(\tilde{g}_1 p_1^{-1}, p_1) c_{\tilde{h}_2}(\tilde{g}_2 p_2^{-1}, p_2) \\ &\quad \times | \psi_{u_B}^{(\tilde{h}_1, \tilde{g}_1 p_1^{-1}), (\tilde{h}_2, \tilde{g}_2 p_2^{-1})} \rangle. \end{aligned} \quad (\text{B15})$$

The key property of these formal tensor product operators is that they commute with any local operator at end  $A_i$ ,  $\forall i$ . That is why they are topological operators for the quasiparticles at end  $A_i$ 's.

Here  $h_B$  should be understood as an operator that measures the gauge flux in the 2-simplex  $t_B$ . The order between the  $F$  term and the  $\omega$  term on the right-hand side is therefore important. Equation (B11) already describes the physical counterclockwise braiding ( $180^\circ$ ) operations  $\hat{R}_{CC}^{n, n+1}$  between quasiparticles at end  $A_n$  and end  $A_{n+1}$  in  $\mathcal{L}(A_1, \dots, A_N, B)$  completely:

Because of Eq. (B4), the multiplication of the formal operators  $D_{(h, p)}^{(n)}(B)$  ( $\forall h, p \in GG$ ) satisfy the following algebra:

$$D_i^{(n)}(B) D_j^{(n)}(B) = \Omega_{ij}^k D_k^{(n)}(B), \quad (\text{B16})$$

where we used the tensor  $\Omega_{ij}^k \equiv \delta_{h_i, h_j} \delta_{h_k, h_i} \delta_{g_k, g_i g_j} c_{h_k}(g_i, g_j)$  defined in Eqs. (86).

Equation (B16) tells us that the quasiparticles created by ribbon  $\Gamma_n$  at end  $A_n$  form representation of this algebra. Mathematically, the algebra in Eq. (B16) is called the multiplication in the quasi-quantum double  $\mathbf{D}^{\tilde{\omega}}(GG)$ ,<sup>61,70</sup> where  $\tilde{\omega} \in H^3(GG, U(1))$  is the 3-cocycle induced on  $GG$  by the cocycle  $\omega \in H^3(SG \times GG, U(1))$  in our model by restricting the elements  $x, y, z \in GG$  in  $\omega(x, y, z)$ . Multiplication in  $\mathbf{D}^{\tilde{\omega}}(GG)$  is associative. A representation of the multiplication algebra Eq. (B16) is called a representation of the quasi-quantum double  $\mathbf{D}^{\tilde{\omega}}(GG)$ .

Because we show that the braiding algebra is completely determined by  $D_{(h, p)}^{(n)}(B)$  operators with  $h, p \in GG$ , one knows the braiding properties of a quasiparticle at end  $A_n$  if we know which representation of  $\mathbf{D}^{\tilde{\omega}}(GG)$  this particle is in. In fact, the quasiparticle species (or more precisely, its superselection sector) is labeled by an irreducible representation of  $\mathbf{D}^{\tilde{\omega}}(GG)$ . Different irreducible representations of  $\mathbf{D}^{\tilde{\omega}}(GG)$  correspond to different quasiparticle species.

The physical counterclockwise  $360^\circ$  braiding for the two particle states is  $(\hat{R}_{CC}^{n, n+1})^2$ . Its action in the basis  $|\psi_{u_B}^{k_1, \dots, k_N}\rangle$  is actually very simple, because the  $\omega$  terms in Eq. (B12) cancel out for  $(\hat{R}_{CC}^{n, n+1})^2$ :

$$\begin{aligned} & (\hat{R}_{CC}^{n, n+1})^2 | \psi_{u_B}^{k_1, \dots, k_n, k_{n+1}, \dots, k_N} \rangle \\ &= D_{(h_n, h_{n+1})}^{(n)}(B) \otimes D_{(h_{n+1}, h_n)}^{(n+1)}(B) | \psi_{u_B}^{k_1, \dots, k_n, k_{n+1}, \dots, k_N} \rangle. \end{aligned} \quad (\text{B17})$$

It is also tempting to formally define the general operator

$$\begin{aligned} R_{CC}^{n, n+1} &= R^{qr} D_r^{(n)}(B) \otimes D_q^{(n+1)}(B) \cdot \sigma \\ &= \sigma \cdot R^{rq} D_r^{(n)}(B) \otimes D_q^{(n+1)}(B) \\ &= \sigma \cdot \sum_{h_n, h_{n+1} \in GG} D_{(h_n, \mathbb{1})}^{(n)}(B) \otimes D_{(h_{n+1}, h_n)}^{(n+1)}(B). \end{aligned} \quad (\text{B18})$$

Note that the formal operator  $R_{CC}^{n,n+1}$  does not have a hat, which distinguishes it from the physical braiding  $\hat{R}_{CC}^{n,n+1}$  in Eq. (B12). The  $\omega$  factor in Eq. (B12) tells us that, for multiple-ribbon states, the physical braiding  $\hat{R}_{CC}^{n,n+1}$  is *not* implemented by  $R_{CC}^{n,n+1}$  in the basis  $\{|\psi_{u_B}^{k_1, \dots, k_N}\rangle\}$ . However, we show that if we change into certain different basis,  $\hat{R}_{CC}^{n,n+1}$  is still implemented by  $R_{CC}^{n,n+1}$ .

Let us first consider three-ribbon states:  $|\psi_{u_B}^{k_1, k_2, k_3}\rangle$ . The physical  $\hat{R}_{CC}^{2,3}$  between the end  $A_2$  and the end  $A_3$  are still implemented by  $R_{CC}^{2,3}$ . However, in this basis,  $R_{CC}^{1,2}$  and the physical braiding  $\hat{R}_{CC}^{1,2}$  differ by a phase factor  $\frac{\omega(h_1, h_2, h_3)}{\omega(h_2, h_1, h_3)}$ , due to the  $\omega$  term in Eq. (B11). However, this braiding can still be implemented by  $R_{CC}^{1,2}$  if we choose a different basis.

Let us define the state

$$|\psi_{u_B}^{((k_1, k_2), k_3)}\rangle \equiv \omega^{-1}(h_1, h_2, h_3) |\psi_{u_B}^{k_1, k_2, k_3}\rangle. \quad (B19)$$

For reasons that will become clear in a moment, we also define

$$|\psi_{u_B}^{(k_1, (k_2, k_3))}\rangle \equiv |\psi_{u_B}^{k_1, k_2, k_3}\rangle. \quad (B20)$$

All states  $\{|\psi_{u_B}^{((k_1, k_2), k_3)}\rangle\}$  form another basis of  $\mathcal{L}_{u_B}(A_1, A_2, \dots, A_N, B)$ , which differ from the original basis  $\{|\psi_{u_B}^{(k_1, (k_2, k_3))}\rangle\}$  only by phase factors.

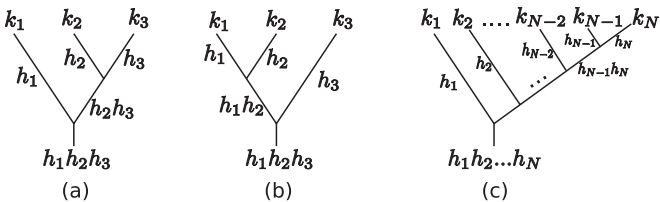
It is then clear that the physical braiding  $\hat{R}_{CC}^{2,3}$  is implemented by  $R_{CC}^{2,3}$  in basis  $\{|\psi_{u_B}^{((k_1, k_2), k_3)}\rangle\}$  (but not in the basis  $\{|\psi_{u_B}^{(k_1, (k_2, k_3))}\rangle\}$ ) and the physical braiding  $\hat{R}_{CC}^{1,2}$  is implemented by  $R_{CC}^{1,2}$  in the basis  $\{|\psi_{u_B}^{((k_1, k_2), k_3)}\rangle\}$  (but not in the basis  $\{|\psi_{u_B}^{(k_1, (k_2, k_3))}\rangle\}$ ). Such a basis change is necessary to maintain the same algebraic form of the formal braiding operator  $R_{CC}^{n,n+1}$  in Eq. (B18).

The two different parentheses configurations:  $(k_1, (k_2, k_3))$  and  $((k_1, k_2), k_3)$  can be viewed as two different ways to “multiply” quasiparticles. For reasons that will become clear later, it is better to call these operations as “comultiplications.” Different orders of comultiplications do not give the same results, which differ by a basis change: Mathematically, the comultiplications are not associative, but are quasiasociative. It turns out that the comultiplications of quasiparticles here have a clear physical meaning: the fusions, which we discuss shortly.

One can generalize the above observation for three-ribbon states to multiple-ribbon states, which turns out to be also very useful to represent the fusion algebra. We define

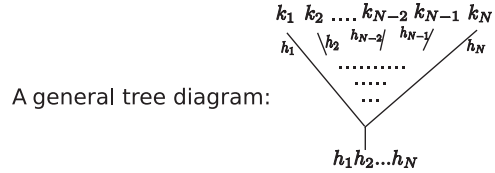
$$|\psi_{u_B}^{(k_1, (k_2, \dots, (k_{N-2}, (k_{N-1}, k_N))))}\rangle \equiv |\psi_{u_B}^{k_1, k_2, \dots, k_{N-2}, k_{N-1}, k_N}\rangle. \quad (B21)$$

We now consider an arbitrary parentheses configuration between  $k_1, k_2, \dots, k_N$ . For convenience, we use a tree diagram to represent it. For example,  $(k_1, (k_2, k_3))$  and  $((k_1, k_2), k_3)$  can be represented as figure (a) and figure (b) below, while  $(k_1, (k_2, \dots, (k_{N-2}, (k_{N-1}, k_N))))$  is represented as figure (c).



Note that we define a tree diagram not only as a geometric object: First, it contains  $k_1 = (h_1, g_1), \dots, k_N = (h_N, g_N)$  assigned to the top end points. Second, every edge (line segment) in a tree diagram is also assigned a group element  $\in GG$ , which is specified as follows. The top edges are assigned as  $h_1, h_2, \dots, h_N$ , and every lower edge coming out of merging two upper edges is assigned by the product of the group elements in the upper two edges.

We can use a tree diagram to represent any parentheses configuration.



A general tree diagram:

We now define a basis for a fixed tree diagram  $\text{Tree}_\alpha$ , where  $\alpha$  labels the tree configuration,

$$|\psi_{u_B}(\text{Tree}_\alpha)\rangle \equiv w(\text{Tree}_\alpha) |\psi_{u_B}^{k_1, k_2, \dots, k_{N-2}, k_{N-1}, k_N}\rangle, \quad (B22)$$

where  $w(\text{Tree}_\alpha)$  is a phase factor which we define below.

Any two tree diagrams with the same set of assigned  $k_1 = (h_1, g_1), \dots, k_N = (h_N, g_N)$  on the top end points can be deformed into each other by a finite number of so-called F moves. An F move is a local deformation of a tree diagram; namely,  $\text{Tree}_\alpha$  and  $\text{Tree}_\beta$  are only different locally as shown in Fig. 18.

When a local F move occurs, we define the state  $\omega^{-1}(h_a, h_b, h_c) |\psi_{u_B}(\text{Tree}_\alpha)\rangle = |\psi_{u_B}(\text{Tree}_\beta)\rangle$ . In this fashion, starting from the tree diagram of the original basis  $(k_1, (k_2, \dots, (k_{N-2}, (k_{N-1}, k_N))))$ , we can find the phase factor  $w(\text{Tree}_\alpha)$  accumulated during a sequence of F moves for any tree diagram  $\alpha$ .

Apparently there are many different possible F-move paths that can connect a given tree diagram with that of  $(k_1, (k_2, \dots, (k_{N-2}, (k_{N-1}, k_N))))$ . One may wonder whether the accumulated phase factor  $w(\text{Tree}_\alpha)$  is the same or not for different F-move paths. It turns out that  $w(\text{Tree}_\alpha)$  is independent of which path one chooses. This is a consequence of the 3-cocycle condition. The 3-cocycle condition dictates that the F moves satisfy a crucial self-consistent condition: the pentagon equation, which in turn indicates that  $w(\text{Tree}_\alpha)$  is well-defined, a consequence of the Mac Lane’s coherence theorem.<sup>76</sup> We refer interested readers to Ref. 77 by Kitaev for detailed discussions.

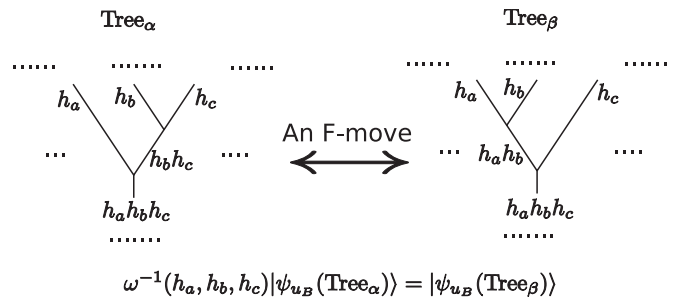


FIG. 18. A general F move.

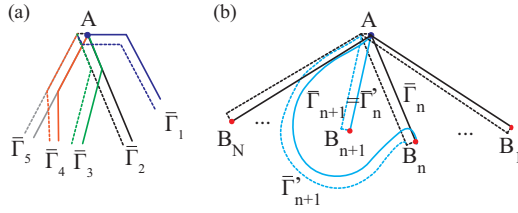


FIG. 19. (Color online) Multiple ribbons sharing end  $A$ , describing quasiparticles at their end  $B$ 's. (a) Example of ordering multiple (five) ribbons, with strings  $\bar{\Gamma}_1, \dots, \bar{\Gamma}_5$ , in a “counterclockwise sense.” The ribbons are allowed to have overlaps only over a finite length starting from end  $A$ . The figure shows a realization possible on a triangular lattice. (b) The counterclockwise  $180^\circ$  braiding of particles  $B_n$  and  $B_{n+1}$  in an  $N$ -particle state. The (blue) strings  $\bar{\Gamma}'$  apply to the braided state.

With this definition of  $|\psi_{u_B}(\text{Tree}_\alpha)\rangle$ , one can show that the physical braiding operation  $\hat{R}_{CC}^{n,n+1}$  between end  $A_n$  and end  $A_{n+1}$  is implemented as  $R_{CC}^{n,n+1}$  in any basis in which  $k_n$  and  $k_{n+1}$  are parenthesized together:  $\dots(k_n, k_{n+1})\dots$

Mathematically, the formal operators  $R_{CC}^{n,n+1}$  do not satisfy the Yang-Baxter equation, a self-consistent equation for braiding algebra. This dictates that an appropriate changing of basis is required, which is discussed in detail above. With this changing of basis, the formal operators satisfy the so-called quasi-Yang-Baxter equation. These mathematical structures are exactly those in the quasi-quantum double  $\mathbf{D}^\omega(GG)$ .

### b. Braiding between the quasiparticles at end $B$ 's

Similarly, we can construct an excited state using multiple ribbons  $\bar{\Gamma}_1, \dots, \bar{\Gamma}_n$  that all share the same end  $A$ :  $A_1 = A_2 = \dots = A_N \equiv A$ , edge  $A_1 = \text{edge } A_2 = \dots =$

edge  $A_N \equiv \text{edge } A$ , and that do not overlap/intersect with each other except for a finite length starting from end  $A$ , while end  $B_n$  are all different from each other. We also choose an ordering:  $\bar{\Gamma}_i$  is on counterclockwise side of  $\bar{\Gamma}_{i+1}$ . [See Fig. 19(a) for a geometric illustration.] We can create an excited state:

$$|\bar{\psi}_{u_A}^{k_1, \dots, k_N}\rangle = \hat{P}_{u_A}(A) \tilde{F}^{k_1}(\bar{\Gamma}_1) \tilde{F}^{k_2}(\bar{\Gamma}_2) \dots \tilde{F}^{k_N}(\bar{\Gamma}_N) |gs\rangle, \quad (\text{B23})$$

which only hosts quasiparticles at end  $B_i$  and end  $A$ . Here  $\hat{P}_{u_A}$  is a projector which enforces  $u_{i_A} = u_A$  for a fixed element  $u_A \in SG$ . [Note that it is important to use  $\tilde{F}^{(h,g)}(\bar{\Gamma})$  operators, *not* the  $F^{(h,g)}(\bar{\Gamma})$  operators to construct  $|\bar{\psi}_{u_A}^{k_1, \dots, k_N}\rangle$ .] We use  $|\bar{\psi}_{u_A}^{k_1, \dots, k_N}\rangle$  to study the braiding properties of the quasiparticles at the end  $B_n$ 's. We denote the sub-Hilbert space spanned by  $\{|\bar{\psi}_{u_A}^{k_1, \dots, k_N}\rangle\}$  as  $\mathcal{L}_{u_A}(B_1, B_2, \dots, B_N, A)$ .

The geometric illustration of the counterclockwise  $180^\circ$  braiding of the end  $B_n$  and the end  $B_{n+1}$  is shown in Fig. 19(b). The following operator identity is crucial to understand its underlying algebraic structure. When  $\bar{\Gamma}_1$  and  $\bar{\Gamma}_2$  share the same end  $A$  but have different end  $B$ 's and  $\bar{\Gamma}_1$  is on the counterclockwise side of  $\bar{\Gamma}_2$ ,

$$\begin{aligned} & \tilde{F}^{(h_1, g_1)}(\bar{\Gamma}_2) \tilde{F}^{(h_2, g_2)}(\bar{\Gamma}_1) \\ &= c_{h_1}(h_2, g_1, h_2^{-1}) \tilde{F}^{(h_2, g_2)}(\bar{\Gamma}_1) \tilde{F}^{(h_1, g_1, h_2^{-1})}(\bar{\Gamma}_2) \frac{\omega(h_2, h_1, h_A^{-1})}{\omega(h_1, h_2, h_A^{-1})}. \end{aligned} \quad (\text{B24})$$

Here  $h_A$  should be interpreted as an operator measuring the gauge flux in  $t_A$ .  $h_A = \mathbb{1}$  in  $|gs\rangle$  and  $h_A = h_1^{-1} h_2^{-1} \dots h_N^{-1}$  in  $|\bar{\psi}_{u_A}^{k_1, \dots, k_N}\rangle$ .

Equation (B24) already describes the physical counterclockwise braiding ( $180^\circ$ ) operations  $\hat{R}_{CC}^{n,n+1}$  between quasiparticles at end  $B_n$  and end  $B_{n+1}$  in  $\mathcal{L}(B_1, \dots, B_N, A)$  completely:

$$\begin{aligned} & \hat{R}_{CC}^{n,n+1} |\bar{\psi}_{u_A}^{k_1, \dots, (h_n, g_n), (h_{n+1}, g_{n+1}), \dots, k_N}\rangle \\ &= \hat{R}_{CC}^{n,n+1} \hat{P}_{u_A}(A) \tilde{F}^{k_1}(\bar{\Gamma}_1) \dots \tilde{F}^{(h_n, g_n)}(\bar{\Gamma}_n) \tilde{F}^{(h_{n+1}, g_{n+1})}(\bar{\Gamma}_{n+1}) \dots \tilde{F}^{k_N}(\bar{\Gamma}_N) |gs\rangle \\ &= \hat{P}_{u_A}(A) \tilde{F}^{k_1}(\bar{\Gamma}_1) \dots \tilde{F}^{(h_n, g_n)}(\bar{\Gamma}_{n+1}) \tilde{F}^{(h_{n+1}, g_{n+1})}(\bar{\Gamma}_n) \dots \tilde{F}^{k_N}(\bar{\Gamma}_N) |gs\rangle \\ &= \frac{\omega(h_{n+1}, h_n, h_{n+2} h_{n+3}, \dots, h_N)}{\omega(h_n, h_{n+1}, h_{n+2} h_{n+3}, \dots, h_N)} c_{h_n}(h_{n+1}, g_n, h_{n+1}^{-1}) \hat{P}_{u_A}(A) \tilde{F}^{k_1}(\bar{\Gamma}_1) \dots \tilde{F}^{(h_{n+1}, g_{n+1})}(\bar{\Gamma}_n) \tilde{F}^{(h_n, g_n, h_{n+1}^{-1})}(\bar{\Gamma}_{n+1}) \dots \tilde{F}^{k_N}(\bar{\Gamma}_N) |gs\rangle \\ &= \frac{\omega(h_{n+1}, h_n, h_{n+2} h_{n+3}, \dots, h_N)}{\omega(h_n, h_{n+1}, h_{n+2} h_{n+3}, \dots, h_N)} c_{h_n}(h_{n+1}, g_n, h_{n+1}^{-1}) |\bar{\psi}_{u_A}^{k_1, \dots, (h_{n+1}, g_{n+1}), (h_n, g_n, h_{n+1}^{-1}), \dots, k_N}\rangle. \end{aligned} \quad (\text{B25})$$

Here the  $h_A^{-1}$  in Eq. (B24) picks up the inverse of the accumulated flux in  $t_A$ :  $h_{n+2} h_{n+3}, \dots, h_N$ .

We can also define the formal braiding operator:

$$\begin{aligned} \bar{R}_{CC}^{n,n+1} &= \bar{R}^{r,q} D_r^{(n)}(A) \otimes D_q^{(n+1)}(A) \cdot \sigma \\ &= \sigma \cdot \bar{R}^{q,r} D_r^{(n)}(A) \otimes D_q^{(n+1)}(A) = \sigma \sum_{h_n, h_{n+1} \in GG} [c_{h_n^{-1}}(h_{n+1}, h_{n+1}^{-1}) c_{h_{n+1}}(h_n, h_n^{-1}) D_{(h_n, h_{n+1})}^{(n)}(A) \otimes D_{(h_{n+1}, \mathbb{1})}^{(n+1)}(A)], \end{aligned} \quad (\text{B26})$$

where  $\sigma$  is the permutation operator, and we define the tensor  $\bar{R}^{(h_1, g_1), (h_2, g_2)}$  as

$$\bar{R}^{(h_1, g_1), (h_2, g_2)} = \delta_{h_1, g_2} \cdot \delta_{g_1, \mathbb{1}} \cdot c_{h_2^{-1}}(h_1, h_1^{-1}) c_{h_1}(h_2, h_2^{-1}). \quad (\text{B27})$$

In fact, one can show that for an Abelian group,  $c_{h_1}(h_2, h_2^{-1}) = c_{h_1}(h_2^{-1}, h_2)$ ,  $\forall h_1, h_2$ .  $D_{(h_n, p_n)}^{(n)}(A)$  with  $h_n, p_n \in GG$  is a formal operator that transforms the  $\bar{\Gamma}_n$  operator  $\tilde{F}^{(h,g)}(\bar{\Gamma}_n)$  as if we are in a single-ribbon state [see Eq. (B5)]. More precisely, for instance, because

$$D_{(h_1, p_1)} |\bar{\psi}_{u_A}^{(\tilde{h}_1, \tilde{g}_1)}\rangle = \delta_{h_1^{-1}, \tilde{h}_1} \cdot c_{p_1}^{-1}(\tilde{h}_1^{-1}, \tilde{h}_1) c_{\tilde{h}_1}^{-1}(p_1, \tilde{g}_1) |\bar{\psi}_{u_A}^{(\tilde{h}_1, p_1, \tilde{g}_1)}\rangle, \quad (\text{B28})$$

we have

$$\begin{aligned} & D_{(h_1, p_1)}^{(1)} \otimes D_{(h_2, p_2)}^{(2)} |\bar{\psi}_{u_A}^{(\tilde{h}_1, \tilde{g}_1), (\tilde{h}_2, \tilde{g}_2)}\rangle \\ &= \delta_{h_1^{-1}, \tilde{h}_1} \cdot \delta_{h_2^{-1}, \tilde{h}_2} c_{p_1}^{-1}(\tilde{h}_1^{-1}, \tilde{h}_1) c_{\tilde{h}_1}^{-1}(p_1, \tilde{g}_1) c_{p_2}^{-1}(\tilde{h}_2^{-1}, \tilde{h}_2) \\ & \quad \times c_{\tilde{h}_2}^{-1}(p_2, \tilde{g}_2) |\bar{\psi}_{u_A}^{(\tilde{h}_1, p_1 \tilde{g}_1), (\tilde{h}_2, p_2 \tilde{g}_2)}\rangle. \end{aligned} \quad (\text{B29})$$

$D_{(h_n, p_n)}^{(n)}(A)$  also satisfy the multiplication algebra Eq. (B16) in the quasi-quantum double  $D^{\hat{\omega}}(GG)$ .

One can show that for two-ribbon states, the  $\omega$  factor in Eq. (B25) is unimportant because it equals one due to the canonical form of a 3-cocycle. In this case one can show that the physical braiding  $\hat{R}_{CC}^{1,2}$  is indeed implemented by the formal operator  $\hat{R}_{CC}^{1,2}$ .

For multiple-ribbon states, the  $\omega$  factor in Eq. (B25) becomes important. Similar to the braiding of end  $A$ 's, one way to get rid of the  $\omega$  factor in Eq. (B25) in the braiding algebra of end  $B$ 's is to introduce appropriate basis changes, which we do not discuss here. After the appropriate basis change, physical braiding  $\hat{R}_{CC}^{n,n+1}$  can still be implemented by the formal operators  $\hat{R}_{CC}^{n,n+1}$ .

Finally, the physical counterclockwise  $360^\circ$  braiding  $(\hat{R}_{CC}^{n,n+1})^2$  also has a simple algebraic form:

$$\begin{aligned} & (\hat{R}_{CC}^{n,n+1})^2 |\bar{\psi}_{u_A}^{k_1, \dots, k_n, k_{n+1}, \dots, k_N}\rangle \\ &= D_{(h_n^{-1}, h_{n+1}^{-1})}^{(n)}(A) \otimes D_{(h_{n+1}^{-1}, h_n^{-1})}^{(n+1)}(A) |\bar{\psi}_{u_A}^{k_1, \dots, k_n, k_{n+1}, \dots, k_N}\rangle. \end{aligned} \quad (\text{B30})$$

### 3. Fusion

We study the fusion of the quasiparticles at the end  $A$ 's only. Let us consider multiple-ribbon states with ribbons all sharing the same end  $B$ , but with different end  $A$ 's.

First let us consider two-ribbon states  $|\psi_{u_B}^{k_1, k_2}\rangle$ . According to the twisted extended ribbon algebra Eq. (B6), the  $D_{(h, p)}(B)$  operators with both  $h, p \in GG$  transform two-ribbon states as

$$\begin{aligned} & D_{(h, p)}(B) |\psi_{u_B}^{(\tilde{h}_1, \tilde{g}_1), (\tilde{h}_2, \tilde{g}_2)}\rangle \\ &= \delta_{h, \tilde{h}_1 \tilde{h}_2} \cdot c_p(h_1, h_2) c_{\tilde{h}_1}(\tilde{g}_1 p^{-1}, p) c_{\tilde{h}_2}(g_2 p^{-1}, p) \\ & \quad \times |\psi_{u_B}^{(\tilde{h}_1, \tilde{g}_1 p^{-1}), (\tilde{h}_2, \tilde{g}_2 p^{-1})}\rangle \\ &= \sum_{h_1 \cdot h_2 = h, h_1, h_2 \in GG} [c_g(h_1, h_2) D_{(h_1, p)}^{(1)}(B) \otimes D_{(h_2, p)}^{(2)}(B)] \\ & \quad \times |\psi_{u_B}^{(\tilde{h}_1, \tilde{g}_1), (\tilde{h}_2, \tilde{g}_2)}\rangle \\ &= \Lambda_{(h, p)}^{ij} D_i^{(1)}(B) \otimes D_j^{(2)}(B) |\psi_{u_B}^{(\tilde{h}_1, \tilde{g}_1), (\tilde{h}_2, \tilde{g}_2)}\rangle, \end{aligned} \quad (\text{B31})$$

where we have used the formal operators  $D_i^{(n)}(B)$  introduced in Eq. (B13), and the tensor  $\Lambda_k^{ij} = \delta_{g_i, g_j} \delta_{g_k, g_i} \delta_{h_k, h_i h_j} c_{g_k}(h_i, h_j)$  defined in Eqs. (86).

This motivates us to generally define formal operators for multiribbon states,

$$D_r^{(n)(n+1)}(B) \equiv \Lambda_r^{ij} D_i^{(n)}(B) \otimes D_j^{(n+1)}(B). \quad (\text{B32})$$

Basically, when acting on a multiribbon state,  $D_r^{(n)(n+1)}(B)$  only transforms the  $\Gamma_n$  and  $\Gamma_{n+1}$  ribbons as if we are in a two-ribbon state. Mathematically, the operation in Eq. (B32) is called comultiplication in the quasi-quantum double  $D^{\hat{\omega}}(GG)$ ,

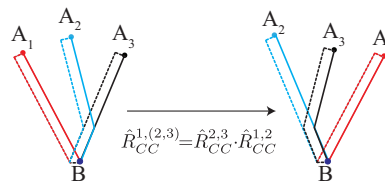


FIG. 20. (Color online) Braiding quasiparticle  $A_1$  with the fused quasiparticle  $A_2 A_3$  can be calculated using the shown formula for a two-step process. The resulting braiding operator is determined by the action of two topological operators [Eq. (B35)], analogously to the simple case of two-particle braiding; however, in this case one topological operator relates to particle  $A_1$ , but the other is a “comultiple” [Eqs. (B32) and (B33)] of topological operators acting on particles  $A_2$  and  $A_3$ .

and is often denoted in mathematical literature by

$$\Delta(D_r) \equiv \Lambda_r^{ij} D_i \otimes D_j. \quad (\text{B33})$$

$D_r^{(n)(n+1)}(B)$  turns out to be very useful; we will show soon that braiding properties of the fused quasiparticle of  $\Gamma_n$  and  $\Gamma_{n+1}$  ribbons are completely determined by  $D_r^{(n)(n+1)}(B)$ .

Because  $D_r^{(n)(n+1)}(B)$  has a physical interpretation of acting  $D_r(B)$  on the two-ribbon states,  $D_r^{(n)(n+1)}(B)$  clearly also satisfy the multiplication algebra Eq. (B16) in the quasi-quantum double  $D^{\hat{\omega}}(GG)$ . Therefore, if we know the irreducible representations of  $D^{\hat{\omega}}(GG)$  (i.e., superselection sectors) for the quasiparticles at end  $A_n$  and end  $A_{n+1}$ , the comultiplication Eq. (B32) induces another representation of  $D^{\hat{\omega}}(GG)$ , which is generally reducible. One can decompose this induced representation into its irreducible components. Every irreducible component corresponds to one fusion channel. *This procedure defines the fusion rule.*

Now let us consider three-ribbon states  $|\psi_{u_B}^{k_1, k_2, k_3}\rangle$ , which allows us to study the braiding of a fused quasiparticle with another quasiparticle. Let us imagine that we fuse the end- $A_2$  and the end- $A_3$  quasiparticles first and braid the fused particle with the end- $A_1$  quasiparticle. We should physically braid both end  $A_2$  and end  $A_3$  with end  $A_1$ , which we define as  $\hat{R}_{CC}^{1,(2,3)} \equiv \hat{R}_{CC}^{2,3} \cdot \hat{R}_{CC}^{1,2}$  [see Fig. 20]. To understand the algebraic structure of this procedure, the basis change that we introduced earlier becomes useful now. One can straightforwardly show that

$$\begin{aligned} & \hat{R}_{CC}^{1,(2,3)} |\psi_{u_B}^{(k_1, (k_2, k_3))}\rangle \\ &= (\hat{R}_{CC}^{2,3} \cdot \hat{R}_{CC}^{1,2}) |\psi_{u_B}^{(k_1, (k_2, k_3))}\rangle \\ &= c_{h_1}(h_2, h_3) c_{h_2}(g_2 h_1^{-1}, h_1) c_{h_2}(g_3 h_1^{-1}, h_1) \\ & \quad \cdot |\psi_{u_B}^{((h_2, g_2 h_1^{-1}), (h_3, g_3 h_1^{-1})), (h_1, g_1)}\rangle \\ &= \sigma \cdot c_{h_1}(h_2, h_3) D_{(h_2, h_1)}^{(2)}(B) \otimes D_{(h_3, h_1)}^{(3)}(B) |\psi_{u_B}^{(k_1, (k_2, k_3))}\rangle \end{aligned} \quad (\text{B34})$$

$$= \sigma \cdot R^{r,q} D_r^{(1)}(B) \otimes D_q^{(2)(3)}(B) |\psi_{u_B}^{(k_1, (k_2, k_3))}\rangle, \quad (\text{B35})$$

where the permutation operator  $\sigma$  is defined as  $\sigma |\psi_{u_B}^{(k_1, (k_2, k_3))}\rangle = |\psi_{u_B}^{((k_2, k_3), k_1)}\rangle$ . Therefore, the braiding algebra of the fused particle satisfies the same algebra as in Eq. (B18) after using  $D_q^{(2)(3)}(B)$  operator.

Similarly, one can imagine to fuse the end- $A_1$  and the end- $A_2$  quasiparticles first and braid the fused particle with the



end- $A_3$  quasiparticle. This physical process is  $\hat{R}_{CC}^{(1,2),3} \equiv \hat{R}_{CC}^{1,2} \cdot \hat{R}_{CC}^{2,3}$ . One can also show that

$$\begin{aligned} \hat{R}_{CC}^{(1,2),3} |\psi_{u_B}^{((k_1, k_2), k_3)}\rangle \\ = \sigma \cdot R^{r,q} D_r^{(1)(2)}(B) \otimes D_q^{(3)}(B) |\psi_{u_B}^{((k_1, k_2), k_3)}\rangle, \end{aligned} \quad (\text{B36})$$

where the permutation operator  $\sigma$  is defined as  $\sigma |\psi_{u_B}^{((k_1, k_2), k_3)}\rangle = |\psi_{u_B}^{(k_3, (k_1, k_2))}\rangle$ .

This discussion can be easily generalized to multiple-ribbon states. One can show that the braiding algebra of the fused particle is always represented using the  $D_r^{(n)(n+1)}(B)$  in a basis where  $(k_n, k_{n+1})$  are parenthesized together.

Finally, the fusion algebra is formally represented by the comultiplication in  $\mathbf{D}^\omega(GG)$  in Eq. (B32) only in a basis where  $(k_n, k_{n+1})$  are parenthesized together. Comultiplication is not associative but is quasiassociative; namely, it becomes associative after the changing of basis: the F move introduced earlier. Because F moves satisfy the pentagon equation, one can show that the fusion algebra also satisfy the pentagon equation,<sup>70,77</sup> the self-consistent equation for fusion algebra.

#### 4. Summary

In this section we find the operator realizations of the twisted extended ribbon algebra and also study the braiding and fusion properties of the topological quasiparticles created by ribbon operators. We find that the topological order in our model is described by the quasi-quantum double  $\mathbf{D}^{\tilde{\omega}}(GG)$ , where the cocycle  $\tilde{\omega} \in H^3(GG, U(1))$  is the one naturally induced by the cocycle  $\omega \in H^3(SG \times GG, U(1))$  in our model.

The core mathematical structures of the quasi-quantum double  $\mathbf{D}^{\tilde{\omega}}(GG)$  include the multiplications in Eq. (B16), the comultiplications in Eq. (B32) and the changing of basis described by Fig. 18 (mathematically called associator). The superselection sector of a quasiparticle is determined by the irreducible representation of the multiplication algebra Eq. (B16). The braiding algebra of quasiparticles is determined by the formal braiding operator in Eq. (B18), together with the changing of basis (associator), which satisfy the quasi-Yang Baxter equation. The fusion algebra of quasiparticles is determined by the comultiplication algebra Eq. (B32), together with the changing of basis (associator), which satisfy the pentagon equation. One can further show that the braiding algebra and the fusion algebra are compatible: They satisfy the hexagon equation.<sup>77</sup>

We have not studied the interplay between the global symmetry  $SG$  and the topological order  $\mathbf{D}^{\tilde{\omega}}(GG)$  here. For instance, we have not used  $D_{(h,g)}(A)$ ,  $D_{(h,g)}(B)$  operators when  $g \notin GG$  except for stating their basic properties in the twisted extended ribbon algebra Eqs. (B4)–(B7). However, in Sec. V, we carefully study the interplay between the global symmetries and the topological orders in some examples. We believe that those studies can be generalized to any phase in our classification.

#### APPENDIX C: PARTICLE STATISTICS DIRECTLY FROM CROSSING STRINGS

Here we provide an alternative, direct approach to braiding statistics, and compare it to that of Sec. IV D.

The braiding statistics of two quasiparticles is a topological property that therefore cannot depend on the details of the ribbon operator at its ends. When the system is a torus, the statistical phase of quasiparticles (meaningful for Abelian quasiparticles only) follows from the commutation of operators  $\mathcal{T}_a$  which describe the following process: creating a particle-antiparticle pair, tunneling the particle across the system in direction  $a = x, y$ , and finally annihilating the pair, as described by the formula<sup>78</sup>

$$\mathcal{T}_x \mathcal{T}_y = e^{-i2\theta} \mathcal{T}_y \mathcal{T}_x, \quad (\text{C1})$$

with  $\theta$  the (exchange) statistical angle of the quasiparticles; see Fig. 21(a). The ribbon operator  $\hat{F}^{(h,g)}(\Gamma)$  represents exactly the operation  $\mathcal{T}$  along its  $\Gamma$ . Since the string ends are not involved, we can actually also use  $\hat{w}_h^\Gamma(g)$  (see Fig. 13).

The angle in Eq. (C1) depends only on the commutation relation at the intersection point of the two strings, so even if the system is not a torus, we can consider a braiding operation performed locally<sup>28</sup> and realized by an open and closed string that intersect at a single point, Fig. 21(a).

Figure 21 shows the ingredients for calculating the phases  $W_{mn} = \langle f | \hat{w}_{h_m}^{\Gamma_m}(g_m) \hat{w}_{h_n}^{\Gamma_n}(g_n) | i \rangle$ , which reveal the statistical angle:

$$e^{-i2\theta} = \frac{W_{12}}{W_{21}}. \quad (\text{C2})$$

The phases  $W_{mn}$  differ due to the 3-simplices positioned on top of two lattice triangles which are shared by the two ribbon operators, as well as due to string phases  $\Theta_{\Gamma_m}^{h_m}$  on two edges, Fig. 21(b).

Using the definition of the 2-cocycle  $c_h$ , Eq. (63), we get for the phase factor ratio due to the 3-simplices

$$\frac{\Psi_{12}}{\Psi_{21}} = c_{h_1}(h_2, a_i) c_{h_2}(h_1, b_{i+1}^{-1}), \quad (\text{C3})$$

with  $i$  the lattice site of intersection.

Since the definition of statistical angle only makes sense for Abelian quasiparticles, we consider only trivial cocycles  $c_h$ . This means that we can rewrite the 2-cocycle using a 1-cochain, as in Eq. (67).

In that case, the phase ratio  $\Theta_{12}/\Theta_{21}$  is given by Eq. (74) and can easily be simplified, giving

$$\frac{\Theta_{12}}{\Theta_{21}} = \frac{\varepsilon_{h_1}(h_2 \cdot a_i)}{\varepsilon_{h_1}(a_i)} \frac{\varepsilon_{h_2}(b_{i+1})}{\varepsilon_{h_2}(h_1^{-1} \cdot b_{i+1})}; \quad (\text{C4})$$

see labels in Fig. 21(a).

Using the property  $\varepsilon_h(g_1^{-1})/\varepsilon_h(g_2^{-1}) = \varepsilon_h^{-1}(g_1)/\varepsilon_h^{-1}(g_2)$ , which holds for any 1-cochain describing a trivial canonical 2-cocycle, the total phase ratio  $\frac{W_{12}}{W_{21}} = \frac{\Psi_{12}\Theta_{12}}{\Psi_{21}\Theta_{21}}$  finally becomes

$$e^{-i2\theta} = \varepsilon_{h_1}(h_2) \varepsilon_{h_2}(h_1) \frac{\varepsilon_{h_1}(g_1) \varepsilon_{h_2}(g_2')}{\varepsilon_{h_1}(g_1') \varepsilon_{h_2}(g_2)}. \quad (\text{C5})$$

The group elements appearing here are  $g_1 = \prod_j a_j$ ,  $g_2 = \prod_k b_k$ , i.e. the values for isolated strings, and  $g_1' = h_2 \prod_j a_j$ ,

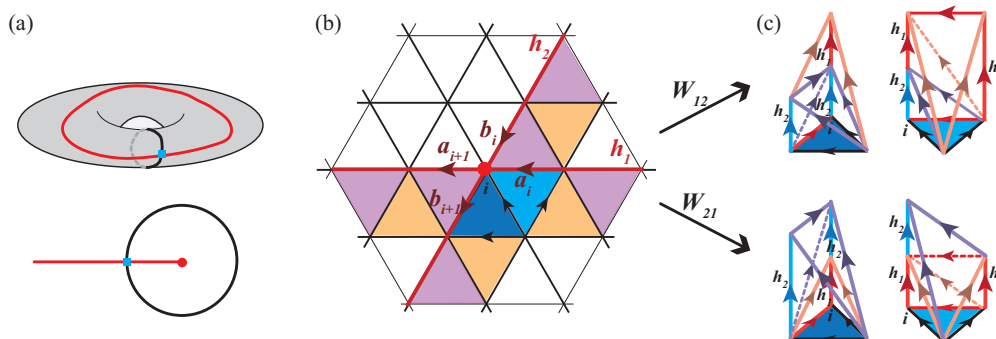


FIG. 21. (Color online) Quasiparticle statistics from ribbon commutation. (a) Commutation of two strings (ribbon operators, black and red) at the intersection point (blue square) gives the braiding statistics. (Top) Strings representing tunneling of particle-antiparticle pairs across the system (the surface of torus) can give the self-statistics. (Bottom) Braiding setup independent of system shape. (b) Near the intersection of two ribbon operators  $\hat{w}_{h_1}^{\Gamma_1}(g_1)$ ,  $\hat{w}_{h_2}^{\Gamma_2}(g_2)$ , the phase difference occurs due to 3-simplices on top of two blue shaded triangles, detailed in (c) with phases  $W_{mn} = \langle f | \hat{w}_{h_m}^{\Gamma_m}(g_m) \hat{w}_{h_n}^{\Gamma_n}(g_n) | i \rangle$  shown in top ( $W_{12}$ ) and bottom ( $W_{21}$ ) rows. Note that elements  $b_i$  are defined to be oriented oppositely to our lattice edge orientations, but consistent with definition of ribbon operator phase, Fig. 13, hence the appearance of  $b_{i+1}^{-1}$  in Eq. (C3).

$g'_2 = h_1 \prod_k b_k$ , i.e. the values after the other string is already applied.

After using the 1-cochain, Eq. (67), on Eq. (100), the result obtained by calculating the braiding matrix by using the algebra of local operators at the string ends almost exactly matches the one here (up to replacing  $g_1 \rightarrow h_2 \cdot g_1$  here). The difference involves a deeper subtle issue we address now. The obtained angle  $2\theta$  [either following from Eq. (100) or Eq. (C5)] should represent  $2\pi$  braiding of Abelian quasiparticles in systems with trivial cocycle  $c_h$ . However, for the statistical angle to be physical, one expects that it is invariant under changes of the 3-cocycle by a 3-coboundary, as introduced in Eq. (10), because this change does not alter the physical content of the theory. Such transformations of  $\omega$  by a coboundary lead to the following transformation of the 1-cochain  $\varepsilon$  by an arbitrary function  $u(x, y)$ :

$$\varepsilon_h(g) \rightarrow \varepsilon_h(g) \frac{u(h, g)}{u(g, h)}. \quad (\text{C6})$$

One can see that the factor  $\varepsilon_{h_1}(h_2) \varepsilon_{h_2}(h_1)$  in the result Eq. (C5) is invariant, but the rest of the expression is not. [The same is true for the result following from Eq. (100).]

The resolution of this puzzle is instructive. Namely, the ribbon operator  $F^{(h, g)}(\Gamma)$  we used here and in Sec. IV D, when acting on the ground state, does not necessarily create a quasiparticle pair state with well-defined flux  $h$  and gauge charge  $h_g$ . As explicitly shown in the examples of Sec. V, the gauge charge operator may act nontrivially within the quasiparticle Hilbert space. [This Hilbert space is created by the action of  $F^{(h, g)}(\Gamma)$  on the ground state, but has to be specified further by discriminating different values of  $SG$  elements  $u_C$  at the ends  $C = A, B$  of string  $\Gamma$ ; see Sec. V A.] This means that physical states, having well-defined gauge charge, can actually be nontrivial linear combinations of states spanned by  $F^{(h, g)}(\Gamma)$ .

Of course, the braiding matrix Eq. (100) contains all information necessary to specify braiding properties of quasiparticles; one only has to pose the right question, which would involve explicit use of physical flux and charge states constructed using the formalism in Sec. V.

In the present discussion of Abelian quasiparticles, it becomes obvious that the physical quasiparticle states with fixed flux and charge are simply obtained by absorbing the noninvariant factors in Eq. (C5). This is achieved easily by using  $\bar{F}^{(h, g)}(\Gamma) \equiv F^{(h, g)}(\Gamma) \varepsilon_h(g)$ , which leads to the statistical angle independent on the cocycle within a fixed cocycle equivalence class:

$$e^{-i2\theta} = \varepsilon_{h_1}(h_2) \varepsilon_{h_2}(h_1). \quad (\text{C7})$$

[The same is obtained starting from expression given by Eq. (100).]

Let us now use Eq. (C7) on two Abelian topological theories with  $Z_2$  order, namely the toric code (TC) and double semion (DS) models (see Appendix D). These two orders are physically distinguished exactly by the statistics of their quasiparticles.

As demonstrated explicitly in Appendix D, the TC is recovered by choosing the trivial cocycle  $\omega(g_1, g_2, g_3) = 1, \forall g_1, g_2, g_3 \in G$ . From these constraints we need to obtain the values of the 1-cochain  $\varepsilon_h(g)$ . The constraint  $\omega(g_1, g_2, g_3) = 1$  leads to

$$c_h(g_1, g_2) = 1 \text{ (TC)}, \quad (\text{C8})$$

which implies that

$$\varepsilon_h(g_1) \varepsilon_h(g_2) = \varepsilon_h(g_1 \cdot g_2) \text{ (TC)}; \quad (\text{C9})$$

i.e. the 1-cochain  $\varepsilon$  actually becomes a 1-cocycle. There are two representations of the  $Z_2$  group, i.e., in total four solutions for  $\varepsilon$  given by  $\varepsilon_0(g) = 1$  or  $\varepsilon_0(g) = (-1)^g$ , and  $\varepsilon_1(g) = 1$  or  $\varepsilon_1(g) = (-1)^g$ .

In the present formalism, a particular ribbon is determined by its flux  $h_v$  and one of the particular solutions for the 1-cochain  $\varepsilon$ .

The TC has four quasiparticles,  $\{\mathbb{1}, e, m, em\}$ , the trivial, charge, flux, and charge-flux bound state, respectively. Assigning  $h_v = 0$  to  $\mathbb{1}, e$ , and  $h_v = 1$  to  $m, em$ , we make a choice (not unique) of assigning each of the four solutions to one particular quasiparticle: (1) to  $\mathbb{1}$ :  $\varepsilon_h(g) = 1$ ; (2) to  $e$ :  $\varepsilon_h(g) = (-1)^g$ ; (3) to  $m$ :  $\varepsilon_1(g) = (-1)^g$ ; and (4) to  $em$ :  $\varepsilon_0(g) = (-1)^g$ .

This solution recovers the well-known TC result that  $\mathbb{1}, e, m$  are bosons and  $em$  a fermion, and nontrivial mutual statistics is given by  $2\theta = \pi$  among the  $\{e, m, em\}$ .

According to the explicit demonstration in Appendix D, the DS theory is obtained by choosing the second representative 3-cocycle for  $G = Z_2$  given by  $\omega(g_1, g_2, g_3) = -1$  for  $g_1 = g_2 = g_3 = 1$ , and 1 otherwise. Repeating the analysis from the TC case above, the difference lies in the constraint

$$c_1(1,1) = -1 \text{ (DS)}, \quad (\text{C10})$$

which leads to solutions given by  $\varepsilon_0(g) = 1$  or  $\varepsilon_0(g) = (-1)^g$ , and  $\varepsilon_1(1) = i$  or  $\varepsilon_1(1) = -i$ , while  $\varepsilon_1(0) = 1$  always.

The nontrivial excitations in the Abelian topological phase described by DS theory are two semions  $s_1, s_2$ , and their bound state  $s_{12}$ . Assigning  $h_v = 0$  to  $\mathbb{1}, s_{12}$ , and  $h_v = 1$  to  $s_1, s_2$ , we make a choice (not unique) of assigning each of the four solutions to one particular quasiparticle: (1) to  $\mathbb{1}$ :  $\varepsilon_1(1) = i$ ; (2) to  $s_{12}$ :  $\varepsilon_0(g) = (-1)^g, \varepsilon_1(1) = -i$ ; (3) to  $s_1$ :  $\varepsilon_0(g) = (-1)^g, \varepsilon_1(1) = i$ ; and (4) to  $s_2$ :  $\varepsilon_1(1) = -i$ .

This solution indeed recovers the well-known quasiparticle properties:  $\mathbb{1}, s_{12}$  are bosons;  $s_1, s_2$  are semions ( $2\theta = \pi$ ); and the nontrivial mutual statistics is  $2\theta = \pi$  between  $s_{12}$  and either  $s_1$  or  $s_2$ .

#### APPENDIX D: EXPLICIT FORM OF MODELS FOR $Z_2$ TOPOLOGICALLY ORDERED PHASES

Here we consider the well-understood case of  $Z_2$  topological order, to demonstrate that our general model explicitly yields models for the two inequivalent phases having such order. Two well-known models for the two distinct  $Z_2$  topological phases are Kitaev's toric code, TC,<sup>65</sup> and the double semion, DS, theory.<sup>69</sup> We make a direct comparison to the TC and DS model variants presented in Ref. 28.

For that purpose, we set the symmetry group to be trivial,  $SG = Z_1$ , and the gauge group to  $GG = Z_2$ . There are only two group elements, which we can label by  $G = \{\mathbb{1} \equiv +1, a \equiv -1\}$ , with  $a = a^{-1}$ . The group element  $g_{ij} = \pm 1$  assigned to the  $ij$  edge (of the triangular lattice) we call "spin" ( $\pm 1 = \text{"up/down"}$ ) positioned at the midpoint of the edge  $ij$ . We now switch to the dual lattice, which is honeycomb, as shown in Fig. 22. The spins are still on the edges of the honeycomb lattice, and the honeycomb plaquette  $ph$  contains the same six spins as our original plaquette  $p$ .

Let us start with the operator  $Q_t$ , which is the same in both topologically ordered theories. This operator forces the product of three spins adjacent to a honeycomb lattice site to  $+1$ ; see Fig. 22. It therefore acts as the projector,

$$Q_v = \frac{1}{2} \left( 1 + \prod_{i \in v} \sigma_z^{(i)} \right), \quad (\text{D1})$$

on three spins  $i$  neighboring the vertex  $v$ . Comparing directly to the variant of TC and DS models presented in Ref. 28, the first term in  $H$ , Eq. (57), becomes up to an overall constant just the standard vertex contribution  $\sum_v \prod_{i \in v} \sigma_z^{(i)}$  to  $H^{TC}$  or  $H^{DS}$  in Ref. 28. Further, the product  $\prod_{t \in p} Q_t$  appearing in the plaquette terms of  $H$  exactly becomes the  $\prod_{v \in ph} Q_v$  term in  $H^{TC}$  or  $H^{DS}$  which projects the flux in the honeycomb plaquette  $ph$  to zero (this is the  $P_p$  factor in Ref. 28).

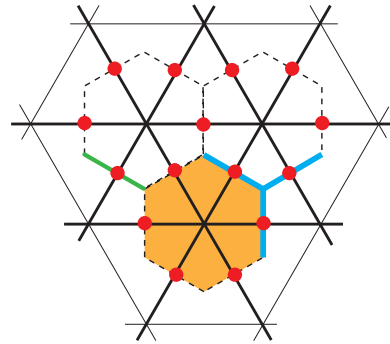


FIG. 22. (Color online) Recovering the two  $Z_2$  topological phases from the exactly solvable models: toric code (TC) and double semion theory (DS). The dual lattice is honeycomb (dashed). Red dots mark the positions of group elements  $g_{ij}$  assigned to edges  $ij$ , becoming "spin- $\frac{1}{2}$ " states in TC and DS. A honeycomb lattice plaquette  $ph$  is shaded. The plaquette operator  $\hat{B}_p$  (Fig. 9) acts on the six "spins" of  $ph$ . The DS model differs from TC by having an additional phase in its plaquette operator. This phase depends on spins on the six outer legs of  $ph$ , one of which is marked by a green line. These six "outer" spins belong to the six tetrahedrons in our  $\hat{B}_p$ ; see Fig. 9. The  $Q_t$  operator in both models just acts on the three spins nearest to a site (spins on blue lines).

At this point, we can discuss the physical interpretation of  $Q_v$  and the outcome of this subsection more precisely. In our model,  $Q_v = 1, \forall v$  gives the zero-flux rule on the lattice. One should recall that if we had been considering the *dual* of the globally symmetric  $SG = Z_2, GG = Z_1$ , the zero-flux rule would have been automatically satisfied [see Eq. (46)]. This fact is equivalent to saying that in the undualized theory the domain walls separating regions of up and down spins have to form closed loops, i.e., "closed strings" in the language of string-net models.<sup>69</sup> No matter if we start from the dualized  $SG = Z_2$  model or the  $GG = Z_2$  model, the restriction to states satisfying  $Q_v = 1$  (which is automatic or chosen, respectively) leads to  $Z_2$  gauge theory models, and this is clearly shown below. In fact, Ref. 28 clarifies that there are still two physically distinguishable  $Z_2$  gauge theories, which represent two different topological orders; both of these were obtained there by dualizing  $Z_2$  spin models, automatically enforcing the closed-string rule. We explicitly show that our  $G = GG = Z_2$  model indeed reduces to the two inequivalent  $Z_2$  gauge theories when  $Q_v = 1$ .

One can now ask: How do the Kitaev's TC<sup>65</sup> and the DS theory<sup>69</sup> fit in this? Simply, the two different  $Z_2$  topological orders are also described by these two different models. (TC and DS can be seen as Ising matter coupled to the two different  $Z_2$  gauge fields.<sup>28</sup>) The TC and DS models are expected to arise when the restriction to  $Q_v = 1$  is lifted; i.e., they are open-string models. We explicitly show below that our  $G = GG = Z_2$  model indeed gives rise to TC in the absence of that restriction.

Let us move on to the plaquette operator and the Hamiltonian of our model. Under  $\hat{B}_{p \equiv i}^a$ , the six group elements  $g$  on edges (of triangular lattice) which share the lattice site  $i$  are multiplied by  $a$ . Therefore, the six spins on the honeycomb  $ph$  plaquette are "flipped,"  $g = \pm 1 \rightarrow \mp 1$ , i.e., acted on by

Pauli matrix  $\sigma_x$ . Obviously,  $\hat{B}_{p=i}^{\mathbb{1}}$  does not change the state (no flipped spins).

Next we consider the phase factor of  $\hat{B}$ . There are exactly two inequivalent classes of 3-cocycles  $\omega$  for the group  $G = Z_2$ , as dictated by  $H^3(Z_2, U(1)) = Z_2$ . They are represented by the two distinct choices:<sup>60</sup>

$$\omega(-1, -1, -1) = \pm 1. \quad (\text{D2})$$

In both cases,  $\omega(g_1, g_2, g_3) = 1$  for any  $g_1, g_2, g_3 \in G$  when they are not all equal to  $-1$ .

To obtain a model for TC phase, we choose a trivial cocycle, i.e.,  $\omega(g_1, g_2, g_3) = 1$ ,  $\forall g_1, g_2, g_3 \in G$ . The amplitude from Eq. (52) then becomes trivial,  $B_p^{TC} = 1$ . The action of the plaquette operator is

$$\hat{B}_p^{TC} = \frac{1}{2} \left( 1 + \prod_{l \in ph} \sigma_x^{(l)} \right), \quad (\text{D3})$$

with six spins  $l$  in the honeycomb plaquette  $ph$ . This is equivalent to the standard plaquette operator of TC model in Ref. 28, although in the present case there is a constant term added to the  $\sigma_x$  term. This constant shift can be removed by smoothly deforming the  $\hat{B}_p^{TC}$  operator without ever closing the gap in the Hamiltonian. (The constant shift is there to make our  $\hat{B}_p^{TC}$  a projector, which is its general property.) Our model with  $\omega = 1$  is consequently equivalent to the TC model. Under the  $Q_v = 1$  constraint, obviously we obtain the standard  $Z_2$  gauge theory on the honeycomb lattice.

We now turn to the DS model.<sup>69</sup> Compared to the TC model, the only difference is that the honeycomb plaquette operator now has an additional phase factor determined by the value of six spins on ‘‘outer legs’’ of the plaquette;<sup>28</sup> one of six such legs of the plaquette  $ph$  is marked by green line in Fig. 22. This phase in the DS model is assigned by the following rule. If exactly two, or exactly six, of the outer leg spins are in state  $-1$ , there is a phase factor  $-1$  in the plaquette operator. If we again restrict to a closed-string theory, i.e.,  $Q_v = 1$ , the lines of  $-1$  spins on the honeycomb lattice physically represent the closed domain walls of the dual  $Z_2$  spin theory, and therefore there is always an even number of  $-1$  legs entering a plaquette  $ph$ . As mentioned, this closed-string restriction of DS model is the second type of  $Z_2$  lattice gauge theory.

Let us show that under  $Q_v = 1$  our model indeed reduces to the  $Q_v = 1$  restricted DS model from Ref. 28. The six outer leg spins of the honeycomb lattice are actually lying on the six outer edges of the plaquette  $p$  in our model on the triangular lattice (compare Figs. 22 and 9). Although our  $\hat{B}_p$  does not change them, they are on the edges of the six tetrahedrons which determine the phase of the operator.

Given the restriction  $Q_v = 1$ , i.e., the zero-flux rule on the triangular lattice, and using  $\omega(-1, -1, -1) = -1$ , it is straightforward to show that the phase coming from six tetrahedrons [see  $B_p^{s=1}$  in Eq. (51)] is equal to  $-1$  only in two cases: (1) when the only outer leg spins in state  $-1$  are on two legs separated by  $120^\circ$ ; (2) when beside the two legs as in case (1), there are two more legs with spin  $-1$  separated by  $60^\circ$ .

These rules seem strange; however, this is remedied by a simple change of basis. As explained, for an arbitrary basis

state there is an even number of  $-1$  outer legs, i.e., segments of dual domain walls, entering the honeycomb plaquette  $ph$ . These segments of domain walls have to be connected (they do not have ends) in some way along the six edges of the hexagonal plaquette  $ph$ . Given the configuration of  $-1$  legs entering the  $ph$ , no matter how we choose to connect them, the number of  $ph$  edges we use for that will have fixed parity. It is therefore well defined to use this number,  $\# \text{int.legs}(ph)$ , for any basis state. After redefining the basis by  $|\text{state of plaquette } p\rangle \rightarrow (-1)^{\# \text{int.legs}(ph)} |\text{state of plaquette } p\rangle$ , our ‘‘strange’’ phase factors become exactly the DS model’s phase factors described above. Therefore, within the zero-flux manifold of states, our model with  $G = Z_2$  and  $\omega(-1, -1, -1) = -1$  explicitly reduces to the closed-string version of the DS model, which was firstly understood in that form in Ref. 28.

#### APPENDIX E: ALL TWO-PARTICLE STATES ARE GIVEN BY ACTION OF RIBBON OPERATOR, AND LOCAL OPERATORS ACT PROJECTIVELY ON THESE STATES

Let us first show that the local operators form a projective representation of the group  $G$  in the Hilbert space  $\mathcal{L}(A, B)$  of two excitations at the ends  $A, B$  of the ribbon  $\Gamma$ . Let us for concreteness focus on the projected subspace  $\mathcal{L}_{u_A}(A, B)$  defined in Eq. (84), and the exact same results follow for  $\mathcal{L}_{u_B}(A, B)$ . For brevity, let us also use the double index notation, i.e.,  $i \equiv (h_i, g_i), j \equiv (h_j, g_j), \dots$ , with  $h_i, h_j, \dots \in GG$  and  $g_i, g_j, \dots \in G$ . Directly combining the definition of excited states Eq. (84) and the operator algebra from Eqs. (81), we get

$$D_j(A) |\psi_{u_A}^k\rangle = \delta_{h_j, h_k^{-1}} c_{g_j}^{-1}(h_k, h_k^{-1}) c_{h_k}^{-1}(g_j, g_k) |\psi_{\tilde{g}_j u_A}^{(h_k, g_k g_j)}\rangle, \quad (\text{E1})$$

$$D_j(B) |\psi_{u_A}^k\rangle = \delta_{h_j, h_k} c_{h_k}(g_j^{-1} g_k, g_j) |\psi_{u_A}^{(h_k, g_j^{-1} g_k)}\rangle, \quad (\text{E2})$$

where we used the usual factorization  $g_j = h'_j \cdot \tilde{g}_j$  with  $\tilde{g}_j \in SG$ ,  $h'_j \in GG$ . Applying the operators twice and using the 2-cocycle identities Eqs. (87b) and (87a), we get

$$D_i(A) D_j(A) |\psi_{u_A}^k\rangle = c_{h_k}^{-1}(g_i, g_j) D_{ij}(A) |\psi_{u_A}^k\rangle, \quad (\text{E3a})$$

$$D_i(B) D_j(B) |\psi_{u_A}^k\rangle = c_{h_k}(g_i, g_j) D_{ij}(B) |\psi_{u_A}^k\rangle, \quad (\text{E3b})$$

where we used the obvious shorthand notation  $ij \equiv (h_i h_j, g_i g_j)$ . The 2-cocycle  $c_h$ , with  $h \in GG$ , therefore determines the projective representation of  $G$ .

The projective representation of local operators is actually unitary, as we next show. In the basis  $|\psi_{u_A}^k\rangle$  labeled by  $k$  ( $u_A$  is fixed), the matrix elements of operator  $D_{(h, g)}(A)$  from Eq. (E1) are

$$M(h, g)_{k', k} = c_g^{-1}(h^{-1}, h) c_{h^{-1}}^{-1}(g, g_k) \delta_{g_k', g_k} \delta_{h, h_k^{-1}} \delta_{h_k, h_k'}. \quad (\text{E4})$$

Using the multiplication law, Eq. (E3a), it further follows that  $M(h, g) M(h^{-1}, g^{-1}) = c_h(g, g^{-1}) M(\mathbb{1}, \mathbb{1})$ , where the identity operator  $M(\mathbb{1}, \mathbb{1})$  in the basis  $|\psi_{u_A}^k\rangle$  is represented by the unit matrix. This determines the inverse of the matrix  $M(h, g)$ .

On the other hand, in the orthonormal basis the matrix of adjoint operator is given by the conjugated transpose  $M_{k', k}^\dagger = M(h, g)_{k, k'}^*$ .

The matrices  $M^\dagger$  and  $M^{-1}$  differ only by a phase factor containing five 2-cocycle factors. Using the cocycle rules Eqs. (87b), (87a), and (87c) it is easy to show that the phase factor is equal to one, and the representation  $M$  is unitary. The same can be shown for the representation of  $D(B)$ .

We note that the projective representation of  $G$  formed by local operators  $D(A)$  or  $D(B)$ , as discussed here, is *not* the algebra defining the quasi-quantum double. The operator algebra within the quasi-quantum double is formed by the ‘‘topological operators’’ and depends on cocycle of elements in  $GG$  only. This is discussed in detail in Appendix B.

Let us next consider the problem of determining the two-quasiparticle Hilbert space  $\tilde{\mathcal{L}}(A, B)$ , where we fix the two excitations at positions  $A$  and  $B$ . We prove that the Hilbert space  $\mathcal{L}(A, B) = \oplus_{u_C} \mathcal{L}_{u_C}(A, B)$  ( $C$  is either  $A$  or  $B$ ), as introduced after Eq. (84), indeed contains all the states of the two excitations; i.e., it contains  $\tilde{\mathcal{L}}(A, B)$ . Our proof follows the one given in Ref. 65 for the model generalizing the  $Z_2$  toric code to arbitrary finite groups (the ‘‘generalized toric code’’); however, our proof has significant changes, rooted in the fact that our model differs significantly from the generalized toric code. (For the present proof, the presence of global symmetries in our model makes the most important difference.)

We note that since clearly the two-quasiparticle Hilbert space  $\tilde{\mathcal{L}}(A, B)$  is a subspace of  $\mathcal{K}(\Gamma)$ , the action of  $F(\Gamma)$  and  $D$  operators appearing below is always well defined.

To establish our result, we need to define additional useful tensors related to the ones in Sec. IV C. We recall the double index notation using Latin indices:  $i \equiv (h_i, g_i), j \equiv (h_j, g_j), \dots$ , with  $h_i, h_j, \dots \in GG$  and  $g_i, g_j, \dots \in G$ , while the Kronecker  $\delta$  function  $\delta^i_j \equiv \delta_{h_i, h_j} \delta_{g_i, g_j}$ . The antipode tensor  $S$  is defined such that the element  $S^k_l F^l \otimes D_k$  is the inverse of the element  $F^i \otimes D_i$  in the algebra  $\mathbb{F} \otimes \mathbb{D}$ . This definition results in the following identity and solution for  $S$ :

$$S^k_l \Lambda_p^{lm} \Omega_{kn}^q \delta_m^n = \epsilon_p e^q, \quad (\text{E5})$$

$$S_{(h_2, g_2)}^{(h_1, g_1)} = \delta_{h_1, h_2^{-1}} \delta_{g_1, g_2^{-1}} c_{g_2}^{-1}(h_2, h_1) c_{h_1}^{-1}(g_1, g_2). \quad (\text{E6})$$

One can check that the defining identity Eq. (E5) holds for the given form of  $S$  by using the 2-cocycle identities Eqs. (87b) and (87d).

Recall from Sec. IV C the functions  $\epsilon_i \equiv \delta_{h_i, \mathbb{1}}$  and  $e^i \equiv \delta_{g_i, \mathbb{1}}$ , which define the unit and counit of the algebras  $\mathbb{F}, \mathbb{D}$ . Using these functions we now define  $\tau_s \equiv N_G^{-1} e^s$  and

$$\hat{C}(A) \equiv \frac{1}{N_{GG}} \epsilon_i D_i(A), \quad (\text{E7})$$

where  $N_{GG} = |GG|$  is the order of the gauge group and  $N_G = |G|$  is the order of the group  $G$ . It is important to notice that by its definition, the  $\epsilon_i$  constrains only the gauge group element  $h_i \equiv \mathbb{1}$  of the double index  $i = (h_i, g_i)$ . This means that the operator  $\hat{C}(A)$  in Eq. (E7) projects out any nonzero flux in triangle  $t_A$ ; i.e., it ensures there are no *flux* excitations at that lattice plaquette. However, the action of operator  $D(A)$  in  $\hat{C}(A)$  is still nontrivial, e.g., since the element  $g_i \in G$ , in principle, modifies the lattice site element  $u_{i_A}$ .

We now arrive at the central identity,

$$\begin{aligned} \tau_s \Omega_{mp}^s S_q^p F^m(\Gamma) \hat{C}(A) F^q(\Gamma) & \quad (\text{E8}) \\ &= \frac{1}{N_{GG} N_G} \delta_{h_r, \mathbb{1}} \delta_{g_j, \mathbb{1}} D_j(A) F^r(\Gamma) \\ &= \frac{1}{N_{GG} N_G} \mathbb{1}_{\mathbb{D}_A \otimes \mathbb{F} \otimes \mathbb{D}_B}, \quad (\text{E9}) \end{aligned}$$

where we again used the double summation convention, i.e.,  $\sum_p = \sum_{h_p \in GG, g_p \in G}$ , etc. The first equality can be proved by using the explicit definitions of all tensors, the operator algebra, and the 2-cocycle properties. The last line of Eq. (E8) is slightly more subtle. Consider an arbitrary matrix element of the operator in Eq. (E9). The  $\delta$  functions ensure that the ribbon and local operators do not change any edge or site elements between the initial and final state. Further, their phase factors containing cocycles are also trivial due to our choice of standard cocycle; see Eq. (87c). Consider then the matrix element contribution from the ribbon operator:  $\delta(u_{i_A} u_{i_B}^{-1}, \tilde{g}_r)$ , with the obvious factorization  $r \equiv (h_r, g_r) = (h_r, h'_r \cdot \tilde{g}_r)$ ,  $h_r, h'_r \in GG$ ,  $\tilde{g}_r \in SG$ . However, there is a summation over  $r$ , and therefore over  $\tilde{g}_r \in SG$ , so the  $\delta$  function is harmless. The same is true for the  $\delta$  function coming from the local operator. We therefore see that the quantum amplitude is 1, and indeed the action equals the identity operator  $\mathbb{1}$  in the algebra  $\mathbb{D}_A \otimes \mathbb{F} \otimes \mathbb{D}_B$ .

Let us now consider an arbitrary state  $|\psi\rangle$  in the Hilbert space  $\tilde{\mathcal{L}}(A, B)$ . We can define

$$\begin{aligned} |\eta^q\rangle & \equiv \hat{C}(A) F^q(\Gamma) |\psi\rangle, \\ G_q & \equiv N_{GG} N_G \tau_s \Omega_{mp}^s S_q^p F^m(\Gamma), \end{aligned} \quad (\text{E10})$$

so that

$$|\psi\rangle = G_q |\eta^q\rangle \quad (\text{E11})$$

holds due to the identity Eq. (E8). The states  $|\eta^q\rangle$  actually have *no flux* excitations at  $A$  due to the action of  $\hat{C}(A)$ . Elementary gauge and charge excitations must be in pairs and by construction are symmetric, so  $|\eta^q\rangle$  can only describe the ground state  $|gs\rangle$  or a one-particle state that breaks the global symmetry. Since the site elements  $u_{i_A}, u_{i_B}$  are the local ( $A, B$ ) degrees of freedom acted on by the global symmetry, we conclude that the  $|\eta^q\rangle$  states can be written as linear combinations of the form

$$|\eta^q\rangle = \sum_{u_1, u_2 \in SG} k_{u_1, u_2}^q \hat{P}_{u_1}(A) \hat{P}_{u_2}(B) |gs\rangle, \quad (\text{E12})$$

with some coefficients  $k_{u_1, u_2}^q$ . (These states include the ground state itself.)

Equations (E11) and (E10) show that an arbitrary two-particle state is a combination of the form

$$|\psi\rangle = \sum_{\substack{u_1, u_2 \in SG \\ m}} K_{m, u_1, u_2} F^m(\Gamma) \hat{P}_{u_1}(A) \hat{P}_{u_2}(B) |gs\rangle. \quad (\text{E13})$$

By the definition of the ribbon and projector operators, the  $|\psi\rangle$  is the zero vector unless  $u_1 \cdot u_2^{-1} = \tilde{g}_m$ , where  $m \equiv (h_m, g_m) = (h_m, h'_m \cdot \tilde{g}_m)$ ,  $h_m, h'_m \in GG$ ,  $\tilde{g}_m \in SG$ . One of the three sums over  $SG$  in Eq. (E13) is therefore superfluous for physical states in  $\tilde{\mathcal{L}}(A, B)$ .

We can use  $u_1 \cdot u_2^{-1} = \tilde{g}_m$  to eliminate either of the  $u_{1,2}$  in Eq. (E13), which immediately shows that the arbitrary state  $|\psi\rangle \in \tilde{\mathcal{L}}(A,B)$  is indeed a linear combination of projected ribbon states from Eq. (84).

#### APPENDIX F: SYMMETRY FRACTIONALIZATION FOR MULTIPLE QUASIPARTICLES

In the examples of Sec. VB, we describe the scheme to find the fractionalized symmetry transformations  $U_\sigma(C)$  ( $C = A, B$ ) for a quasiparticle at location  $C$  in the single-ribbon states; see Eq. (108), where we assumed Eq. (110). In this section, we show that at least when the nontrivial symmetry fractionalization only occurs in a  $Z_2$  gauge sector (namely for visons in a gauge sector  $Z_2 \in GG$ ), the definition of local operators  $U_\sigma(C)$  in Eq. (108) implements the fractionalized symmetry transformations for multiparticle states created by ribbon operators defined for ribbons  $\Gamma_1, \Gamma_2, \dots, \Gamma_N$  that all

share the same end  $B$ :

$$U_\sigma(A_1)U_\sigma(A_2) \cdots U_\sigma(A_N)U_\sigma(B)|\psi_{u_B}^{k_1, k_2, \dots, k_N}\rangle = U(\sigma)|\psi_{u_B}^{k_1, k_2, \dots, k_N}\rangle, \quad \forall \sigma \in SG. \quad (F1)$$

In our simple examples in the main text, it is always true that when nontrivial symmetry fractionalization occurs, it always only occurs in one  $Z_2$  gauge sector. In addition, we believe that all states  $\{|\psi_{u_B}^{k_1, k_2, \dots, k_N}\rangle\}$ ,  $\forall u_B, k_1, k_2, \dots, k_N$  span a Hilbert space  $\mathcal{L}(A_1, A_2, \dots, A_N, B)$  that contains all possible excitations at those locations. Therefore, Eq. (F1), which we prove below, indicates that the  $U_\sigma(C)$  operators are the general fractionalized symmetry transformations in our examples.

It is straightforward to show that (both  $GG$  and  $SG$  are Abelian)

$$U(\sigma)|\psi_{u_B}^{k_1, k_2, \dots, k_N}\rangle = |\psi_{\sigma^{-1}u_B}^{k_1, k_2, \dots, k_N}\rangle, \quad (F2)$$

while

$$\begin{aligned} & D_{(h_1^{-1}, \sigma^{-1})}(A_1)D_{(h_2^{-1}, \sigma^{-1})}(A_2) \cdots D_{(h_N^{-1}, \sigma^{-1})}(A_N)D_{(h_1, h_2, \dots, h_N, \sigma^{-1})}(B)|\psi_{u_B}^{k_1, k_2, \dots, k_N}\rangle \\ &= \epsilon_{h_1, \sigma^{-1}, u_{A_1} u_B^{-1}} \epsilon_{h_2, \sigma^{-1}, u_{A_2} u_B^{-1}} \cdots \epsilon_{h_N, \sigma^{-1}, u_{A_N} u_B^{-1}} \cdot \xi(g, h_1, h_2, \dots, h_N) \cdot |\psi_{\sigma^{-1}u_B}^{k_1, k_2, \dots, k_N}\rangle \\ &= \epsilon_{h_1, \sigma^{-1}, u_{A_1}} \epsilon_{h_2, \sigma^{-1}, u_{A_2}} \cdots \epsilon_{h_N, \sigma^{-1}, u_{A_N}} \epsilon_{h_1, h_2, \dots, h_N, \sigma^{-1}, u_B^{-1}} \cdot \xi(g, h_1, h_2, \dots, h_N) \cdot |\psi_{\sigma^{-1}u_B}^{k_1, k_2, \dots, k_N}\rangle \\ &= \epsilon_{h_1^{-1}, \sigma^{-1}, u_{A_1}}^{-1} \epsilon_{h_2^{-1}, \sigma^{-1}, u_{A_2}}^{-1} \cdots \epsilon_{h_N^{-1}, \sigma^{-1}, u_{A_N}}^{-1} \epsilon_{h_1, h_2, \dots, h_N, \sigma^{-1}, u_B}^{-1} \cdot \xi(g, h_1, h_2, \dots, h_N) \cdot |\psi_{\sigma^{-1}u_B}^{k_1, k_2, \dots, k_N}\rangle, \end{aligned} \quad (F3)$$

where we used the assumption:  $\epsilon_{h, \sigma^{-1}, h'} = 1$ ,  $\forall h, h' \in GG$  and  $\sigma \in SG$ , and the basic properties of the tensor  $\epsilon_{x,y,z}$ . The extra phase  $\xi(g, h_1, h_2, \dots, h_N)$  is defined as

$$\begin{aligned} & \xi(g, h_1, h_2, \dots, h_N) \\ &= c_{\sigma^{-1}}^{-1}(h_1^{-1}, h_1) c_{\sigma^{-1}}^{-1}(h_2^{-1}, h_2) \cdots c_{\sigma^{-1}}^{-1}(h_N^{-1}, h_N) \cdot c_{\sigma^{-1}}(h_1, h_2, h_3, \dots, h_N) c_{\sigma^{-1}}(h_2, h_3, \dots, h_N) \cdots c_{\sigma^{-1}}(h_{N-1}, h_N) \end{aligned} \quad (F4)$$

In our examples, nontrivial symmetry fractionalization occurs for a single  $Z_2$  subgroup  $Z_2^{\text{SF}} \in GG$  and  $GG = Z_2^{\text{SF}} \times GG'$ . Let us denote a group element  $h \in GG$  as  $h = (h_{\text{SF}}, h')$ , with  $h_{\text{SF}} \in Z_2^{\text{SF}}$  and  $h' \in GG'$ . This indicates that  $c_{\sigma^{-1}}(h_a, h_b) \neq 1$  can occur only when both  $h_{a, \text{SF}}$  and  $h_{b, \text{SF}}$  have nontrivial components in  $Z_2^{\text{SF}}$ , i.e.,  $h_{a, \text{SF}} = h_{b, \text{SF}} = 1$ , and generally  $c_{\sigma^{-1}}(h_a, h_b) = c_{\sigma^{-1}}(h_{a, \text{SF}}, h_{b, \text{SF}})$ . Let us denote  $c_{\sigma^{-1}}(h_a, h_b) = 1, h_{b, \text{SF}} = 1) = \eta$  (we use the  $\{0, 1\}$  notation for  $Z_2^{\text{SF}}$ ). Under

these conditions, it is easy to show that  $\xi(g, h_1, h_2, \dots, h_N) = \eta^{-N_{\text{SF}}/2}$ , where  $N_{\text{SF}}$  is the total number of visons (at the end  $A_i$  and end  $B$ ) in the  $Z_2^{\text{SF}}$  sector for the state  $|\psi_{u_B}^{k_1, k_2, \dots, k_N}\rangle$ . Therefore, using  $U_\sigma(C)$  defined in Eq. (108) for an excitation with a gauge flux  $h$ ,

$$U_\sigma(C) = \sqrt{c_{\sigma^{-1}}(h, h^{-1})} \cdot \epsilon_{h, \sigma^{-1}, u_C} \cdot D_{(h, \sigma^{-1})}(C), \quad (F5)$$

it follows that Eq. (F1) is indeed satisfied.

<sup>1</sup>V. L. Ginzburg and L. D. Landau, Zh. Eksp. Teor. Fiz. **20**, 1064 (1950).

<sup>2</sup>X.-G. Wen and Q. Niu, Phys. Rev. B **41**, 9377 (1990).

<sup>3</sup>X.-G. Wen, Int. J. Mod. Phys. B **5**, 1641 (1991).

<sup>4</sup>The phrase ‘‘topological order’’ has been widely used in literature, sometimes with different meanings. In this paper, we particularly reserve the phrase ‘‘topological order’’ for those quantum phases that feature nontrivial topological ground state degeneracies, and in  $2 + 1$  dimensions have quasiparticles with anyonic statistics.

<sup>5</sup>A. M. Turner, Y. Zhang, R. S. K. Mong, and A. Vishwanath, Phys. Rev. B **85**, 165120 (2012).

<sup>6</sup>R. S. K. Mong, A. M. Essin, and J. E. Moore, Phys. Rev. B **81**, 245209 (2010).

<sup>7</sup>L. Fu, Phys. Rev. Lett. **106**, 106802 (2011).

<sup>8</sup>T. L. Hughes, E. Prodan, and B. A. Bernevig, Phys. Rev. B **83**, 245132 (2011).

<sup>9</sup>Z.-X. Liu and X.-G. Wen, Phys. Rev. Lett. **110**, 067205 (2013).

<sup>10</sup>Z.-X. Liu, Z.-B. Yang, Y.-J. Han, W. Yi, and X.-G. Wen, Phys. Rev. B **86**, 195122 (2012).

<sup>11</sup>Z.-C. Gu and X.-G. Wen, arXiv:1201.2648.

<sup>12</sup>X.-G. Wen, Phys. Rev. B **85**, 085103 (2012).

<sup>13</sup>R.-J. Slager, A. Mesaros, V. Juricic, and J. Zaanen, Nat. Phys. **9**, 98 (2013).

<sup>14</sup>M. Z. Hasan and C. L. Kane, Rev. Mod. Phys. **82**, 3045 (2010).

<sup>15</sup>X.-L. Qi and S.-C. Zhang, Rev. Mod. Phys. **83**, 1057 (2011).

- <sup>16</sup>M. Z. Hasan and J. E. Moore, *Annu. Rev. Condens. Matter Phys.* **2**, 55 (2011).
- <sup>17</sup>A. P. Schnyder, S. Ryu, A. Furusaki, and A. W. W. Ludwig, *Phys. Rev. B* **78**, 195125 (2008).
- <sup>18</sup>A. Kitaev, in *American Institute of Physics Conference Series*, edited by V. Lebedev and M. Feigel'Man (American Institute of Physics, Melville, NY, 2009), Vol. 1134, pp. 22–30.
- <sup>19</sup>Y.-M. Lu and A. Vishwanath, *Phys. Rev. B* **86**, 125119 (2012).
- <sup>20</sup>X. Chen, Z.-C. Gu, Z.-X. Liu, and X.-G. Wen, *Phys. Rev. B* **87**, 155114 (2013).
- <sup>21</sup>F. D. M. Haldane, *Phys. Lett. A* **93**, 464 (1983).
- <sup>22</sup>A. Y. Kitaev, *Phys. Usp.* **44**, 131 (2001).
- <sup>23</sup>L. Fidkowski and A. Kitaev, *Phys. Rev. B* **81**, 134509 (2010).
- <sup>24</sup>A. M. Turner, F. Pollmann, and E. Berg, *Phys. Rev. B* **83**, 075102 (2011).
- <sup>25</sup>E. Tang and X.-G. Wen, *Phys. Rev. Lett.* **109**, 096403 (2012).
- <sup>26</sup>I. Affleck, T. Kennedy, E. H. Lieb, and H. Tasaki, *Phys. Rev. Lett.* **59**, 799 (1987).
- <sup>27</sup>F. Pollmann, E. Berg, A. M. Turner, and M. Oshikawa, *Phys. Rev. B* **85**, 075125 (2012).
- <sup>28</sup>M. Levin and Z.-C. Gu, *Phys. Rev. B* **86**, 115109 (2012).
- <sup>29</sup>R. B. Laughlin, *Phys. Rev. Lett.* **50**, 1395 (1983).
- <sup>30</sup>H. Yao, L. Fu, and X.-L. Qi, [arXiv:1012.4470](https://arxiv.org/abs/1012.4470).
- <sup>31</sup>S.-P. Kou, M. Levin, and X.-G. Wen, *Phys. Rev. B* **78**, 155134 (2008).
- <sup>32</sup>S.-P. Kou and X.-G. Wen, *Phys. Rev. B* **80**, 224406 (2009).
- <sup>33</sup>M. B. Hastings, *Phys. Rev. B* **69**, 104431 (2004).
- <sup>34</sup>E. Lieb, T. Schultz, and D. Mattis, *Ann. Phys.* **16**, 407 (1961).
- <sup>35</sup>S. Yan, D. A. Huse, and S. R. White, *Science* **332**, 1173 (2011).
- <sup>36</sup>H.-C. Jiang, Z. Wang, and L. Balents, *Nat. Phys.* **8**, 902 (2012).
- <sup>37</sup>S. Depenbrock, I. P. McCulloch, and U. Schollwöck, *Phys. Rev. Lett.* **109**, 067201 (2012).
- <sup>38</sup>Y.-M. Lu, Y. Ran, and P. A. Lee, *Phys. Rev. B* **83**, 224413 (2011).
- <sup>39</sup>F. Wang and A. Vishwanath, *Phys. Rev. B* **74**, 174423 (2006).
- <sup>40</sup>G. Misguich, D. Serban, and V. Pasquier, *Phys. Rev. Lett.* **89**, 137202 (2002).
- <sup>41</sup>S. Sachdev, *Phys. Rev. B* **45**, 12377 (1992).
- <sup>42</sup>Y. Huh, M. Punk, and S. Sachdev, *Phys. Rev. B* **84**, 094419 (2011).
- <sup>43</sup>J. Maciejko, X.-L. Qi, A. Karch, and S.-C. Zhang, *Phys. Rev. Lett.* **105**, 246809 (2010).
- <sup>44</sup>B. Swingle, M. Barkeshli, J. McGreevy, and T. Senthil, *Phys. Rev. B* **83**, 195139 (2011).
- <sup>45</sup>M. Levin and A. Stern, *Phys. Rev. B* **86**, 115131 (2012).
- <sup>46</sup>G. Y. Cho, Y.-M. Lu, and J. E. Moore, *Phys. Rev. B* **86**, 125101 (2012).
- <sup>47</sup>A. Kitaev and J. Preskill, *Phys. Rev. Lett.* **96**, 110404 (2006).
- <sup>48</sup>M. Levin and X.-G. Wen, *Phys. Rev. Lett.* **96**, 110405 (2006).
- <sup>49</sup>S. Furukawa and G. Misguich, *Phys. Rev. B* **75**, 214407 (2007).
- <sup>50</sup>Y. Zhang, T. Grover, and A. Vishwanath, *Phys. Rev. B* **84**, 075128 (2011).
- <sup>51</sup>S. V. Isakov, M. B. Hastings, and R. G. Melko, *Nat. Phys.* **7**, 772 (2011).
- <sup>52</sup>R. Dijkgraaf and E. Witten, *Commun. Math. Phys.* **129**, 393 (1990).
- <sup>53</sup>We consider PBC systems for simplicity. For open boundary systems, one can put quasiparticles on the edge and there can be only one quasiparticle in the bulk. However, this does not modify the argument below.
- <sup>54</sup>The general topological orders are mathematically described by tensor category theories. See, for instance, Refs. 77 and 69 for detailed discussions.
- <sup>55</sup>More precisely, we discuss projective representations determined by a gauge group, so the topological order is described by a discrete gauge group. However, symmetry fractionalization can be studied in topologically ordered phases beyond this subclass.
- <sup>56</sup>X.-G. Wen, *Phys. Rev. B* **65**, 165113 (2002).
- <sup>57</sup>D. Robinson, *Course Theory Groups*, Graduate Texts in Mathematics Series (Springer-Verlag, Berlin, 1996).
- <sup>58</sup>A. Kitaev in Ref. 47, Ying Ran and Xiao-Gang Wen (unpublished, 2002), Michael Hermele (private communication, 2012) and in Ref. 74.
- <sup>59</sup>One may wonder how we fix our convention, because for a usual finite Abelian gauge theory  $GG$  in  $2+1$  dimensions, the gauge charges and gauge fluxes are self-dual. In fact, for a general gauge theory with finite gauge group  $GG$ , the gauge fluxes and gauge charges are physically distinct. For example, gauge fluxes are labeled by conjugacy classes of  $GG$ , while gauge charges are labeled by the irreducible representations of the centralizer group of a conjugacy class. We show that in our exactly solvable models it is clear that the  $H^2(SG, GG)$  classification corresponds to the symmetry fractionalization classes of the gauge fluxes.
- <sup>60</sup>M. de Wild Propitius, [arXiv:hep-th/9511195](https://arxiv.org/abs/hep-th/9511195).
- <sup>61</sup>F. A. Bais, P. van Driel, and M. de Wild Propitius, *Nucl. Phys. B* **393**, 547 (1993).
- <sup>62</sup>M. de Wild Propitius, *Nucl. Phys. B* **489**, 297 (1997).
- <sup>63</sup>In Ref. 28, string-net models are used to construct the exactly solvable models for DW theories. It appears to us that this construction may not be general; namely, not all DW theories can be described by string-net models using the construction in Ref. 69. In the present work, we use a different way to construct exactly solvable models for DW discrete gauge theories, which is general.
- <sup>64</sup>M. Wakui, *Osaka J. Math.* **29**, 675 (1992).
- <sup>65</sup>A. Y. Kitaev, *Ann. Phys.* **303**, 2 (2003).
- <sup>66</sup>See, for instance, the web page by John Baez at: <http://math.ucr.edu/home/baez/qg-winter2005/w05week06.pdf>.
- <sup>67</sup>F. Verstraete, J. I. Cirac, J. I. Latorre, E. Rico, and M. M. Wolf, *Phys. Rev. Lett.* **94**, 140601 (2005).
- <sup>68</sup>For simplicity, let us consider  $G = Z_2$  and use the trivial 2-cocycle  $\omega(x, y) = 1, \forall x, y \in Z_2$ . We can construct the projector  $P$  for a circle following the discussion in Sec. III A2, after triangulating it by  $N$  line segments. Let us use  $g_I = \pm 1$  as the group element for the colored line segment  $I$ . The twofold ground-state sector  $\text{Im}(P)$  of the induced TQFT can be easily found:  $|\psi_1\rangle = 1/2^{(N-1)/2} \sum_{\prod_I g_I = +1} |g_I\rangle$ , and  $|\psi_2\rangle = 1/2^{(N-1)/2} \sum_{\prod_I g_I = -1} |g_I\rangle$ . Naively, the second ground state corresponds to a trapped  $Z_2$  gauge flux inside the circle. However, the degeneracy between  $|\psi_1\rangle$  and  $|\psi_2\rangle$  is not protected. One can consider a local perturbation  $\delta H = \epsilon |g_I = -1\rangle \langle g_I = +1| + \text{H.c.}$  for a certain line segment  $I$ . Straightforward perturbative calculation shows that this perturbation lifts the ground-state degeneracy by a finite energy gap.
- <sup>69</sup>M. A. Levin and X.-G. Wen, *Phys. Rev. B* **71**, 45110 (2005).
- <sup>70</sup>R. Dijkgraaf, V. Pasquier, and P. Roche, *Nucl. Phys. B (Proc. Suppl.)* **18**, 60 (1990).
- <sup>71</sup>F. A. Bais, P. van Driel, and M. de Wild Propitius, *Phys. Lett. B* **280**, 63 (1992).
- <sup>72</sup>Although we do not have a general proof, we believe that this is true, which is also confirmed in the examples in Sec. V that we solved.
- <sup>73</sup>L.-Y. Hung and X.-G. Wen, [arXiv:1211.2767](https://arxiv.org/abs/1211.2767).

<sup>74</sup>A. M. Essin and M. Hermele, [arXiv:1212.0593](#).

<sup>75</sup>Y. Hu, Y. Wan, and Y.-S. Wu, [arXiv:1211.3695](#).

<sup>76</sup>S. M. Lane, *Categories for the Working Mathematician*, Graduate Texts in Mathematics (Springer, Berlin, 1998).

<sup>77</sup>A. Kitaev, *Ann. Phys.* **321**, 2 (2006).

<sup>78</sup>M. Oshikawa and T. Senthil, *Phys. Rev. Lett.* **96**, 060601 (2006).

<sup>79</sup>As usual with duality, the flux, i.e.,  $\prod_{ij} u_{ij}$ , automatically vanishes through a closed loop  $ij$  on the lattice. The dual  $\widetilde{SG}$  therefore has no flux particles. Also, note that the duality transformation is not a 1-to-1 mapping, since configurations  $\{u_i\}$  and  $\{u_i \cdot \tilde{s}^{-1}\}$  are mapped to the same configuration  $u_{ij}$  in  $\widetilde{SG}$ , with  $\widetilde{SG}$  understood as the group  $SG$  acting in the dual theory.